Design and Simulation of Combined Accelerator and Brake Pedal

Udesa Getachew Shunu

A Thesis Submitted to

The Department of Mechanical Engineering,

School of Mechanical, Chemical, and Materials Engineering

Presented in Partial Fulfillment of the Requirement for the Degree of Master's in Automotive Engineering

Office of Graduate Studies

Adama Science and Technology University

June 2023

Adama, Ethiopia

Design and Simulation of Combined Accelerator and Brake Pedal

Udesa Getachew Shunu

Advisor: Siraj Kedir Busse (Ph.D.)

A Thesis Submitted to

The Department of Mechanical Engineering,

School of Mechanical, Chemical, and Materials Engineering

Presented in Partial Fulfillment of the Requirement for the Degree of Master's in Automotive Engineering

Office of Graduate Studies

Adama Science and Technology University

June 2023

Adama, Ethiopia

DECLARATION

I hereby declare that this Master thesis entitled "**Design and Simulation of Combined Accelerator and Brake Pedal"** is my original work. That is, it has not been submitted for the award of any academic degree, diploma, or certificate in any other university. All sources of materials that are used for this thesis have been duly acknowledged through citation.

__________________________ _______________________ ________________

Name of student Signature Date

RECOMMENDATION OF ADVISOR

I, the advisor of this thesis, hereby certify that I have read the revised version of the thesis entitled "**Design and Simulation of Combined Accelerator and Brake Pedal**" prepared under my guidance by **Udesa Getachew Shunu** submitted in partial fulfillment of the requirements for the degree of Masters of Science in Automotive Engineering. Therefore, I recommend the submission of a revised version of the thesis to the department following the applicable procedures.

__________________________ _______________________ ________________

Major Advisor Signature Date

APPROVAL PAGE

I, the advisor of the thesis entitled "**Design and Simulation of Combined Accelerator and Brake Pedal**" developed by **Udesa Getachew Shunu**, hereby certify that the recommendation and suggestions made by the board of examiners are appropriately incorporated into the final version of the thesis**.**

_________________________	_____________________	_______________
Major Advisor	Signature	Date

We, the undersigned, members of the board of Examiners of the thesis by **Udesa Getachew Shunu** have read and evaluated the thesis entitled "**Design and Simulation of Combined Accelerator and Brake Pedal**" and examined the candidate during the open defense. This, therefore, is to certify that the thesis is accepted for partial fulfillment of the requirement of the degree of Master's Science in Automotive Engineering.

_________________________	_______________	_________________
Chairperson	Signature	Date
_________________________	_______________	_________________
Internal Examiner	Signature	Date
_________________________	_______________	_________________
External Examiner	Signature	Date

Finally, approval and acceptance of the thesis are contingent upon the submission of its final copy to the Office of Postgraduate Studies (OPGS) through the Department Graduate Council (DGC) and School Graduate Committee (SGC).

___________________________	_______________	__________________
Department Head	Signature	Date
.___________________________	_______________	__________________
School Dean	Signature	Date
___________________________	_______________	__________________
Office of Postgraduate Studies, Dean	Signature	Date

ACKNOWLEDGEMENT

First, I want to thank God for helping me in every way. Next, I would like to sincerely thank my advisor Dr. Siraj Kedir Busse for his guidance and advice during the completion of this work. I would like to express my sincere gratitude to my friend Mr. Daniel Haile and Mr. Adane Seifu for their support and appreciation in carrying out this work. Finally, I want to thank my friends for sharing the idea and helping me.

TABLE OF CONTENTS

LIST OF TABLES

LIST OF FIGURES

ACRONYMS

DC	Direct Current
GND	Ground
IDS	Iowa Driving Simulator
IDE	Integrated Development Environment
LEDs	Light Emitting Diodes
NHTSA	National Highway Traffic Safety Administration
PAE	Pedal Application Error
SAE	Society of Automotive Engineering
TfL	Transport for London
UN	United State
UNECE	United Nations Economic Commission for Europe
UNSS	United Nations Safety Standard
WHO	World Health Organization
ASTU	Adama Science and Technology University

NOMENCLATURE

A	Area(m2)
a	Acceleration of the vehicle (m/s2)
D	Pitch diameter (mm)
D_b	Braking distance (m)
d_c	Minor diameter (mm)
Dc	Coil diameter (mm)
D_{nr}	New reaction distance (m)
d_r	Reaction distance (m)
F	Force (N)
g	Acceleration Due to Gravity (m/s2)
h	Tread depth (mm)
H	Height
K	Spring constant (N/mm)
KE	Kinetic energy (KJ)
m_v	Mass of the vehicle in (kg)
N	Number of engaged threads
n	Revolutions
N	Number of coils
P	Pitch (mm)
P	Power (W)
S	Distance (m)
S_d	Stopping distance (m)
S_{nd}	New stopping distance (m)
t	time (s)
T	The torque required to rotate the screw (N. m)
t_b	Braking time (s)
t_r	Reaction time (s)
V	Speed (m/s)
V	Voltage (v)
W	Load to be pushed (N)

W	Work (KJ)
A	Helix angle (°)
μ	Coefficient of friction
Σ	Axial stress (N/mm2)
σ_b	bending stress (N/mm2)
σ_c	compressive stress (N/mm2)
τ	Shear stress (N/mm2)
Φ	Friction angle (°)

ABSTRACT

The vehicle is the most used transport alternative and the major source of road traffic accident cause in the world. Even if there are many reasons like over-speed, inability to keep distance, unexpected local driving practices and street livestock. Damages, fatalities, and injuries were caused by longer stopping distances, pedal application errors, the requirement of driver effort to apply the sudden brake, and delay in transferring one's foot from the accelerator to the brake, drivers may encompass those persons whose legs may not be as strong to apply the brake pedal and leg Tonus during an emergency, especially in a situation that involve frequent start and stop of the vehicle. Attempts have also been made to solve the problem through different types of combined brake-accelerator pedals. However, the designs were subjected to ergonomic problems, needs driver effort to apply brake and also do not totally illuminate pedal application Error. Therefore, the purpose of this thesis work is to solve these problems, a combined brake and accelerator pedal was designed and simulated for taxis. The method employed for this work is data collection, SOLID WORKS modeling, simulation, and motion analysis. Finally, System programming with Arduino software, and circuit diagram using potentiometric position sensor, Arduino Uno, L293N Motor driver, stepper motor and code simulation using Proteus software. The analysis results of four reports of the Federal Police Commission from 2016 to 2020 show that in Ethiopia, taxis account for 25.03% of deaths, 43.04% of serious injuries, 47.3% of injuries and 49.84% of property damages caused by public transportation. The average property damage over the four years by taxis equals 203,036,437.9ETB, which equals the budget needed to build several full-cycle elementary schools in remote areas of the country. In addition, two years traffic report analysis based on causes of the accident shows that brake inefficiency was responsible for 34.64% of death, 44.26% of serious injuries, 42.88% of a slight injuries, and 37.94% of property damage caused by vehicle side. A designed pedal illuminates the requirement of driver-foot transfer between pedals and pedal application error in conventional systems. In addition to a decrease in stopping distance by 7m, a reduction in brake reaction time from 0.7sec to 0.5sec and rid-off driver from applying the brake pedal. Therefore, the designed combined pedal fits our country Ethiopia's traffic conditions especially, for vehicles that involve frequent start and stop. Finally, it is recommended that this combined pedal be manufactured and used to reduce accidents that may happen every day.

Keywords: *Combined pedal, Position sensor, Arduino Uno, and brake pedal actuator.*

CHAPTER ONE

INTRODUCTION

1.1 Background of the study

People move from one place to another to work, study, do business, or enjoy using multiple modes of transport. Vehicle is the most used mode of transport and the biggest cause of traffic accidents in the world. Nowadays, traffic accidents have been both a public and a growing problem and have attracted the attention of the world. According to a report by the World Health Organization (WHO), more than 1.35 million people are killed on the world's roads every year, and 20 to 50 million people are disabled or injured in traffic accidents (WHO, 2018).

Low-income and middle-income countries have higher road traffic fatality rates 21.5 and 19.5 per 100,000 population, respectively than high-income countries (10.3 per 100,000)(Gupta & Bandyopadhyay, 2020). Over 90% of the world's fatalities on the road occur in low-income and middle-income countries, which have only 48% of the world's vehicles (Mehsen et al., 2020). WHO predicts that "Road traffic injuries will rise to become the eighth leading cause of death by 2030" The rate of road traffic death is highest in Africa (26.6/100,000 people) (WHO, 2018).

According to this report, Ethiopia has not implemented at least 7 or all of the 8 priority UN vehicle safety standards and is subjected to the death of 37% of pedestrians and 63% of others. Road traffic accidents are a significant public health issue in Ethiopia and are getting worse (WHO, 2018).

According to the Ethiopian Transport Authority, the result of the statistical vehicle reports of 2021 shows that there are only 1,339,005 registered vehicles in the country in total. Out of this total number of public vehicles covers 61.67%. The remaining 38.33% consists of commercial vehicles and machinery vehicles. The analysis results of the four reports of the Federal Police Commission from 2016 to 2020 show that Ethiopian taxis cover 14.4% of the total number of vehicles in Ethiopia, but they cause 25.03% of deaths, 43.04% of serious injuries, 47.3% of injured injuries, and 49.84% of property damage caused by public vehicles. This result shows that taxis need serious attention. Because the average property loss over four years is Two Hundred Three Million Thirty-Six Four Hundred Thirty-Seven and Nine-Tenths Birr

(203,036,437.9 ETB), which is equivalent to the budget needed to build several full-cycle primary schools in remote areas.

National Highway Transportation Safety Administration (NHTSA) reports that an estimated 16,000 accidents resulting from pedal errors occur each year. This number means that, on average, 44 accidents occur each day as a result of the driver confusing the gas for the brake. Because of these reasons, several victims' families live on roadsides. This accounts for an annual average of 23 million birrs in property damage, 56.1 serious injuries, 99.1 fatalities, and 66.6 minor injuries. (Hs, 2015). Therefore, this research is intended to highly reduce the percentages stated above.

Automated Pneumatic braking control system research conducted by Yared and Intelligent braking with brake failure indicator by Yonas was based on using software called Catia to model parts, Arduino to program, and Proteus to simulate. Finally, the prototype was developed using an Arduino Uno microcontroller, ultrasonic sensor, solenoid plunger, relay, etc. for demonstration and checked for its functionality. (Woldu, 2021) (Admasu, 2019)

The study investigates how automotive pedal design has changed over time. Despite being in use since the Model A Ford, the traditional accelerator and stop pedals have two fundamental drawbacks. At start-up, it takes about 0.2 seconds to switch the foot from the accelerator pedal to the brake pedal, allowing the vehicle to travel a long distance at high speed. The possibility of pressing the wrong pedal is another danger that can lead to an accident.

The study suggests alternative remedies to these problems, including altering the size of the pedals, expanding the space between the pedals, shifting the pedal's pivot point, and using various brake and accelerator pedal types. The history, evolution, and changes to foot controls that have taken place over time are also covered in this research. The Transport for London (TfL) Safety Manager was consulted early on in the study's development by Human Engineering. To find potential answers, prior Human Engineering initiatives and pertinent scientific studies were examined.

The thesis also offers a thorough analysis of car pedal design and suggests potential fixes for problems with conventional brake and accelerator pedals. To find feasible solutions, the study was carried out by Human Engineering in cooperation with TfL, and relevant scientific studies and earlier initiatives were examined.

This article has practical relevance in that it suggests potential remedies for problems with conventional accelerators and brake pedals in automobiles. These options include altering the pedal size, expanding the space between them, shifting the pivot point, and switching up the brake and accelerator pedals. By putting these suggestions into practice, it will be easier for drivers to react while switching from the accelerator to the brake, and the risk of pushing the wrong pedal, which can cause accidents, will be reduced. The research offers a thorough examination of how car pedal designs have evolved for designers and engineers working in the sector. The well-known SOLIDWORKS 2019 software, an Arduino (ATmega328P microcontroller), and Proteus 8 software were also utilized in this study to model the parts, write the programs, and test the operation of the programs. Finally, SOLIDWORKS software was used to simulate and analyze the motion of the modeled elements.

1.2 Statement of Problem

According to the findings of the federal police commission's four-year report analysis from 2016 to 2020, taxi-related traffic accidents in Ethiopia are a severe problem that result in property damage, fatalities, and injuries to pedestrians, passengers, and other road users. This report demonstrates that, despite the fact that there are numerous contributing factors, including excessive speed, driving out of lanes, failing to signal, failing to maintain a safe following distance, making quick turns and overtaking other vehicles, unpredictable local driving customs, livestock in the road, pedestrians, and a failure to adhere to basic vehicle safety standards. Damages, fatalities, and injuries were caused by brake system inefficiency, longer stopping distance due to brake reaction time, braking pedal error due to repeated driver’s effort as a result of frequent start and stop of the vehicle in high traffic congestion, the requirement of driver effort to apply the sudden brake, and difficulty in transferring one’s foot from the accelerator to the brake quickly because of leg tonus during an emergency. Also, due to a delay in switching the leg the accelerator brake pedal to the brake pedal. For instance, in conventional braking, the time taken to shift the foot from one pedal to the other will lead to an accident. It takes at least

0.2 seconds to move your foot from one pedal to the other and hence, at 80 kilometers per hour this adds five (5) meters to the vehicle's stopping distance (Jadhav et al., 2019).

Last but not least, drivers of vehicles include people whose legs might not be as powerful to press the brake pedals. With the population increasing and becoming older when the drivers become over the age of 65. Older drivers may find it more challenging to operate a car safely due to age-related losses in their cognitive and physical capacities, including clouded eyesight, slow reflexes, and a constrained range of limb motions. They are consequently more prone to be injured in crashes. Older drivers are more prone to engage in PAEs when operating a vehicle (Xi et al., 2018). The study's scholarly contribution is its thorough examination of the development of car pedal design over time. The study also makes design ergonomically safe and suggests for potential remedies to deal with the problems posed by conventional accelerator and brake pedals in vehicles. The effectiveness and safety of automotive pedals can be enhanced by these techniques. For designers and engineers in the automotive sector who are interested in bettering the design of automobile pedals, the research can be helpful.

1.3 Objectives

1.3.1 General Objective

The general objective of this thesis is to design and simulate the pedal that serve for both braking and accelerating purpose.

1.3.2 Specific Objectives

The following are the precise objectives:

- ✓ To design a combined pedal and actuation mechanism.
- ✓ To model the combined accelerator and brake pedal for further analysis.
- ✓ To program and simulate the system to test its functionality.
- ✓ To make motion analysis and simulation to check its response with average pedal application force of 58N.

1.4 Significance of the Study

The significance of this study is that it proposes a new design for a combined accelerator and brake pedal that could potentially increase brake efficiency and reduce driver effort, particularly for vehicles that frequently start and stop. This could ultimately lead to a reduction in accidents and improve overall vehicle safety. The study also offers a thorough literature analysis on the subject, which may be helpful for future studies in this field. The main advantages of this study are;

- ✓ It introduces a system of braking that uses the mechanism of inverse braking i.e., the vehicle will be in braking condition when the combined pedal is not pressed. Once the pedal is pressed the braking force is released and when further pressed the car will accelerate.
- ✓ It reduces driver burden and PAEs, especially for passenger cars (taxis) which involve frequent start and stop.
- ✓ It reduces brake reaction time which may result in fatal traffic accidents.
- ✓ It helps automatic braking when the vehicle is stopped while idling.
- ✓ It helps to stop the vehicle easily and safely.
- ✓ It helps in the emergency he/she has to take his foot off the pedal to apply the sudden brake.
- ✓ Braking is carried out without the possibility of error, and without interfering one function with the other.

In general, it aids in lowering driver effort, traffic accidents, and property damages, to reduce pedestrian deaths and traffic injuries, and as a result, lessens problems with public health and economic growth in our country Ethiopia.

1.5 Beneficiaries of the Study

All road traffic users including vehicle owners, researchers, drivers, pedestrians, traffic police, society, and the country as a whole get benefitted from this work.

The beneficiaries of this study could include:

- ✓ Automotive engineers and designers who are interested in developing new and innovative vehicle control systems.

- ✓ Vehicle manufacturers could potentially implement the new combined pedal design in their vehicles to improve safety and performance.
- ✓ The enhanced braking efficacy and reduced pedal effort may be advantageous to drivers, making driving safer and more pleasant.
- ✓ Other scholars or groups with an interest in vehicle safety and control systems may find the study's findings and recommendations helpful.

1.6 Scope of the Study

The goal of this work is to develop and model a combined accelerator and brake pedal utilizing finite element analysis simulations and computer-aided design (CAD) tools. To highlight research gaps and constraints, the study also includes a thorough literature assessment on the subject of brake and accelerator pedals integrated with autonomous braking systems. The ultimate goal of the study is to reduce brake reaction time, stopping distance increase brake efficiency and reduce driver effort, particularly for vehicles that frequently start and stop, to improve overall vehicle safety.

1.7 Organization of the Thesis

There were five chapters in the thesis. The study's background, a synopsis of the issue, goals, significance, beneficiaries, and scope are presented in **Chapter One. Chapter Two** discusses in-depth studies of the literature on combined accelerator and brake pedals in order to identify research limitations, provide solutions for them, and determine the primary causes of those constraints. The resources used for the study and the procedures that were followed step by step are discussed in **Chapter Three**. Additionally, the raw analysis and numerical designs are examined in this chapter. The results of the research are discussed in **Chapter Four**, and several comparisons between the current system and this thesis work are made using computer simulations. Finally, discusses the implications of the results, and limitations, and concludes remarks with key findings of the present investigation with recommendations and future work summarized in **Chapter Five.**

CHAPTER TWO

LITERATURE REVIEW

2.1 Introduction

This chapter starts with brief evolution of foot controls the extensive reviews of the recent literature reviews related to the combined pedal for brake and accelerator, also automatic braking system was made for knowing the research gap, and the main reasons behind the limitations and improvements.

2.2 A brief history of Vehicles foot controls

To understand recent automotive pedal design, it is best to understand the origins and development of early automotive foot pedals and the changes over time. The development of pedals is an important starting point for the study of recent pedal design. The way drivers accelerate and decelerate cars is thought to have undergone major changes since the late 19th century when vehicles were invented (Xi et al., 2018) as shown in Fig. 2.1.

The birth of the car was not accompanied by the birth of the foot control. In 1866, Benz's current car was the first universally recognized car. It was operated primarily by a hand lever and steering wheel on the left side of the vehicle and had no foot controls. The first known automotive foot switch was introduced in 1890, when the French manufacturer Panhard introduced a foot pedal switch to control the transmission. Early forms of foot switches were not necessarily well received by most manufacturers and drivers as foot controls began to take on functions previously performed by manual controls. Evidence of the side effects of foot control emerged in repeated discussions that appeared in an early automotive journal (Bellis, 2019).

In the early stages of car design, control functions, such as acceleration, were still transferred to footswitches in the form of buttons or pedals. In 1912, Cadillac introduced the first foot-operated starter motor. The first foot-operated reflection-dazzle handle was introduced in 1927 and was located in the pan for about fifty years until it was moved to the steering wheel. Other functions, such as the windshield, were also once controlled by the driver's foot. The foot controls of early auto divers had two main functions. First, you had to control more functions with your foot than in modern cars. Second, foot switches existed in many forms, such as switches other than pedals as we see them today (Xi et al., 2018).

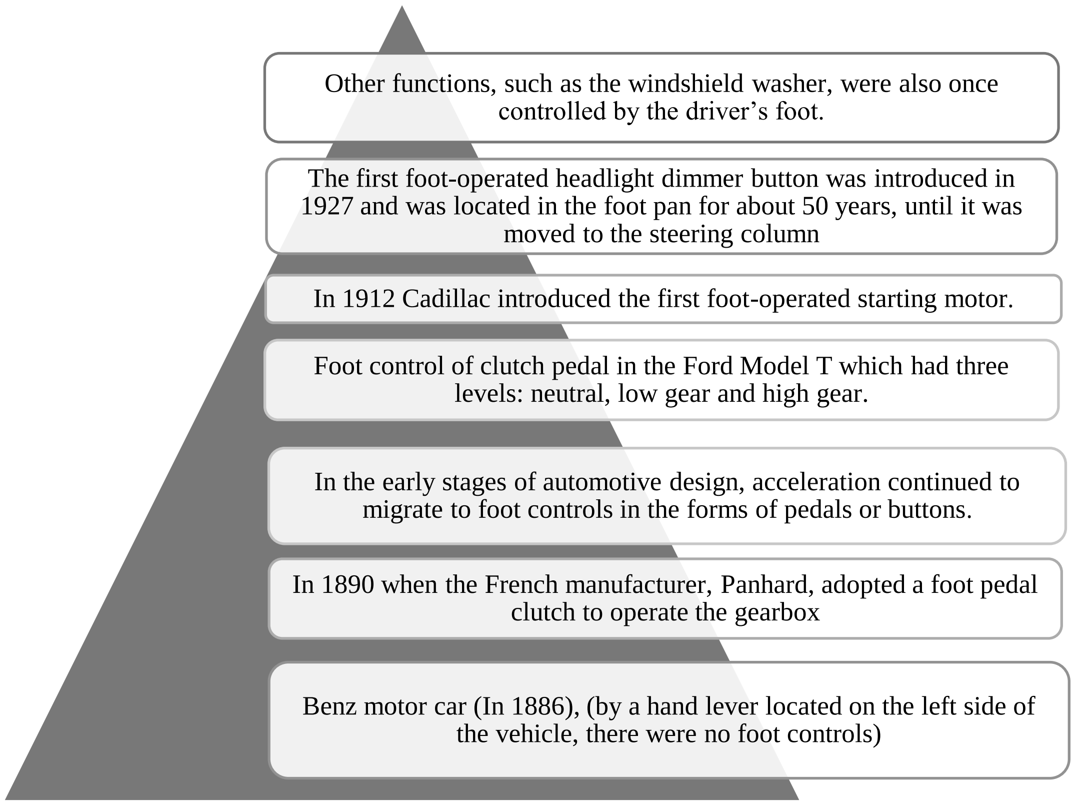

Figure 2.1: Origins and Development of foot controls

In general, the pedal system plays a major role in controlling the vehicle, due to its high functional density at the driver/vehicle interface.

2.3 Review of recent related works on pedals

It is preferable to have an awareness of the origins and development of foot controls in early automobiles and advances that have occurred over time through reviews of articles in order to comprehend current vehicles, pedal design, and why the pedals perform as they do today. The traditional separate accelerator and brake pedals, which appeared at the same time as the model A Ford, are technically simple and functionally safe, however, they involve two crucial drawbacks. First, the reaction time for a driver to move his or her foot from the accelerator to the brake is about 0.2 s; If a vehicle is traveling at 90 km/h it moves 5 m during that time. Second, there is the hazard of pressing the wrong pedal, i.e., a poor depression on the brake pedal or simply contacting the wrong pedal (e.g., pressing the accelerator rather than the brake pedal) (Nilsson, 2018).

To identify potential solutions, Human Engineering had early discussions with the Transport for London (T f L) Safety Manager on the issue, reviewed relevant scientific reports and previous projects undertaken by Human Engineering and Provided potential solutions like changing the size of pedals, increasing the distance between pedals, changing the pivot point of the pedal, use different pedal types for brake and accelerator (suspended vs. organ pedal, etc.) to increase awareness of foot location (Bright et al., 2011). In addition, the installation of a barrier between pedals, bus drivers to use left-foot braking, redesigning the throttle so drivers must accelerate using hand controls, etc. to make it more difficult to place the foot in the wrong place. Increasing the difference in the level of the two pedals can reduce the risk of pressing the wrong pedal (Bright et al., 2011; Nilsson, 1989). This tactic, however, has a serious disadvantage in that it increases the operator's reaction time in braking. Attempts have also been made to solve the problem through different types of combined brake–accelerator pedals.

As shown in Fig. 2.2. Winkelman developed and patented the compound pedal mechanism in 1959 (US Patent No. 2878908).

The gas pedal engages when pressed with the front of the pedal with the toes, and the brake engages when pressed with the back of the heel.

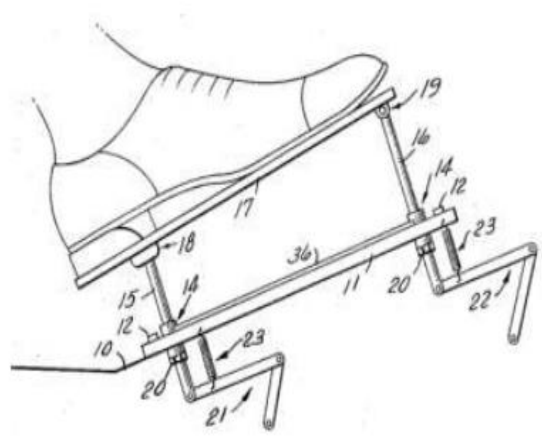

Figure 2.2: Wikelman's innovative accelerator and brake pedal design (U.S. Patent No. 2878908)

Over the years, designers have developed various combined brake–accelerator pedals to eliminate the operator's risk of pressing the wrong pedal as well as to reduce his or her reaction time in braking. According to (Senthil Kumar et al., 2020) the development of a new combination pedal for one-foot braking and acceleration, shown in Figure 2.3, reduces braking time and the stopping distance is improved and accessible for people with physical disabilities. The most effective is thought and planned optimizing different ways of use. The brake can be pressed from under the pedal, which is activated by pressing. The accelerator is placed directly above the brake, using a rotary mechanism to activate the accelerator, the accelerator is connected to the accelerator by a throttle cable. They used the bell crank mechanism to avoid pressing the wrong pedal.

However, they used mechanically controlled components and ergonomic problems if the driver has difficulty in relaxing because of concern for unintentional braking, physical tension and strain are likely to occur.

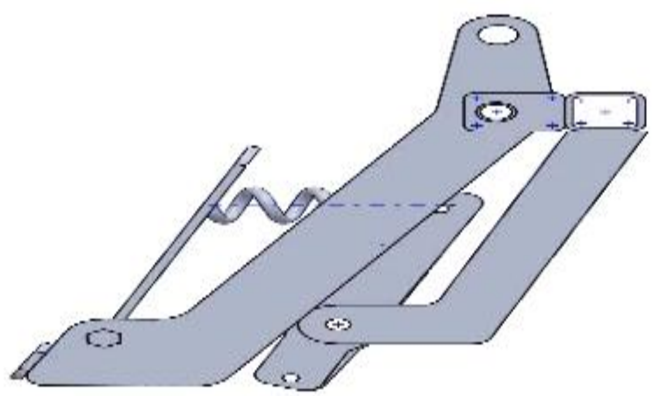

Figure 2.3: Senthil Kumar combined pedal side view (Senthil Kumar et al., 2020)

Also, (Jadhav et al., 2019; Mugundhan et al., 2018) designed a pedal that can provide both accelerating and braking functions. The main objective behind this work is to get rid-off drivers' efforts and reduce road accidents. Also, to avoid misapplication of the accelerating pedal instead of the brake pedal & also to reduce the time required to transfer the foot from the accelerating pedal to the brake pedal. The vehicle can be accelerated by rotating the pedal about the upper pivot point with a torsion spring. The forward motion of the lever with a helical spring will be used for the braking circuit. The helical spring will bring back the lever which pivoted to the ground to its original position.

According to Chandira & Kanuru, (Chandra & Kanuru, 2020), a study shows the day's death rate because of accidents increased a lot and is around 27%. This system can at least reduce the percentage by 1-2%. (Girish et al., 2021) also used the same design which involves accelerating a foot's movement and, while braking comes from extending the whole leg. to avoid the problem of the foot may be inaccurately placed on the brake resulting in bad braking performance due to inaccurate foot transfer while switching between pedals during an emergency. Transport for London Bus Safety Standard Report pedal application error prevention & recovery reported that the brake/accelerator light indicator solution is a simple and clear method for providing feedback to drivers regarding which pedal they are pressing, which could help drivers to recover from pedal application error incidents (Runham et al., 2018).

Prithiviraj et al., (Prithiviraj et al., 2018) also used the same principle as above with a slight difference in which the pedal is mounted in the same position as the conventional accelerator as shown in Fig. 2.4. The right foot is placed on the pedal and should stay there during the drive. A heel support prevents the foot from slipping off the pedal. When accelerating, the driver pushes with the forefoot in the usual manner and when breaking the driver pushes with the whole foot. The main aim is to avoid interference of braking during acceleration and vice versa by a combination of the pedal for brake and accelerator. (Ramachandran & Raghul, 2017) using on/off and cutoff limit switches for electronic vehicles this same technique is also applicable to normal vehicles and it can be used for physically challenged persons.

One of the worst cases occurred in Santa Monica in 2003 when an 86-year-old man pressed the wrong pedal killing 10 people and injuring 63 when his speeding car plowed through an outdoor market his incident happened because of pedal misapplication. However, it is observed that it is difficult to operate the pedal during climbing on hills. To overcome that problem, we should use a handbrake. It will be uncomfortable for the user.

The same principle was used by Chandra and Kanuru (Chandra & Kanuru, 2020), with the main goal of this innovation being to eliminate the operator's risk of pressing the wrong pedal during an emergency, as well as to reduce the driver's reaction time when switching from accelerator to brake or vice versa.

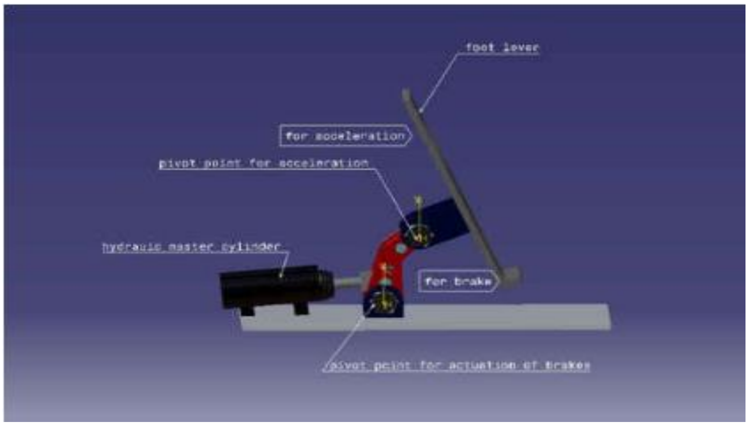

Figure 2.4: Jadhav combined pedal design (Jadhav et al., 2019)

Another combined pedal shown in Fig. 2.5 was developed by researchers (Nilsson, 2002; Shanmugasundar et al., 2018). The new combined brake–accelerator pedal was devised by Sven Gustafsson and further developed by the Swedish company Nomix Development, Inc. The pedal is mounted approximately where the accelerator is normally placed. The combined pedal consists of a brake pedal arm on which is mounted an accelerator. To prevent accidental braking during, e.g., vigorous acceleration the pedal arm is held in place by an electromagnet. The strength of the magnet can be adjusted to adapt to each individual.

During braking, acceleration is automatically disengaged independent of the accelerator's position. Thus, it is unnecessary to reduce the speed of acceleration at the time of braking.

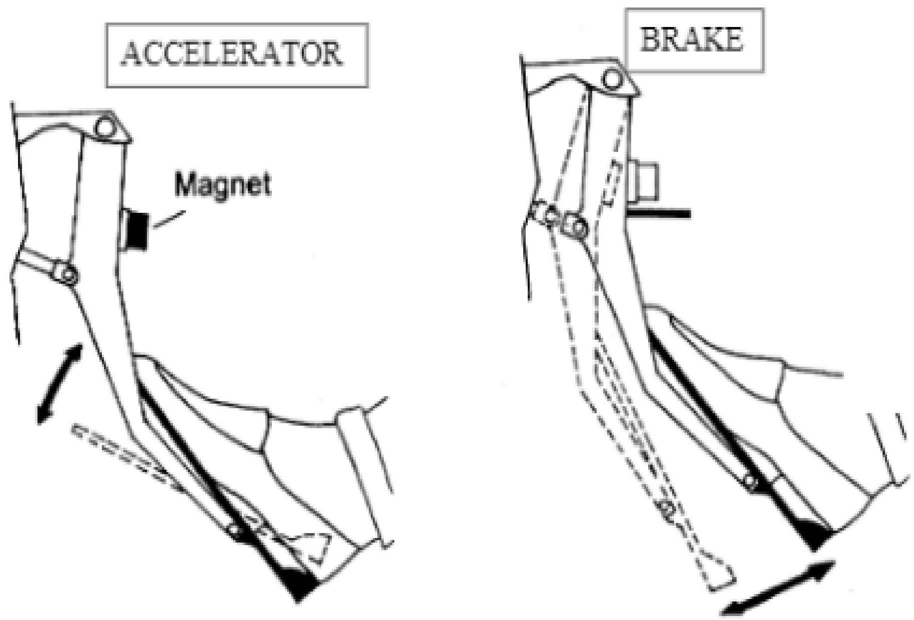

Figure 2.5: Combined brake and accelerator setup (Shanmugasundar et al., 2018)

The study of Khakhar et at., (Khakhar et al., 2018) contributed to eliminating the possibility of a driver pressing the wrong pedal or he/she may take more time in switching his/her leg and this may lead to fatal accidents during emergencies. To solve this problem, they designed another brake pedal and accelerator system. Various components were individually designed and then assembled. In this mechanism, the vehicle is in braking condition when the pedal is not pressed. When the pedal is pressed it will first slowly disable braking. Half of the pedal play is given for braking. When the braking is completely disengaged, by further pressing the pedal we can throttle the vehicle. However, the system is carried out manually and mechanically.

In 1991, a new combined pedal system Naruse Fig. 2.6. When the foot was turned to the right to control the lever, the gas pedal was engaged, and when the pedal was pressed, the brake was engaged. (Matsunaga et al., 1996) compared the time when the foot moves from the gas pedal to the brake pedal and the braking distance using both traditional pedals and the Naruse pedal. The average leg transfer time with the Naruse pedal system was 0.16 seconds shorter than with the traditional pedal system.

The stopping distance of the Naruse pedal has been reduced by 1.6 m compared to the stopping distance of a conventional pedal system.

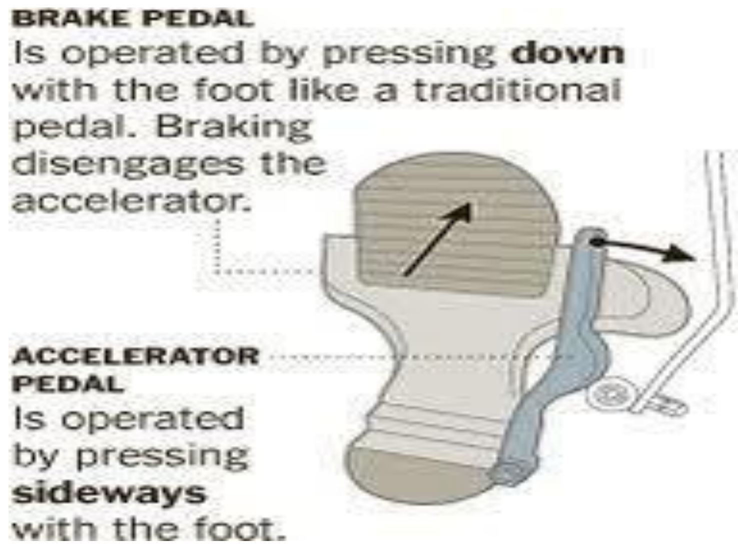

Figure 2.6: The Naruse's pedal operation (Xi et al., 2018)

(Lakew, 2018) In order to prevent accidents brought on by brake system failure, Lakew developed an intelligent braking system for buses with a brake failure indicator system that makes use of an IR sensor to gauge the distance to an obstruction as well as other parts like an Arduino Uno microcontroller, a buzzer, and so forth. In summary, electronic control techniques were applied in this study, which decreased the braking distance from the existing (62.1m) to 49.4m at the maximum speed (105 km/h). However, because to the identification of impediments when turning, it has an IR sensor constraint (Yared, 2019) Using the same idea, Yared also created a prototype for an automated pneumatic braking control system for a Sinotruck. The goal of his research is to alter the design and development of an automated pneumatic braking control system by using Catia for software modeling parts and Arduino programming tools. This will change the brake system of Sinotruck. Additionally, a solenoid for activating the brake and an ultrasonic sensor (IR) for detecting objects or obstacles were incorporated into the design. When compared to the old system's 42.2m stopping distance at 75 km/h, it was found that the automated braking system reduced stopping distance by 27.6m. However, it involves the limitation related to IR sensors due to the detection of obstacles while taking a turn.

Nisson (Nilsson, 2002) in his study highlighted problems that drivers may face when they switch between pedal systems. The results indicate that drivers were able to learn the combined pedal mechanism quickly and effortlessly. The number of mistakes was extremely low during the acquisition phase in learning the combined pedal system. The drivers reported that the combined pedal offered greater physical comfort and was considerably more natural to operate. Forward movements are advantageous in that they make the handling of the vehicle quite ‘natural’. (Wevj- et al., 2015).

2.4 Summary of the Review

Cars have been equipped with the same foot-pedal arrangement since the days of the A-Ford. The clutch is to the left, the accelerator to the right, and the brake in the middle. The right foot should be used for pressing the accelerator and the brake. This arrangement guarantees, that the throttle is released as the driver brakes. However, it also means that the foot almost always is placed at a distance from the brake, that is, on the accelerator, thus movement time adds to brake reaction time. During foot movement, the foot may also be inaccurately placed on the brake resulting in bad braking performance and it may even miss the brake and hit the accelerator. To reduce the risk of misapplication the pedals are usually mounted at different levels, the brake is higher and closer to the driver. However, different levels cost extra movement time.

To overcome the drawbacks of the traditional pedals various combined accelerator-brake pedals have been constructed with different mechanisms of application. All of these constructions focused on decreasing reaction time, avoiding misapplication (pedal error), and providing greater physical comfort which were the major problems with conventional ones. Most of the studies try to develop different types of combined pedal braking systems for various vehicles based on manual (mechanical) systems of braking (i.e., it needs driver force to brake “press or push action”) by combining the pedal. The others are based on objects/obstacles sensed by the ultrasonic sensors and in combination with other signals like the speed of the vehicle, brake oil pressure, and application brake in both pneumatic and hydraulic power-assisted brake systems to control and archiving of reducing traffic accidents as well as road users’ death and injuries. However, the latter case is automatic and does not involve a combined pedal system.

Additionally, some studies demonstrated the development of intelligent braking, automated pneumatic braking control systems, and brake failure indicator circuits that continuously monitor the condition of the brake using a variety of techniques, such as adjusting the rider before the wire is severed or using a sensor that detects the brake shoe's wear and leakage and sends a signal to the microcontroller. Finally, when an obstacle is detected, the vehicle may automatically apply the brakes or signal the driver. As a result, the vehicle is safer thanks to this.

2.5 Design Guidelines and Standards for automotive pedals

The brake pedal is part of the car that initiates the entire brake system in a vehicle. In automatic cars, it's the pedal on the left side, and in manual cars, it's the middle pedal. When you press down on it, all the components of your braking system swing into action. The following information is gathered through reviews of the existing design standards and recommendations for automobile pedal design. Reviews of the current design standards and recommendations for pedals used in vehicles, as well as a breakdown of the different features of pedal design, such as pedal size and position. Governments, national and international standards groups, professional organizations, and other institutions have all released different standards or guidelines over many years.

The '1958 Agreement' is a framework that the United Nations Economic Commission for Europe (UNECE) devised in 1658 to harmonize the criteria for a vehicle that are connected to safety, the environment, anti-theft difficulties, and energy. The UNECE's Inland Transport Committee includes the World Forum for Harmonization of Vehicle Regulations (WP 29). The WP 29 produced a number of car regulations based on the 1958 Agreement. Regulation No.35 (Uniform Provisions Cornering the Approval of Vehicles concerning the Arrangement of Foot controls) of these laws specifies the arrangement of foot controls in passenger vehicles, including those with automatic and manual transmissions (Xi et al., 2018). The standards focus on the accelerator pedal and brake pedal in a passenger car. Recommendation from perspectives such as pedal resistance, travel, position, and considerations helpful to the pedal design exist in pre-viewed articles, design handbooks, and government reports (Whitfield, 1967).

A. **Pedal position:** The pedal position is measured in three dimensions. The position of the pedal may relate to the driver's safety and comfort in a car. Pedal positioning is dependent upon factors such as a driver's leg length, foot length, and seat position, as well as vehicle footwell size. For this study, the pedal position is assumed as it is in the previous position.

B. **Pedal size:** Proper pedal size will allow for comfortable foot contact and aid in creating distinct sensations for various pedals. This includes things like pedal width, pedal length, and pedal travel.

a) **Pedal length:** The preferred pedal length is indicated by an asterisk; suggestions for the accelerator pedal are provided in green, while recommendations for the brake pedal are shown in red, as seen in Fig.2.7.

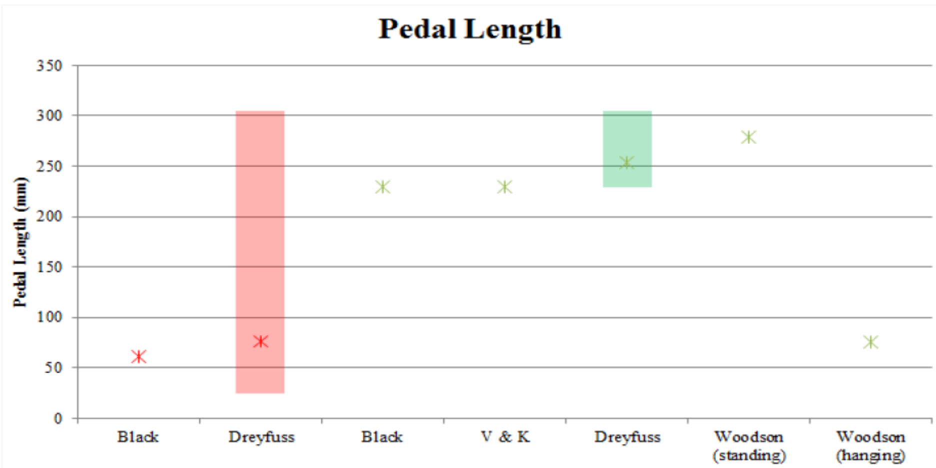

Figure 2.7: Summary of pedal length((Xi et al., 2018))

The ideal length for a standing hinged on-floor accelerator pedal is 254 mm, and the recommended range is 229 mm to 305 mm. (Xi et al., 2018).

b) Pedal width: An overview of the pedal width design suggestions (the preferred pedal width is indicated by an asterisk; the green and red colors correspond to the accelerator and brake pedal recommendations, respectively). as depicted in Fig. 2.8.

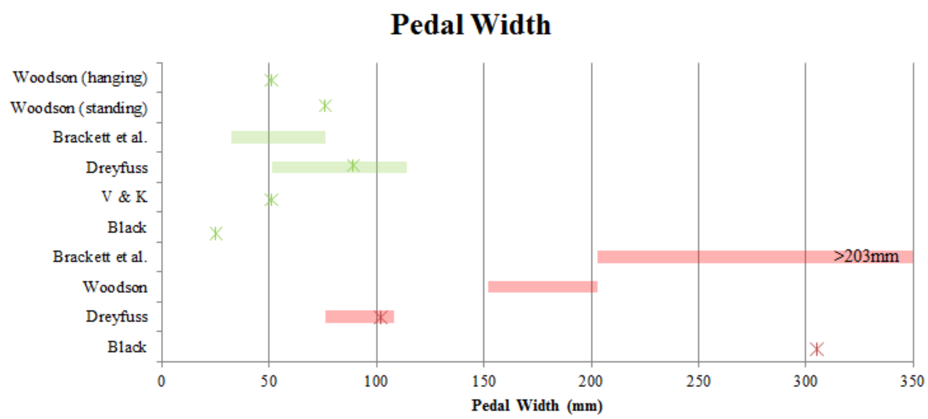

Figure 2.8: Summary of pedal width ((Xi et al., 2018))

It was suggested that the pedal width for a standing accelerator pedal with a floor-mounted hinge should range from 61 mm to 114 mm, with 89 mm being ideal.

c) **Pedal travel:** is also known as "pedal stroke" or "pedal displacement" in the literature. It usually refers to the translational travel of the pedals, but as pedals can also move in a curved path, the translational travel of the pedals can also be characterized by the angular travel of the pedals or by the contour of the journey path. Fig. 2.9 depicts a summary of the pedal design advice for accelerator pedal travel. The preferred accelerator pedal travel is indicated by the asterisk**.**

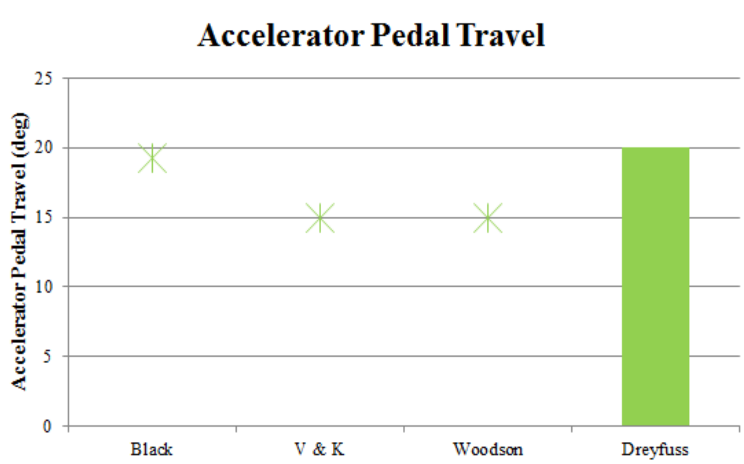

Figure 2.9: Summary of accelerator pedal travel ((Xi et al., 2018))

Said that the angular range of the ankle-operated pedal for an accelerator should not exceed 30 degrees due to the ankle's maximum range of motion. assuming that a 160-degree knee angle will deliver significant foot force without pain based on height.

d) **Pedal angle:** The angle made by the pedal surface and the vehicle floor is referred to as the pedal angle or pedal orientation. Ankle comfort is related to the pedal angle since it determines the foot angle. For the summary of the accelerator pedal angle see Fig. 2.10.

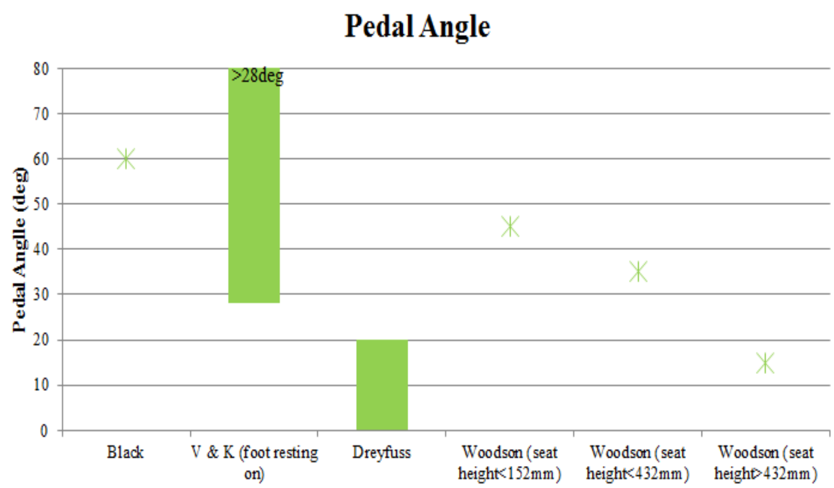

Figure 2.10: Summary of accelerator pedal angle (Xi et al., 2018)

If the seat is 152 mm or lower, such as in a sports car, it is advised that the accelerator pedal should be 45 degrees (from horizontal); 35 degrees if the seat height is between 432 mm and 432; or 15 degrees if the seat height is 432 mm and higher. The advice was based on the comfort of the driver; if the pedal angle is too steep, the ankle will easily tire when the driver releases the pedal.

e) Pedal resistance: Also known as pedal force, is the resistance that the foot experiences when pressing the pedal. It has numerous effects on how the pedals work. For instance, in everyday driving situations, drivers may use pedal resistance as a cue to distinguish one pedal from the other and to vary the force they apply to the pedal. The ideal pedal resistance can support the foot when it is resting on the pedal and is strongly related to the maximum foot/leg force the driver can exert. It can help reduce reaction time and foot travel time. (Xi et al., 2018).

Recommendations for pedal design summarized Fig. 2.11 depicts the pedal resistance. The chosen resistance is denoted by the asterisk. Green denotes suggestions for the acceleration pedal, while red denotes suggestions for the brake pedal.

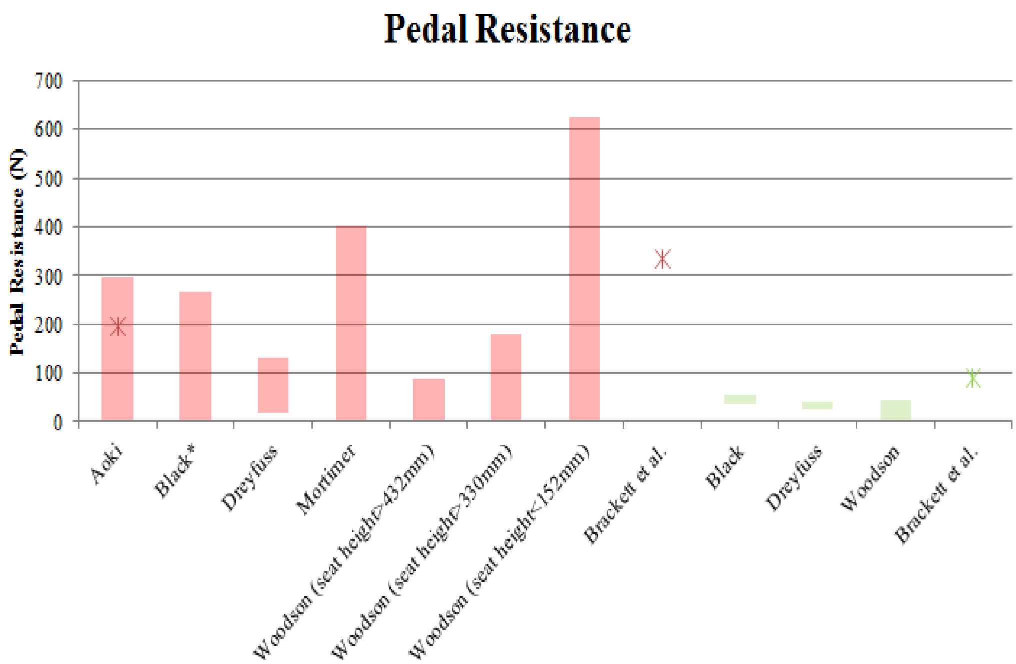

Figure 2.11: Summary of pedal resistance design suggestions (Xi et al., 2018)

Cited the speed regulation and foot comfort as criteria for the accelerator pedal, stating that the lowest pedal resistance should allow the foot to softly rest on the pedal and suggesting the accelerator pedal resistance not exceed 89 N (20 lbs.).

2.6 Summary of relevant design recommendations

As stated in Table 2.1, a summary of pertinent design guidelines for the throttle pedal for this study are found in design handbooks, peer-reviewed studies, and government reports.

Table 2.1: Summary of relevant design recommendations

Design criteria recommendations	Size/type/position
Pedal type	Organ type
Pedal position	As it is (in the previous position)
Pedal length	25cm
Pedal width	8.25cm
Pedal travel	27deg
Pedal angle (when depressed from the floor)	17deg
Maximum Pedal resistance	89N

Therefore, the above summary was used for the design purpose of the combined pedal.

2.7 System Components

The two primary parts of the combined accelerator and brake pedal brake system are as follows:

- ✓ Conventional components and
- ✓ Electronic components,

2.7.1 Conventional Hydraulic Brake Components

The conventional Hydraulic brake components involve the following components shown in Fig. 2.12.

These are:

- ✓ Brake Pedal
- ✓ Brake booster
- ✓ Master Cylinder
- ✓ Oil Reservoir

- ✓ Brake calipers/shoes
- ✓ Pipeline

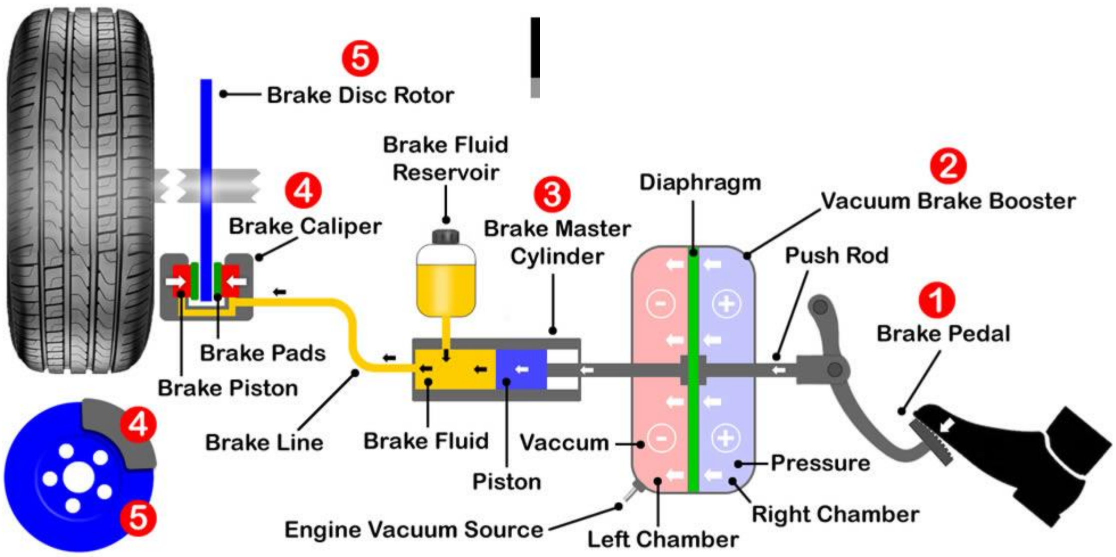

Figure 2.12: Conventional Hydraulic brake components (Winner et al., 2017)

Brake pedal: The brake pedal is part of the car that initiates the entire brake system in a vehicle. In automatic cars, it’s the pedal on the left side, and in manual cars, it’s the middle pedal. When you press down on it, all the components of your braking system swing into action. The foot pedal (accelerator, brake, or clutch pedal) has three important measurements as shown in Fig. 2.13. These are:

Free play: The free stroke of the brake pedal is to measure the distance traveled by the pedal before the master cylinder starts to act for the first time. Depress the pedal until you feel a slight resistance.

Pedal height: The brake pedal height is the travel distance between the brake pedal seat and the floor.

Reserve distance: The brake pedal reserve is the measured value from the floor of the vehicle to the top of the brake pedal when the brake is applied.

These three important pedal measurements work for all brakes. Accelerator and clutch pedal.

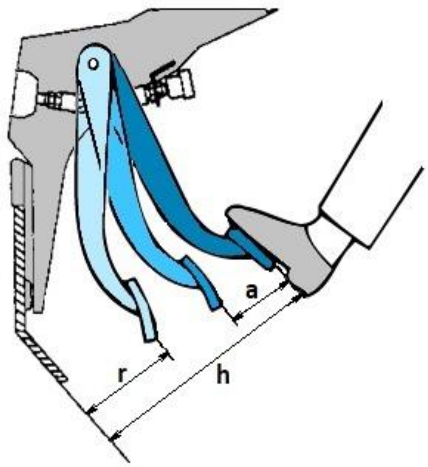

Figure 2.13: Pedal free play (a), Height (h), and Reserve distance (r)

(https://autoedu.info/en/auto-mechanic/brakes/hydraulic-braking-system/checking-brake-pedal/)

2.7.2 The Electronic Components

These parts unite to form a braking system that uses combined accelerator and brake pedal. They are merged with the parts of a traditional brake system. Which are:

- ✓ Arduino UNO
- ✓ Position sensor
- ✓ LED lights
- ✓ Dc motor.
- ✓ L293N Motor Driver Module

Arduino UNO Microcontroller - Arduino UNO is a widely used open-source microcontroller board based on the ATmega328P microcontroller and developed by Arduino.cc. In order to create and upload computer code to the physical board (the hardware boards are reasonably priced), Arduino comprises of both a physical programmable circuit board (commonly referred to as a microcontroller) and a piece of software called an IDE (Integrated Development Environment) that runs on your computer. (B-E-N, 2022).

The board features 14 Digital pins and 6 Analog pins. It can be powered by a USB cable or by an external 9-volt battery, though it accepts voltages between 7 and 20 volts. It's not allowed to use a power supply greater than 20 Volts as you will overpower and thereby destroy the Arduino.

The recommended voltage for most Arduino models is between 6 and 12 Volts. The pins on the Arduino are the places where it will connect wires to construct a circuit probably in conjunction with a breadboard and some wire. They usually have black plastic ‘headers’ that allow you to just plug a wire right into the board (makerspaces, 2018).

The Arduino Uno in Fig. 2.14 includes a variety of pins, each of which is identified on the board and has a particular purpose.

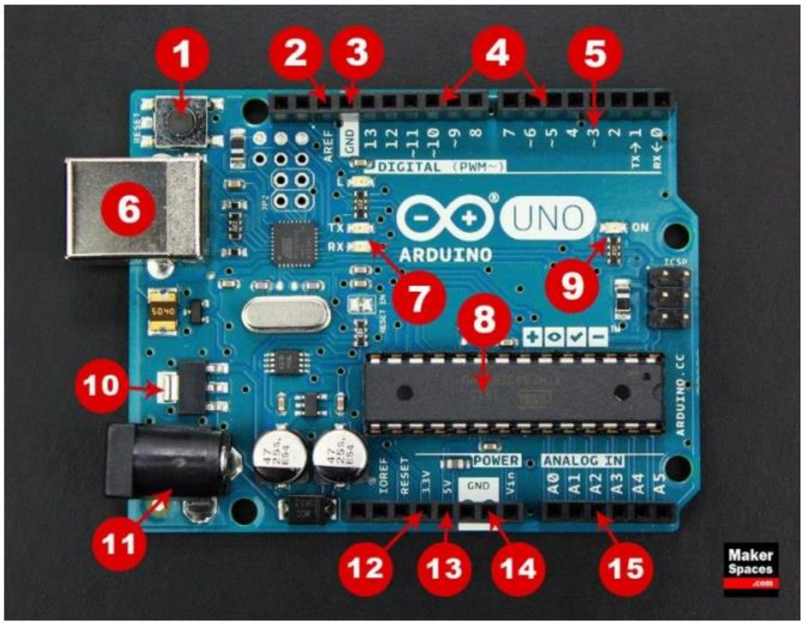

Figure 2.14: Arduino uno microcontroller (makerspaces, 2018)

Board Breakdown

Here are the components that make up an Arduino board and what each of their functions is.

1. **Reset Button** – This will restart any code that is loaded to the Arduino board.
2. **AREF** – Stands for “Analog Reference” and is used to set an external reference voltage.
3. **Ground Pin** – There are a few ground pins on the Arduino and they all work the same.
4. **Digital Input/Output** – Pins 0-13 can be used for digital input or output.
5. **PWM** – The pins marked with the (~) symbol can simulate analog output.
6. **USB Connection** – Used for powering up your Arduino and uploading sketches.
7. **TX/RX** – Transmit and receive data indication LEDs.
8. **AT mega Microcontroller** – This is the brain and is where the programs are stored.

9. **Power LED Indicator** – This LED lights up anytime the board is plugged into a power source.

10. **Voltage Regulator** – This controls the amount of voltage going into the Arduino board.

11. **DC Power Barrel Jack** – This is used for powering your Arduino with a power supply.

12. **3.3V Pin** – This pin supplies 3.3 volts of power to your projects

13. **5V Pin** – This pin supplies 5 volts of power to your projects.

14. **Ground Pins** – There are a few ground pins on the Arduino and they all work the same

15. **Analog Pins** – These pins can read the signal from an analog sensor and convert it to digital

And also, normally additional 3 or 4 voltage pins connect to the Arduino which are:

1 – Ground: connect to the ground on the Arduino.

2 – 5v Vcc: connect to the 5v on the Arduino.

3 and 4 – Signal pins: carries the trigger signal from the Arduino that activates the relay.

Light Emitting Diodes (LED) - An LED is a small light that operates at relatively low power. The LEDs have polarity, which means they only light up when you point legs correctly. The long leg is usually positive and should connect to a digital pin on the Arduino board. The short leg goes to GND; An LED bulb usually also has a flat edge on this side, as shown in Fig. 2.15. It only takes a few lines of code to make the LED light blink. The first thing we do is define a variable that holds the pin the LED is connected to, to make it easy to swap it for another pin. We use an integer variable (called int)(Robbins, 2012). Only in one direction, from the anode to the cathode, does current flow.

Figure 2.15:Light emitting diodes (Robbins, 2012)

Two LEDs have been used. The green LED shows that the brake is not being held while the red LED indicates that the car is braking. The dashboard in front of the driver is equipped with two LEDs (green and red). The red LED shows that the vehicle is braking, while the green LED indicates that the vehicle is in a safe condition (not braking).

Position Sensor - detects the position of something which means that they are referenced either to or from some fixed point or position. They can detect the movement of an object in a straight line using linear sensors or angular movement using rotational sensors. The most commonly used of all the “Position Sensors”, is the **potentiometer** because it is an inexpensive and easy-to-use position sensor. It has a wiper contact linked to a mechanical shaft that can be either angular (rotational) or linear (slider type) in its movement, and which causes the resistance value between the wiper/slider and the two end connections to change giving an electrical signal output that has a proportional relationship between the actual wiper position on the resistive track and its resistance value. In other words, resistance is proportional to position. A DC reference voltage is applied across the two outer fixed connections forming the resistive element. The output voltage signal is taken from the wiper terminal of the sliding contact as shown in Fig. 2.16. This configuration produces a potential or voltage divider-type circuit output which is proportional to the shaft position. Then for example, if you apply the voltage of say 5v across the resistive element of the potentiometer the maximum output voltage would be equal to the supply voltage at 5v, with the minimum output voltage equal to 0v. then the potentiometer wiper will vary the output signal from 0 to 10v, with 2.5v indicating that the wiper or slider is at its half-way or center position.

The output signal from the potentiometer is taken from the center wipe connection as it moves along the resistive track, and is proportional to the angular position of the shaft.

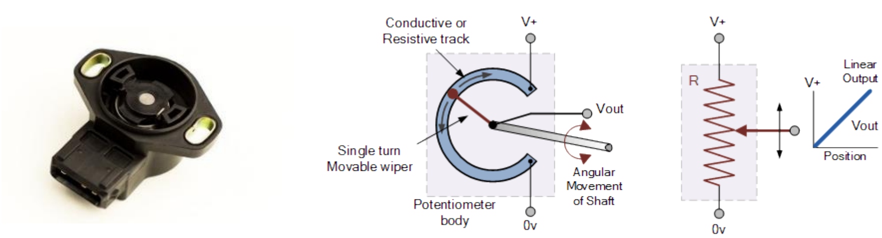

Source:https://www.electronics-tutorials.ws/io/io_2.html) (https://www.thomasnet.com/articles/instruments-controls/all-about-position-sensors/)

Figure 2.16: Potentiometric Position Sensor

Potentiometric Sensor has three pins. These are: Vcc, output, and ground pin

- ✓ **VCC**: The pin power the sensor as the reference voltage, typically with +5V

- ✓ **Output pin**: The pin which sends signal voltage to the Arduino so that it produces an output accordingly.
- ✓ **Ground:** The system's ground is connected to this pin.

The sensor's output is determined by the combined pedal's location; it is an analog voltage signal proportional to movement or position.

DC-motor- A DC motor is an electrical machine that converts mechanical energy into direct current and vice-versa. An electric motor is a machine, which converts electric energy into mechanical energy. Most electric motors operate through the interaction between the motor's magnetic field and electric current in a wire winding to generate force in the form of torque applied on the motor's shaft. Its action is based on the principle that when the current-carrying conductor is placed in a magnetic field (R. S. Khurmi, 2005). In this study, the stepper DC motor for motion control purposes to actuate the brake pedal by pressing the brake pedal through a lead screw has been used.

L293N Motor Driver Module

This L298N Motor Driver Module is a high-power motor driver module for driving DC and Stepper Motors. This module consists of an L298 motor driver IC and a 78M05 5V regulator. L298N Module can control up to 4 DC motors, or 2 DC motors with directional and speed control. The L298N Motor Driver module consists of an L298 Motor Driver IC, 78M05 Voltage Regulator, resistors, capacitor, Power LED, and 5V jumper in an integrated circuit. 78M05 Voltage regulator will be enabled only when the jumper is placed. When the power supply is less than or equal to 12V, then the internal circuitry will be powered by the voltage regulator, and the 5V pin can be used as an output pin to power the microcontroller. The jumper should not be placed when the power supply is greater than 12V and separate 5V should be given through a 5V terminal to power the internal circuitry. ENA & ENB pins are speed control pins for Motor A and Motor B while IN1& IN2 and IN3 & IN4 are direction control pins for Motor A and Motor B (Rittenberry, 2005).

In this study, the L293N motor driver module which is shown in Fig. 2.17 is used to control a single stepper motor.

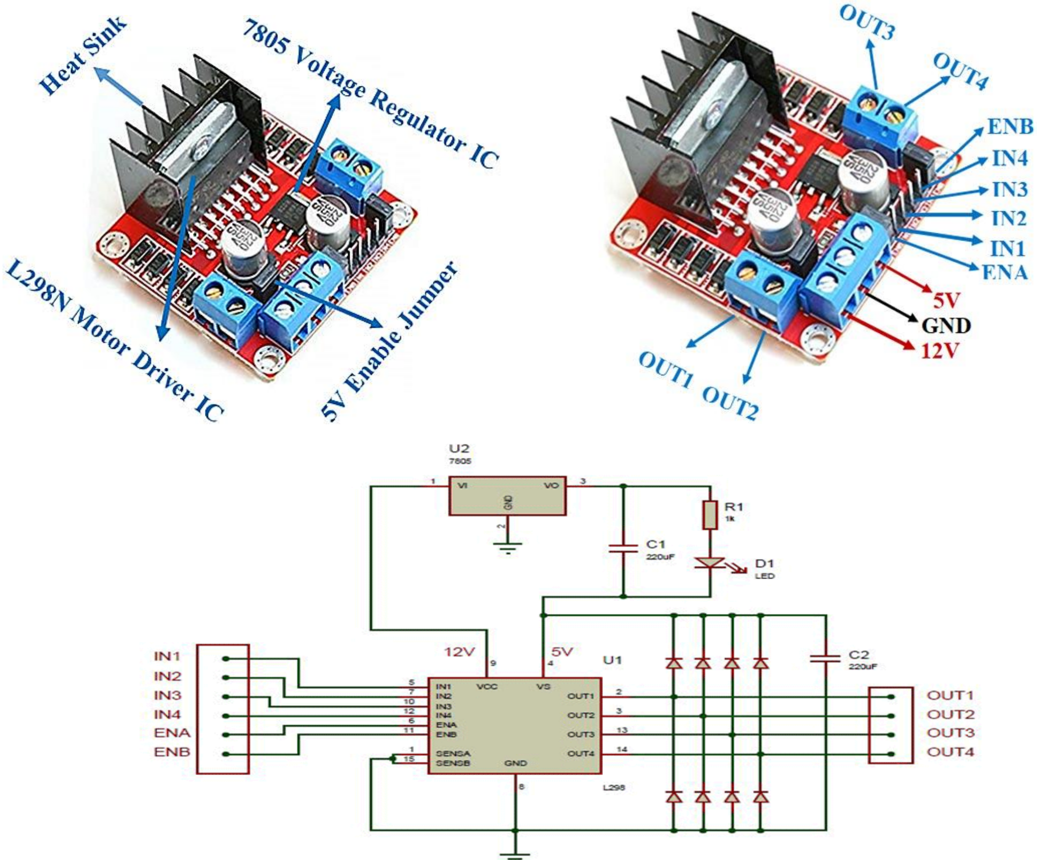

Figure 2.17: L298N-Module-Pinout and Internal-Circuit-Diagram

(https://components101.com/modules/l293n-motor-driver-module)

Resistor

A resistor is a passive two-end electrical component, and the resistor is implemented as a circuit component. Electronic circuits use resistors to reduce current, regulate signal levels, divide voltage, bias active components, and terminate transmission lines. High-power resistors can dissipate watts of electrical energy in the form of heat and can be used as part of a motor control, power distribution system, or generator test load. The resistance of a fixed resistor varies slightly with temperature, time, or operating voltage. Variable resistors can be used to tune circuit elements (such as volume controls and dimmers) or as heat, light, humidity, force, or chemical activity detection devices (R. S. Khurmi, 2005).

2.8 Working principle

The vehicle's engine is what kicks off the entire system. The sensor transmits a voltage signal to the controller when the pedal is close to the brake, and the controller uses the stepper motor to regulate the brake. The microcontroller won't get any signal and the brake won't be applied if the pedal is too far away. The working principle is shown in Fig. 2.18.

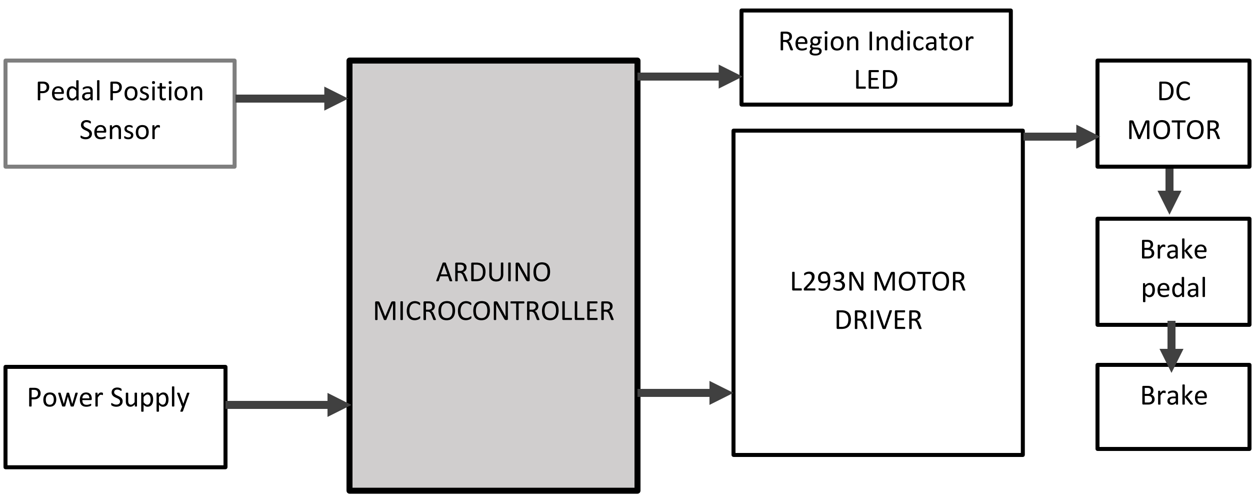

Figure 2.18: Working Principle of combined brake and accelerator pedal.

a. **Braking**: In this mechanism, the vehicle is in braking condition when the pedal is not pressed. It will first slowly disable braking. Half of the pedal play is given for braking in the combined pedal & no acceleration is taken place at this stage.
b. **Acceleration:** When the braking is completely disengaged, by further pressing the pedal we can throttle the vehicle. This can be achieved by setting the cable position to the point where the brake is completely released.

In general, Once the pedal is pressed the braking force is released, and when further pressed the car will accelerate. To apply the brake on the vehicle the operator has to slightly release the force off the brake pedal and in an emergency he/she has to take his foot off the pedal to apply sudden brakes.

2.9 Stopping distance of the vehicle

The distance required to stop a vehicle depends on its speed, weight, drivers' reaction distance, and braking distance in addition to the factors of energy, heat, and friction. The brake power required to stop a vehicle varies directly with its weight and the "square" of its speed. For example, if the weight is doubled, stopping power must be doubled to stop at the same distance. If the speed is doubled, the stopping power must be increased four times to stop at the same distance. When weight and speed are both doubled, stopping power must be increased eight times to stop at the same distance (Yared, 2019).

2.10 Research gap

All investigation stated above has their research gaps. Most of them are limited to manual (mechanical system for both braking and accelerating) braking and accelerating system using a single pedal which needs driver effort or force required to apply both brake and acceleration separately. Most of them involve ergonomic problems and others need the presence of an obstacle for automatic braking using ultrasonic sensors. Thus, the vehicle brakes while taking turn. However, the driver uses the conventional brake system (which does not provide a driving control that permits the quick and smooth transition from acceleration to braking, due to the need to transfer the foot from one pedal to another) to stop the vehicle in the absence of any obstacle. Thus, acceleration and braking cannot be done quickly.

The system also causes issues when the vehicles turn because a sensor could falsely indicate an obstruction and apply the brakes. The detection range of an object depends on its size, shape, and orientation, and curved objects or objects made of sound-absorbing materials like fabrics or non-woven materials reflect less energy back to the sensor. Granular materials' surface variations and/or angle of response may cause them to absorb sound or reflect it away from the sensor. In addition, both sensors and signals may be affected by atmospheric conditions like humid air, and dusty roads, which get damaged easily, since they are exposed or externally fitted and feed external signals. Furthermore, this system is futuristic and difficult to apply in a country like Ethiopia due to high traffic congestion.

In general, in most of the above-combined pedal investigations, they only focused on manual braking which needs driver effort (force application for both brake and accelerator application), and the other's autonomous braking which needs the presence of an obstacle to brake while the numbers of pedals are three (do not involve combined pedal system. Thus, acceleration and braking cannot be done quickly). So, this study aimed to fill the above gap by using the idea of reverse braking (i.e., the brake is applied as we release the combined pedal when it is in the braking region) using position sensor work with a combined pedal system in addition to the existing one. which may be highly useful for the signs stated above, especially for taxis that involves frequent start and stop in denser traffic condition in a country like Ethiopia.

CHAPTER THREE

MATERIALS AND METHODS

3.1 Place of study with geographical location (ASTU)

The study was conducted at Adama Science and Technology University (ASTU), which is 97 kilometers from Addis Abeba in Ethiopia's Oromia region.

3.2. Materials

When choosing the material, the following considerations are taken into account. These considerations include: - Material cost; - Material availability; - Material compatibility for the operating conditions; - Material strength, durability, machinability, and weldability. The best material is one which serves the required objectives.

Safety considerations should take priority over cost or usability concerns in pedal design since it is active safety and the most important driver vehicle interface. The other considerations are next to this based on design requirements.

In Table 3.1 the software applications utilized for electronic simulation in this thesis project are listed.

Table 3.1 lists the supplies (computer programs) needed for the simulation.

Software Tools	Unit	Quantity
Arduino uno Microcontroller	Set	01
DC motor (Stepper)	Pc	01
Position Sensor (Potentiometric)	Pc	01
Battery (12v)	Pc	01
LEDs (Green &Red)	Pc	02
Circuit/Jumper wires	Pc	--
Motor Driver (L293N)	Pc	01
Resistors (220 ohm)	Pc	02

Material Selections

a) Arduino Uno

The Arduino uno selected for this study is shown in Table 3.2 a detailed explanation of which is given in Chapter Two section 2.9.2.

Table 3.2: Arduino uno Specifications

Microcontroller	ATmega328P
Operating voltage	5v
Input voltage (Recommended)	7 – 12v
Input voltage (Limit)	6 – 20v
Digital I/O pins	14 (of which 6 provide PWM output)
Analog Input pins	6
DC per I/O pin	20Ma
DC for 3.3v pin	50Ma
Clock speed	16MHz
LED built-in	13
Length	68.6mm
Width	53.4mm
Weight	25g

https://en.wikipedia.org/wiki/Arduino_Uno

b) Motor Selection

In this study DC motor is selected as the actuator of the brake pedal based available power source which is 12v DC on most vehicles, also there are different types of DC motors used for control like a stepper and servo DC motors, based on the following conditions shown in Table 3.3.

Table 3.3: Application attributes for stepper versus servo motor

Application Requirements	Stepper	Servo
High torque at low speed (<1000rpm)	✓	
Open loop	✓	
Low voltage (<75v)	✓	
High voltage (400-480 +volts)		✓
Low speed (up to 1500rpm)	✓	
Medium to High speed (>1500rpm)		✓
In terms of cost	✓	
Motor life	✓	
Repeatability	✓	

Source:(Gill, 2016)

Once the strengths and weaknesses of servo and stepper motor systems are clearly understood. Stepper motors are a convenient solution due to their low cost, versatility, ease of setup, long motor life, high torque at low speeds, high overload safety, and simplicity of motors. Therefore, the stepper motor was preferred for this study's motion control.

Stepper Motors

A stepper motor shown in Fig. 3.1 is a special brushless DC electric motor that divides a complete rotation into several equal steps (movement in separate steps). Stepping is controlled by a computer for highly accurate positioning and speed adjustment. Computer-controlled stepping can be used to achieve highly accurate positioning and velocity regulators. Stepper motors are excellent for many precision motion control applications. Stepper motors are used in an array of precision moving and measuring devices such as nuclear power plants, aeronautics, robotics, automotive, medicine, manufacturing, etc. (Ahmed M.T. Ibrahim Al-Naib, 2019; Gill, 2016).

Figure 3.1: Stepper motor (Ahmed M.T.Ibraheem Al-Naib, 2019)

Types of stepper motor

By construction, the stepper motors come into three broad classes as shown in Table 3.4.

- ✓ Permanent Magnet Stepper
- ✓ Variable Reluctance Stepper
- ✓ Hybrid Step Motor

Table 3.4: Types of stepper motors

Type	Explanations	Image
Permanent Magnet Stepper	The magnetic poles of the rotor and stator of a permanent magnet stepper motor have no teeth. In contrast, the rotor has alternating north and south poles parallel to the axis of the rotor shaft. When the stator is energized, an electromagnetic pole is generated. The magnetic rotor is aligned with the stator magnetic field. Then the other stator in the sequence is powered, and the rotor moves to adapt to the new magnetic field. Therefore, when the stator is energized in a certain order, the stepper motor rotates at a certain angle	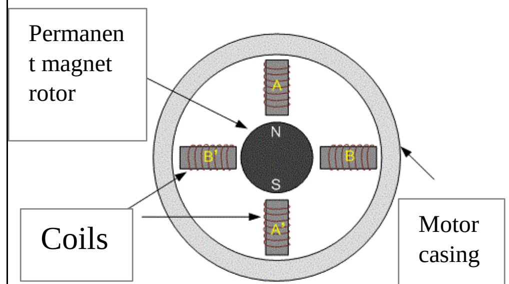 AA’ and BB’ are two phases
Variable Reluctance Stepper	The variable resistance stepper motor has a non-magnetic soft iron-toothed rotor. When the stator coil is energized, the rotor moves to have a minimum clearance between the stator and its teeth. Note that the teeth on the rotor are designed so that when aligned with a phase, they will be misaligned.	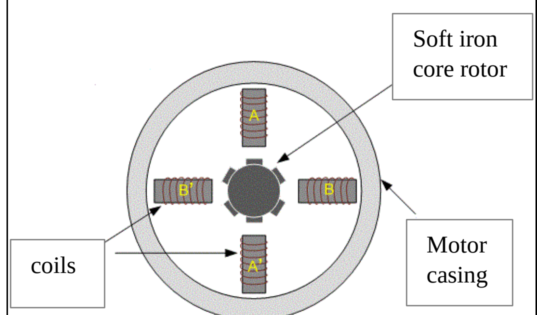 AA’ and BB’ are two phases

(Ahmed M.T.Ibraheem Al-Naib, 2019)

Unipolar and bipolar stepper motors

Unipolar SMs are collected of two windings; everyone has a center tap. The center taps are either carried outside the motor as two individual wires or coupled to each other inside and carried outer the motor as a single wire. A bipolar stepper motor has one winding per stator phase. A two-phase bipolar stepper motor has 4 leads in a bipolar stepper we don’t have a common lead like in a unipolar stepper motor. A bipolar stepper motor has an easy wiring arrangement but its operation is a little complex.

Comparison between unipolar and bipolar

The current runs through the whole coil instead only half coil as in a unipolar motor. As a result, the Bipolar motor will produce more torque than a unipolar motor of the same size. Compared to unipolar motors, the bipolar motor is uncomplicated in structure but necessitates a positive and negative source and an extra complex switching electric circuit. Therefore, bipolar stepper motors are selected for the automatic pedal-controlling system. The selection of the size of the stepper motor was made based on design analysis in section 3.4.2.

c) Selecting the best type of screw

The threading mechanism provides a means of generating linear motion by rotating either the screw or the nut in the assembly. A screw is a cylindrical element with a thread formed on it. The nut is the component that matches the screw. There are three main types of screw technology used in linear actuators: acme, ball, and roller. The difference lies in the design and operation of the matching nut, as well as the design of the shape of the screw (Tlomatic, 2021).

Acme Screws

The Acme screw has a thread form having a trapezoidal tooth shape that is typically rolled into a steel shaft. The thread form itself is very strong and linear force is transmitted to a solid nut from the sliding surfaces on the flanks of the thread form. The efficiency of a solid nut system is determined by the nut material and the lead, it can range from 20% to 40% and is relatively low compared to other screw technologies. However, the disadvantage of the low system efficiency is the increased motor torque input required in comparison to other screw technologies. Common nut materials include brass, bronze, self-lubricating plastics, resins, and metals (Tlomatic, 2021). See a typical Acme power screw in Fig.3.2.

Figure 3.2: Acme power screw (Tlomatic, 2021)

Acme Screw Advantages:

- ✓ Low cost, quiet operation, reduce or remove back driving

- ✓ Ideal for applications with slow to medium speeds, low-duty cycles, and low to medium force capacities.

Acme Screw Limitations

- ✓ Solid nut design may wear, increase backlash, and affect positioning.
- ✓ Lower efficiency ratings require higher input torque.
- ✓ Unpredictable service life.
- ✓ External factors such as environment can affect screw life

Summary

For most applications that require high force, repetitive cycles and long expected life a roller actuator and ball screw are used. The most common applications of ball and roller actuators include robots and aircraft. Acme screws provide a more reliable design for common applications. With no back-drive and low cost, this design is a very flexible solution for most automated linear motion applications. From the above explanation, the automatic vehicle pedal locking electric linear actuator use an Acme type screw because this linear electric actuator works with lower force and vertical actuation and it is low cost, quiet operation, and reduces or removes back driving.

3.3. Methods

The main data sources for this thesis work were secondary and primary data. Most of the thesis work data collection methods were based on the collection of secondary data. However, as primary data observation and oral questions were used somewhere accidents occurred during our study. However, this is not so much acceptable, instead, it is base for motivation for studying this problem and collecting secondary data. Secondary data was obtained from the Ethiopian Federal Police Commission, the Ministry of Transportation, and the Ethiopian Transport Authority. Moreover, different books, journals, articles, and reports publications were also conducted. A literature survey about the different types of combined pedals was the key methodology of this thesis. After reviewing the literature, the design of an appropriate combined pedal mechanism was carried out by using Solid work. The overall methodology followed in achieving the objectives of this thesis work is illustrated in Fig.3.3 in the form of a flowchart. The implementation of a combined acceleration and braking pedal for taxis, namely the Minibus 5L type, is the subject of this thesis work.

- ✓ Data gathering, organization, and analysis.
- ✓ Material choice.
- ✓ Component design, and analysis.
- ✓ Modeling, simulation, and motion analysis using Solid Works.
- ✓ Programming the system with Arduino software.
- ✓ Circuit schematic and simulation using proteus software.

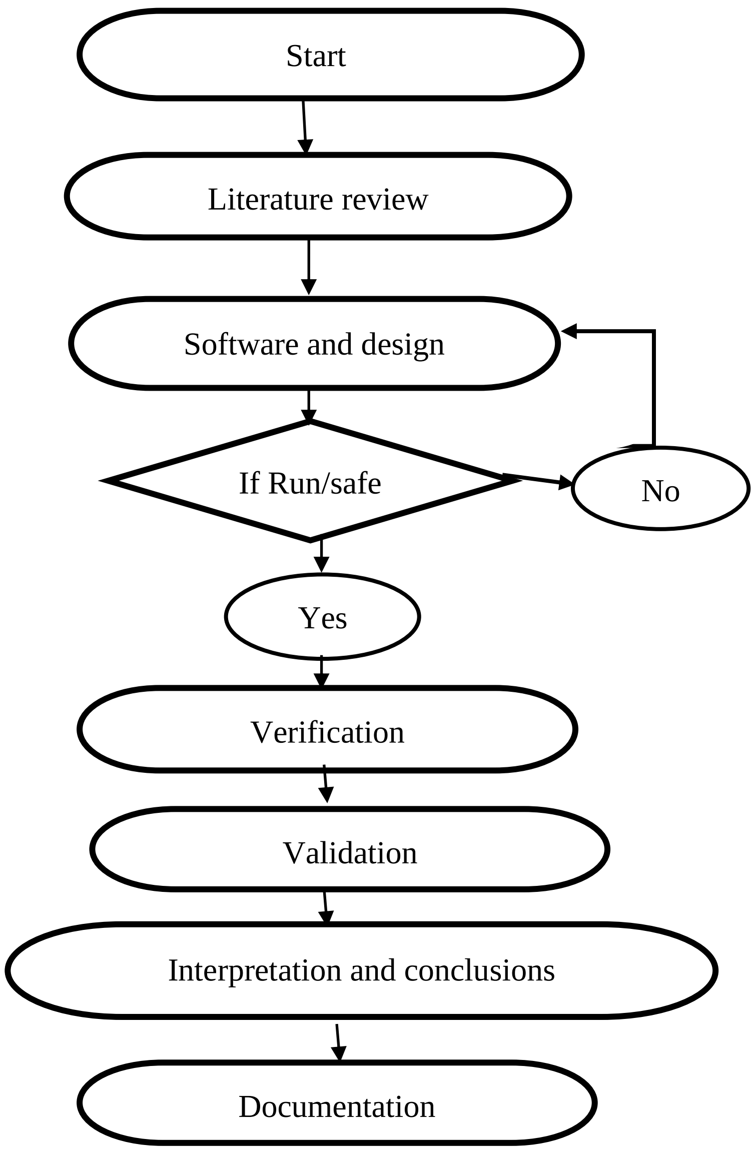

Figure 3.3: Flowchart methodology of the thesis

3.4. Analysis

Under this topic analysis of raw data, design analysis, modeling, and simulation of designed components and circuits was made.

3.4.1. Analysis of Row Data

Data from the four-year total traffic accident statistical data report from the Ethiopian Federal Police Commission show that road accidents are Ethiopia's leading source of mortality, serious injury, minor injury, and property damage. The report's four-year cumulative summary is displayed in Fig.3.4.

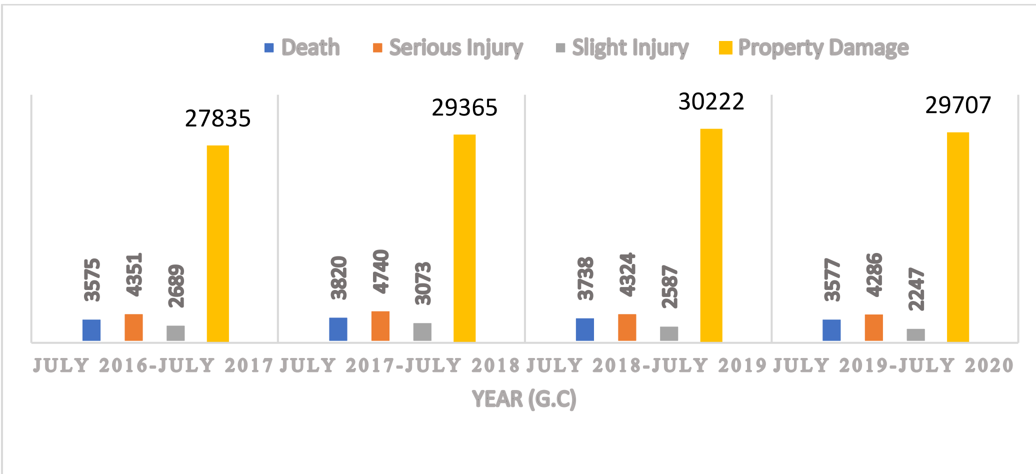

Figure 3.4: Analysis of Ethiopia's four-year total traffic accident record data

The majority of the criteria, according to the report, are rising yearly. This demonstrates how terrible traffic accidents are in Ethiopia and how they require immediate care.

In this study, the data from four years are first divided into three categories according to the functions of the vehicles. The following are these groups.

- ✓ All public means of vehicles
- ✓ All freight or cargo means of vehicles
- ✓ All machinery-type vehicles

All forms of public transportation: Bicycles, motorcycles, cars, station wagons, taxis, minibuses with up to 12 seats, medium buses with up to 45 seats, buses with more than 46 seats, three-wheeled Bajajs, and trains are included in this group. The analysis of four years' worth of traffic accidents involving public transportation is illustrated in Fig. 3.5.

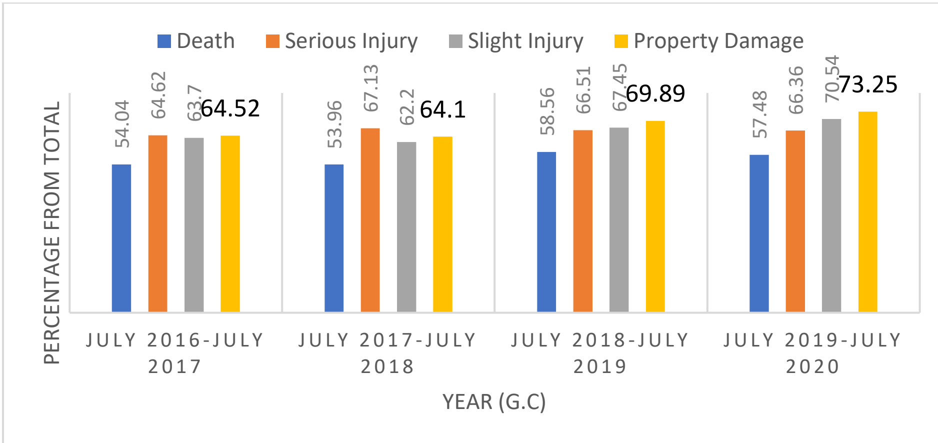

Figure 3.5: Four years of public means of vehicle traffic accient analysis

All cargo means of vehicles: Carts, pick-ups up to one ton, trucks between one and four tons, trucks between five and ten tons, and heavy tracks with trailers fall under this group. See Fig. 3.6 for a four-year analysis of freight vehicle traffic accidents**.**

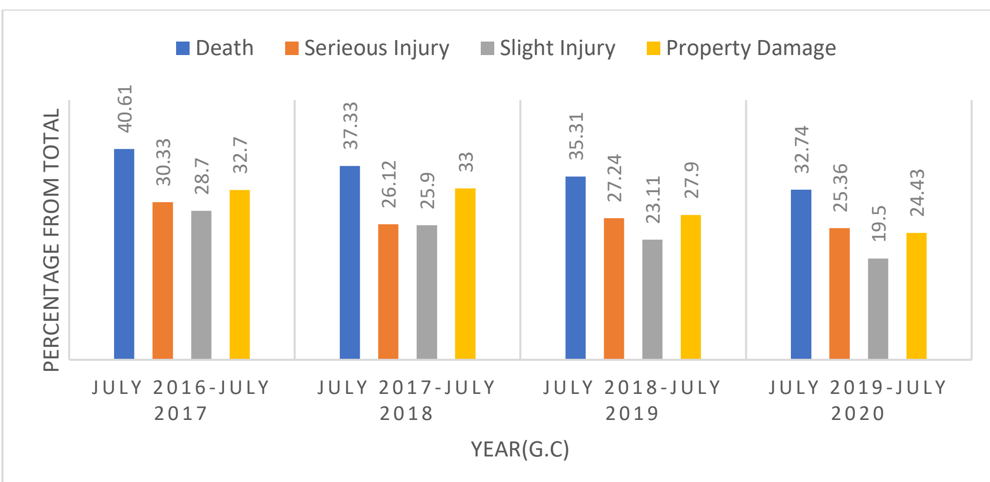

Figure 3.6: Examination of four years' worth of cargo vehicle accidents

All machines type vehicles: Construction vehicles and machinery vehicles fall under this category. Fig. 3.7, which is given , displays data from four years of traffic accident analysis for vehicles of the machinery type.

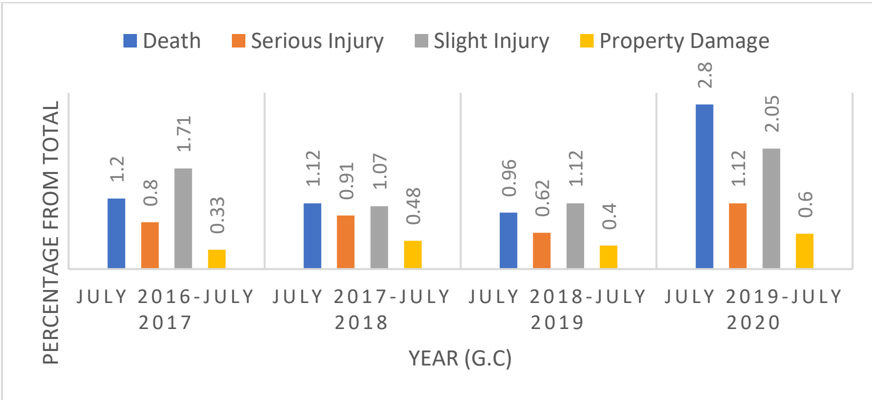

Figure 3.7: Analysis of four years' worth of accidents involving machinery-type vehicles

We use the average accident report from the previous four years to summarize the category analysis. as Fig. 3.8 illustrates.

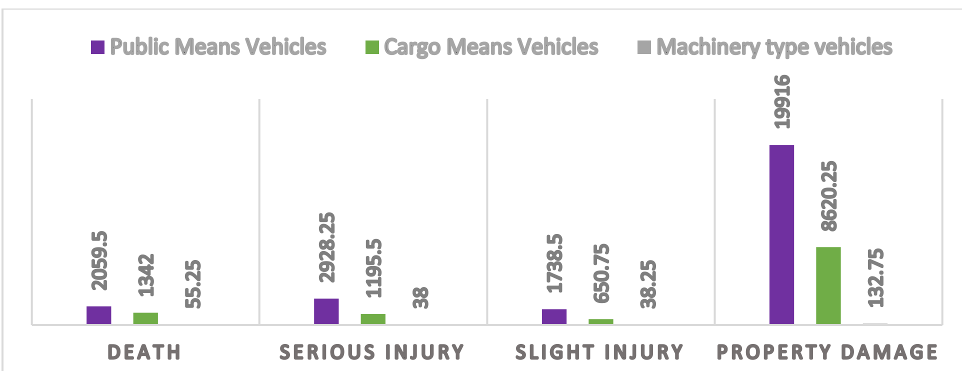

Figure 3.8: An investigation of traffic accidents in Ethiopia over a four-year period.

According to my analysis of the traffic report data from the previous four years:

- ✓ Public transportation accounts for the majority of fatalities, serious injuries, minor injuries, and property damage.
- ✓ Cargo transportation accounts for significantly less of these things.

Screening by category

According to the aforementioned statistical finding, public transportation vehicles are more responsible than cargo and machinery-type vehicles for causing fatalities, serious injuries, minor injuries, and property damage. Look at Table 3.5. As a result, this study emphasizes or pays attention to public transportation.

Table 3.5: Screening by category

Parameters (average)	Public means of vehicles	Freight or cargo vehicles	Machinery-type vehicles
Death	2059.5	1342	55.25
Serious injury	2928.25	1195.5	38
Slight injury	1738.5	650.75	38.25
Property damage	19916	8620.25	132.75
Rank	1	2	3
Remark	Selected	Not selected	Not selected

Therefore, for this study, public means of vehicles are selected.

Public means vehicles or public transportation options

This category also covers various vehicle kinds, so more research is required before choosing just one to focus on. As a result, this group is further divided into two of the following:

- ✓ Private vehicles and
- ✓ Public vehicles

Private vehicles: This category contains bicycles, motorbikes, station wagons, and automobiles. For four years traffic accident analysis for private vehicles sees in Fig. 3.9.

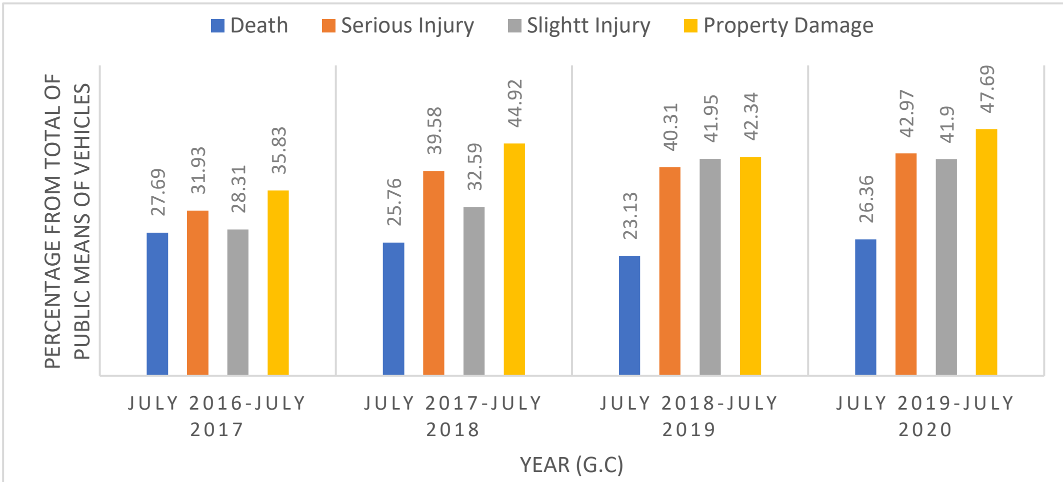

Figure 3.9: Four-year examination of private car traffic accidents

Public Vehicles: Taxis, minibuses with up to 12 seats, medium buses with 13 to 45 seats, buses with more than 46 seats, three-wheel bajajs, and trains are included in the category of public vehicles (see Fig. 3.10).

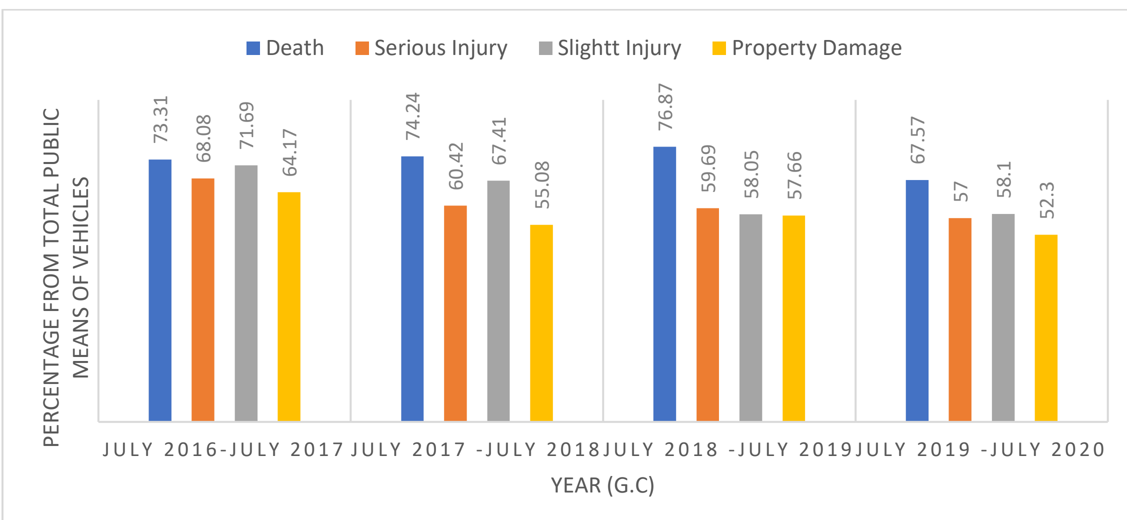

Figure 3.10: Public vehicle traffic accident analysis over four years

As demonstrated in Fig. 3.11, the private vehicle category has the lowest ratio of fatalities, major injuries, minor injuries, and property damage as compared to public vehicles throughout the course of four years of statistical data analysis.

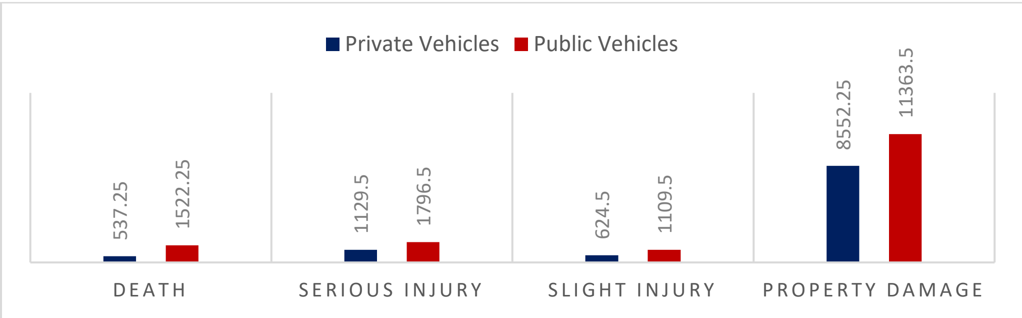

Figure 3.11: Analysis of four years' worth of traffic accidents by kind of vehicle (private and public)

Sub-category Screening

Sub-category screening is shown in Table 3.6.

Table 3.6: Screening by subcategory

Parameters	Private Vehicles	Public Vehicles
Death	537.25	1,522.25
Serious injury	1,129.5	1,796.5
Slight injury	624.5	1,109.5
Property damage	34,209	11,363.5
Rank	2	1
Remark	Not selected	Selected

Therefore, this study focused on public vehicles. Shared vehicles include a variety of vehicles. Thus, the research needs further analysis to choose one type of vehicle. So, this category is further divided into six which are:

- ✓ Taxis
- ✓ Mini busses up to 12 seats
- ✓ Medium busses from 13 -45 seats
- ✓ Buses above 46 seats

- ✓ Three-wheel bajaj
- ✓ Trains

Taxis

Figure 3.12 shows how much of the total number of deaths, serious injuries, minor injuries, and property damage is caused by taxis.

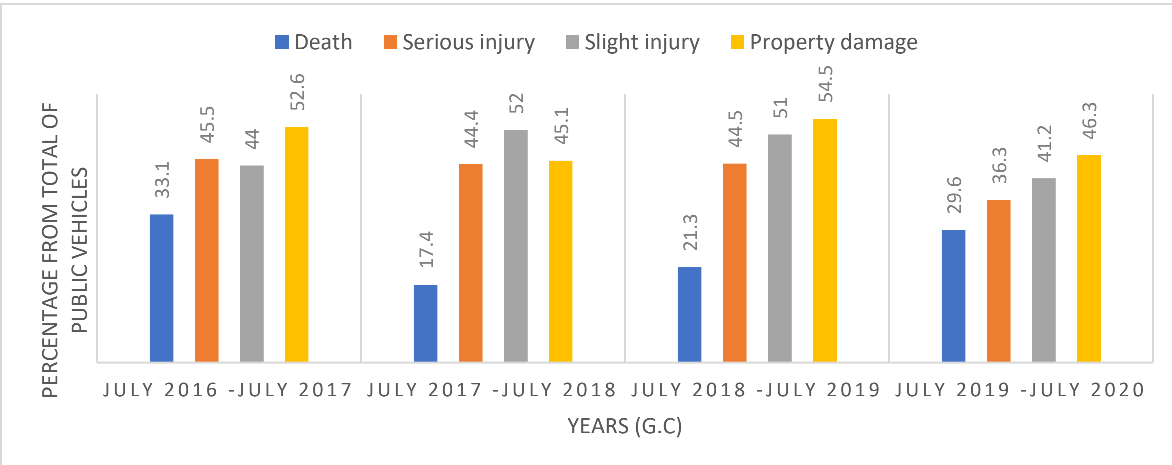

Figure 3.12: Four years traffic accident analysis for Taxis

Mini busses up to 12 seats

Fig 3.13 shows how much of the total number of deaths, serious injuries, minor injuries, and property damage is caused by minibusses with up to 12 seats.

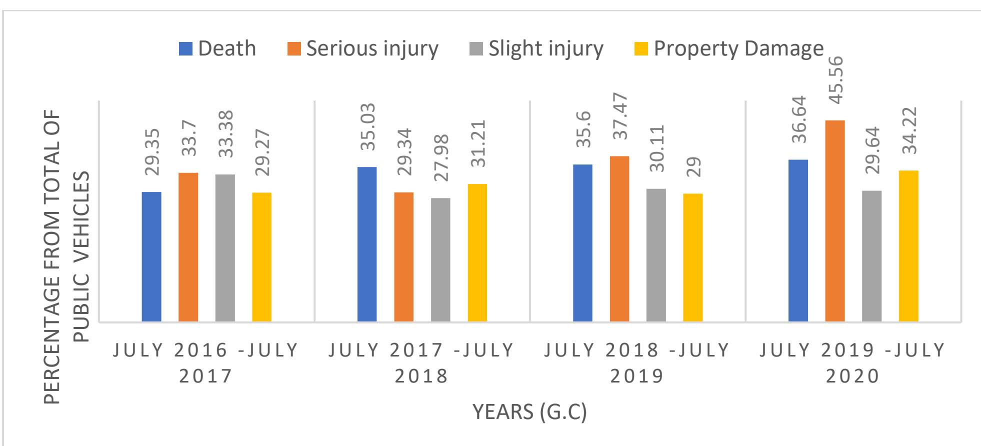

Figure 3.13: Four years traffic accident analysis for mini busses up to 12 seats

Medium busses from 13 -45 seats

Fig 3.14 shows how much of the total number of deaths, serious injuries, minor injuries, and property damage is caused by medium buses with 13-45 seats.

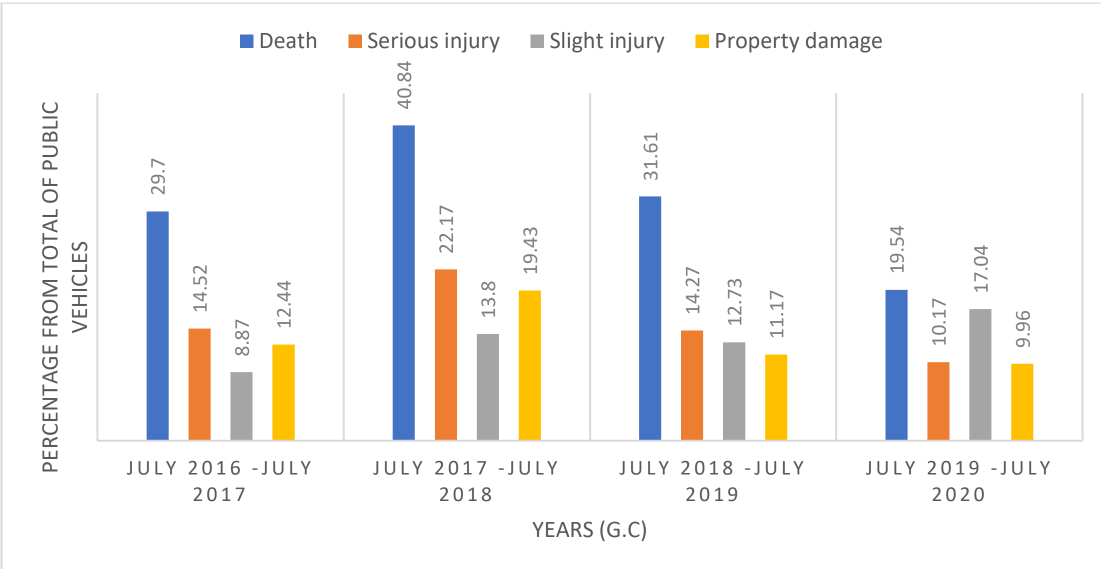

Figure 3.14: Four years traffic accident analysis for medium busses from 13 -45 seats

Buses having above 46 seats

Fig 3.15 depicts the percentage of deaths, serious injuries, minor injuries, and property damage caused by buses with more than 46 seats in comparison to all public vehicles.

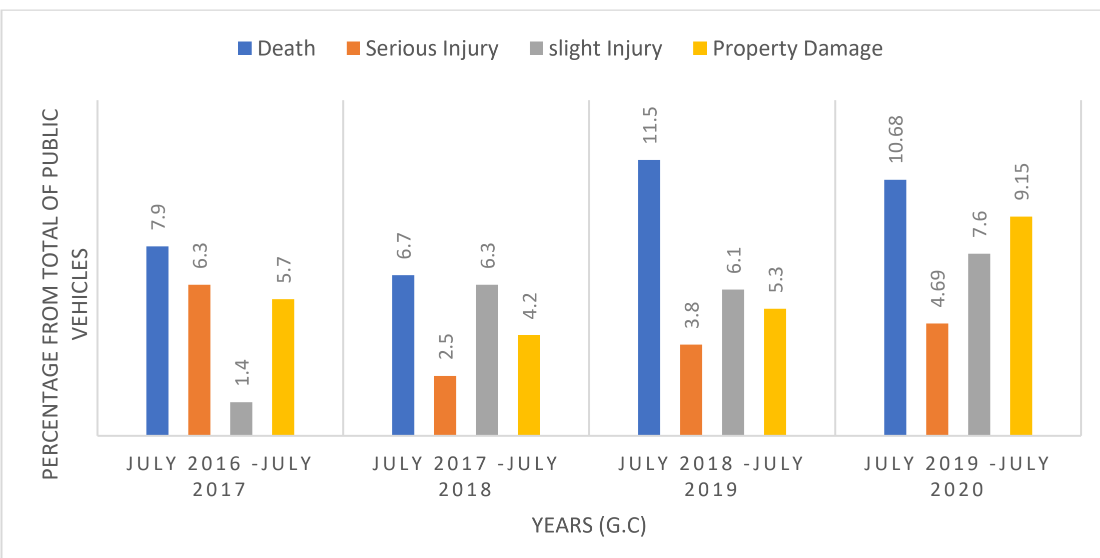

Figure 3.15: Four years traffic accident analysis for buses above 46 seats

Three-wheel bajaj

Recording of deaths, serious injuries, injuries, and property caused by three-wheeled bajaj began in 2018/2019, and no damage was recorded this year. However, death, serious injuries, minor injuries, and property damage in 2019/2020 are 49, 54, 42, and 45 respectively.

Trains

A statistical data reports from the Ethiopian Federal Police Commission on total traffic accidents show that trains are subjected to one (1) slight injury in 2017/2018, again three (3) death in 2019/2020. Therefore, bajaj and trains are responsible for very little cause of the accident. Fig. 3.16 shows the average number of bus fatalities, serious injuries, injuries, and property damage for each public transport vehicle.

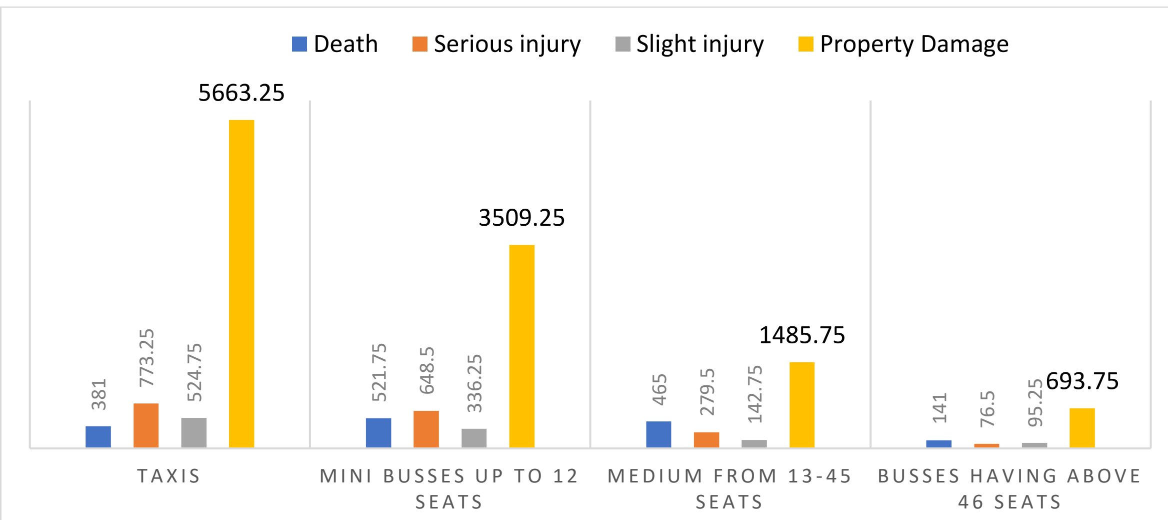

Figure 3.16: Four years average traffic accident analysis by each public vehicle

Sub-sub-category screening

For sub-sub-category screening see Table 3.7.

Table 3.7: Sub-sub-category screening

Parameters (Average)	Taxis	up to 12 seats (minibusses)	Medium-sized buses with 13-45 seats	Bus has more than 46 seats
Death	381	521.75	465	141
Serious injury	773.25	648.5	279.5	76.5
Slight injury	524.75	336.25	142.75	95.25
Property damage	5663.25	3509.25	1485.75	693.75
Rank	1	2	3	4
Remark	Selected	Not selected	Not selected	Not selected

Therefore, among the modes of public transportation, Taxis were chosen for this study. For shared vehicle-related fatalities, serious injuries, minor injuries, and property damage. Fig 3.17 displays the percentage of taxi fatalities, serious injuries, minor injuries, and property damage.

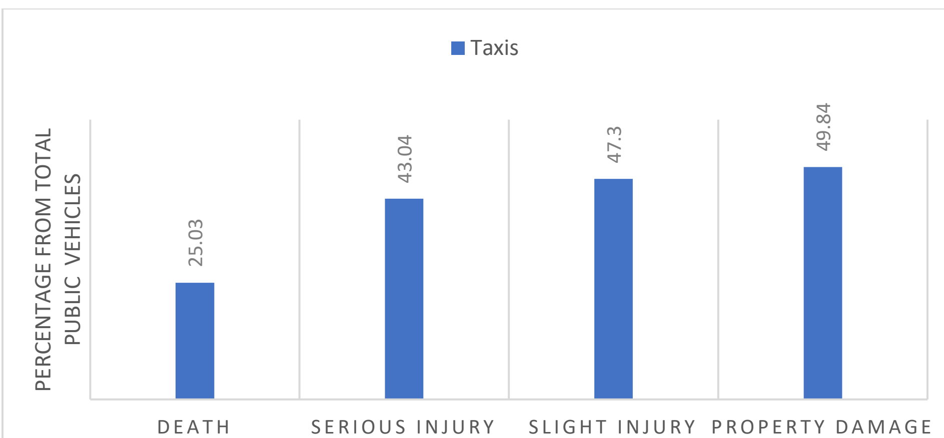

Figure 3.17 The proportion of fatalities, serious injuries, injuries, and property damage that taxis cause.

From above, 25.03% of deaths, 43.04% of serious injuries, 47.3% of minor injuries, and 49.84% of property damage are caused by taxis from shared vehicles.

Property damage

All property damage in Ethiopia

According to the Triennial Traffic Accident Statistics Report of the Ethiopian Federal Police Commission, traffic accidents are a major and gradually increasing cause of property damage. Due to these disasters, our country Ethiopia lost billions of birrs. For three years aggregate property damage report in Ethiopia see Table 3.8.

Table 3.8: Property damage report over three years.

Year	In ETB, all property damages
July 2016 – June 2017	1,187,486,803.00
July 2017 – June 2018	920,771,314.80
July 2018 – June 2019	872.884,881.00

Property damage over three years is (See Fig. 3.18).

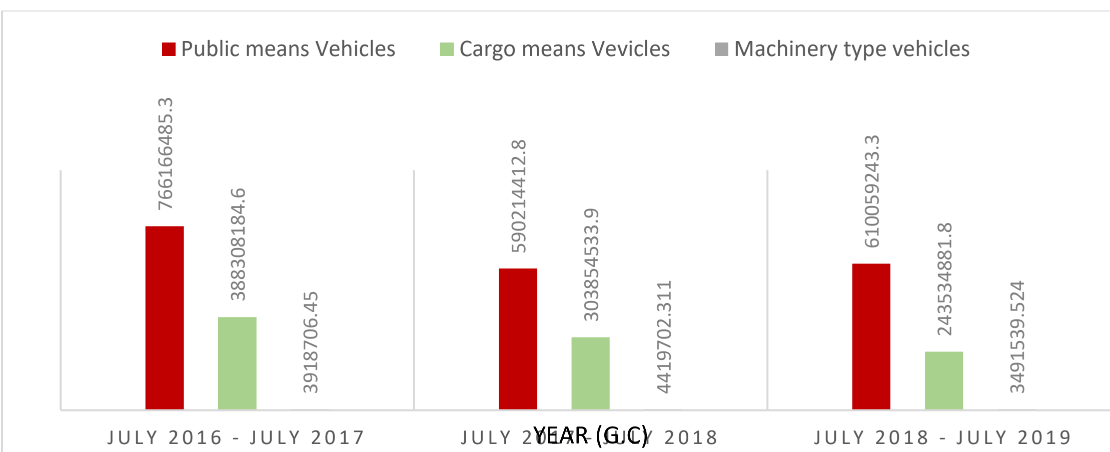

Figure 3.18: Property damage over three years

Here, the result shows that shared vehicles take more responsibility for property damage than others.

Property damage caused by public means vehicles

Based on this, we have two classes. These are:

- ✓ Private Vehicles: Includes bicycles, motorcycles, cars (automobiles), and station wagons
- ✓ Shared (public) vehicles: taxis, minibusses with up to 12 seats, medium-sized buses with 13-45 seats, buses with more than 46 seats, and trains. For comparison see Fig. 3.19.

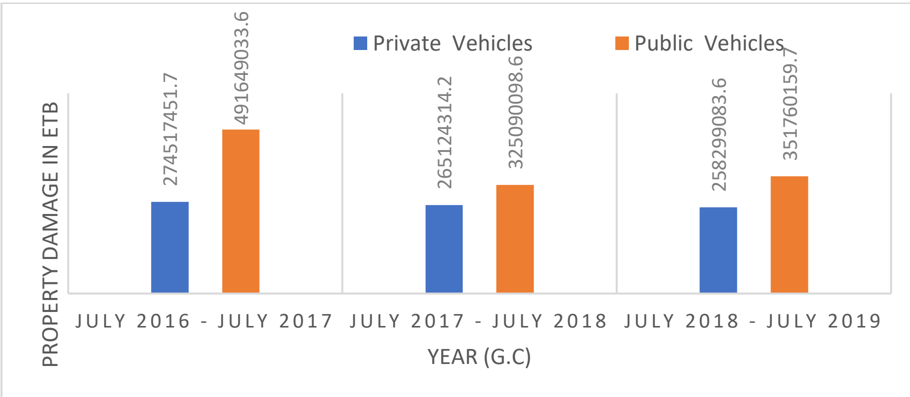

Figure 3.19: Property damage comparison of public transport vehicles

The result shows that shared vehicles receive more credit than private vehicles.

Property damage caused by taxis

From a research point of view, it is very important to know the damages caused by taxis because most of our passengers prefer taxis because they are affordable and the best public transport available (See Fig 3.20).

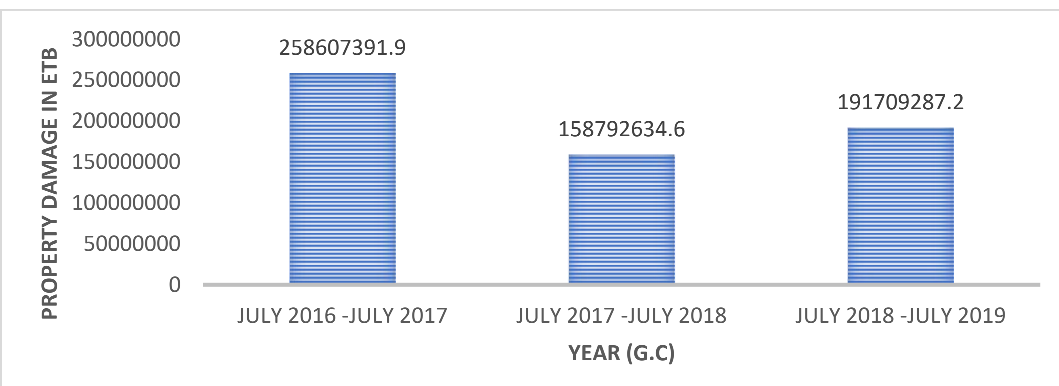

Figure 3.20: Propert damage due to taxis

The result indicates that taxis need serious attention. Because the three-year average property loss is *Two Hundred Three Million Thirty-Six Four Hundred Thirty-Seven and Nine-Tenths Birr* (203,036,437.9 ETB), which is equivalent to the budget needed to build several full-cycle primary schools in remote areas of the country.

Analysis related to accidents caused by vehicle side

The two (2) years of data collected from the Federal police commission show that the causes of traffic accident mainly involve Vehicle-related causes such as brake inefficiency, steering problem, tire explosion, and other tire problem. Driver related causes such as: using alcohol, using cocaine, driving out of right hand, not giving way to another vehicle, not giving way to pedestrians, not keeping distance, not following by keeping distance, overtaking on the tip of a bumpy road, overtaking on a curve, sharp turn after overtaking, overspeed, overtaking by unallowed manner, taking a turn in an unallowed manner, ignorance of traffic police command, refusion to wait for a traffic light, refusion to consider stop traffic sign, refusion to consider give way traffic sign, Improper takeoff, Improper parking, driving with poor healthy (tired/sleep), showing unnecessary signals, overloading, In addition to external causes such as road condition, pedestrians' problem, and other unknown causes. For this study, the analysis was carried out only by considering causes from the vehicle side.

According to the report, a summary of the two years is given in Fig 3.21.

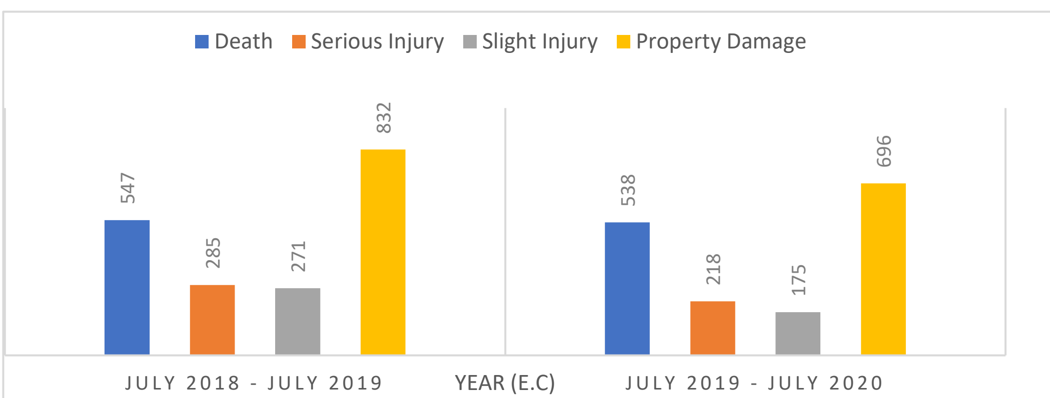

Figure 3.21: Two years aggregate causes from vehicle side in Ethiopia

In this study, the analysis starts by categorizing all causes registered from the vehicle side in two years of data into four categories based on individual causes registered from vehicles. These categories are:

- ✓ Steering problem,
- ✓ Tire explosion,
- ✓ Brake inefficiency and
- ✓ Other tire problem

Accident causes due to Steering problems and output

The two years traffic accident analysis due to the steering problem is shown in Fig. 3.22.

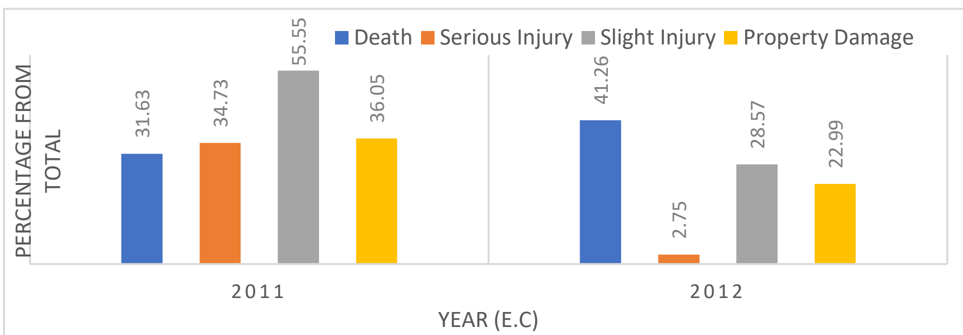

Figure 3.22: Two years accident report analysis caused by steering problem in Ethiopia

Accident causes due to Tire explosion and output

The two years traffic accident analysis due to tire explosion is shown in Fig. 3.23.

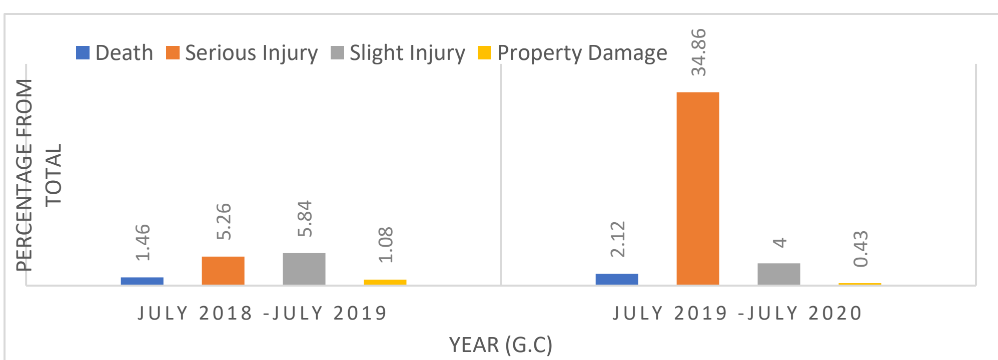

Figure 3.23: Two years accident report analysis caused by tire explosion in Ethiopia

Accident causes due to Brake inefficiency and output

The two years traffic accident due to a tire explosion is shown in Fig. 3.24.

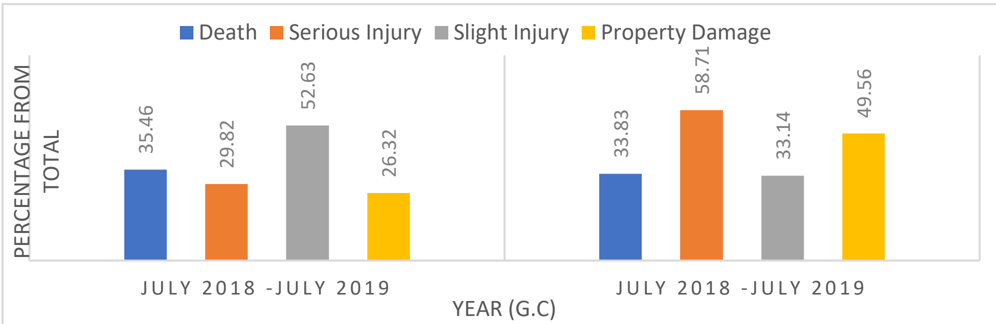

Figure 3.24: Two years accident report analysis caused by brake inefficiency in Ethiopia

Accident causes due to other tire-related problems and output

The two years traffic accident due to other tire problems is shown in Fig. 3.25.

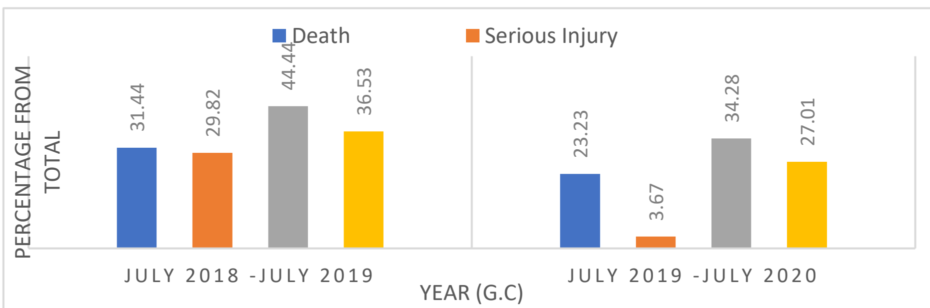

Figure 3.25: Two years accident report analyses caused by other tire-related problems in Ethiopia

To generalize the category analysis, we can make the percentage of two years traffic accident report. as shown in Fig. 3.26.

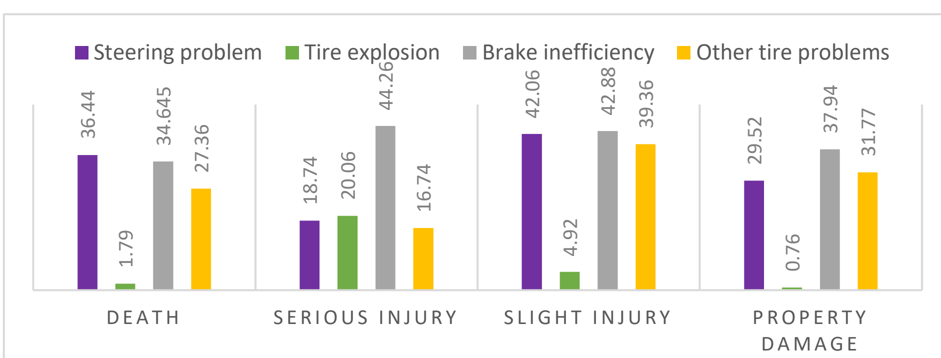

Figure 3.26: The average two years traffic accident analysis registered on the vehicle side in Ethiopia.

From the above two years of traffic report analysis, it was found that:

- ✓ Vehicle brake inefficiency is the leading cause of death, serious injury, minor injury, and property damage.
- ✓ Vehicle tire burst cause relatively fewer deaths, serious injuries, minor injuries, and property damage compared to others.

In general, above brake inefficiency is responsible for 36.44% of death, 18.74% of serious injuries, 42.06% of slight injuries, and 29.52% of property damage caused by the vehicle side (See Appendix C).

Vehicle Statics in 2013

According to data taken from the information communication technology directorate. (See Table 3.9).

Table 3.9: Ethiopian vehicle statics.

<table>
<tr><td>Vehicles category</td><td>Registered</td><td colspan="2" rowspan="2">Percentage from</td></tr>
<tr><td>Total vehicles number</td><td>1339005</td></tr>
<tr><td>Public means vehicles</td><td>825866</td><td>All vehicles registered</td><td>61.67%</td></tr>
<tr><td rowspan="2">Public transport vehicles</td><td rowspan="2">298095</td><td>Total number of vehicles</td><td>22.26%</td></tr>
<tr><td>Total public means</td><td>36.1%</td></tr>
</table>

From the point of view of the research, it is very important to know the area where there is a lot of public transport. According to data taken from the information communication technology directorate the region in which a high number of public vehicles is shown in Fig. 3.27.

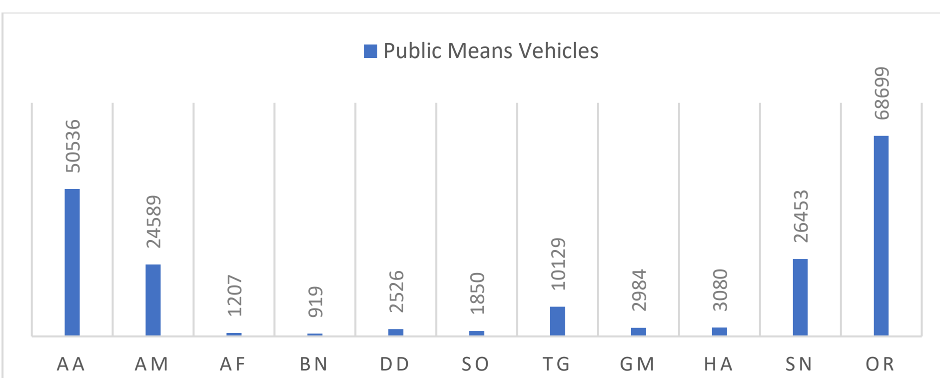

Figure 3.27: Region in which public means vehicles is high.

In comparison with their geographical coverage public transportation (taxis) is high in Addis Ababa. As a result, a city like Addis Ababa is a critical application area in this study due to congested traffic conditions.

3.4.2 Design Analysis, Modeling, and Simulation

Based on the analysis of the original data presented in Section 3.4.1, taxis cause 25.03% of deaths, 43.04% of serious injuries, 47.3% of minor injuries and 49.84% of property damage caused by shared vehicles. Moreover, data from the Ethiopian Police Commission shows that brake failure causes 36.44% of deaths, 18.74% of serious injuries, 42.06% of minor injuries, and 29.52% of deaths, serious injuries, minor injuries, and property damage. damage to the side of the vehicle (see Appendix C). Due to high traffic congestion, it is difficult to control two pedals (brake and accelerator pedals) with a single foot. Therefore, to complete this work the vehicle must be specified.

Toyota 5L 2000 Model minibus shown in Fig. 3.28 is selected because of its higher number and used for public services as a taxi. See the general specification of the Toyota 5L in Table 3.10.

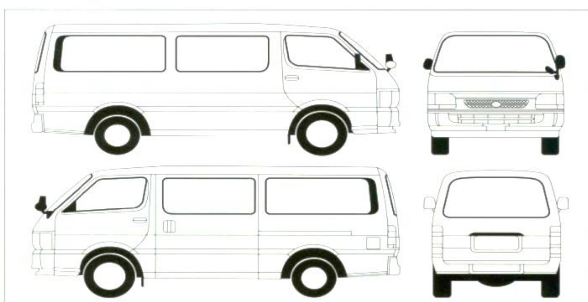

Figure 3.28: TOYOTA 5L model minibus

(http://www.toyota.co.jp/jpn/company/history/75years/vehicle_lineage/catalog/60015447/html5m.html#page=28)

Table 3.10: Vehicle Specification

<table>
<tr><td colspan="2">Vehicle type</td><td>TOYOTA 5L</td></tr>
<tr><td colspan="2">Model Code</td><td>KG-LH172V</td></tr>
<tr><td colspan="2">Engine</td><td>Diesel, SOHC, Straight-4, vertical, Displacement, 3.0 L, 2,986 cm3 (182.20 cu in), Firing (injection) order Mechanical (1-3-4-2).</td></tr>
<tr><td colspan="2">Compression ratio</td><td>22.2:1</td></tr>
<tr><td colspan="2">Maximum power</td><td>91 PS (67 kW; 90 HP) at 4,000 r.p.m</td></tr>
<tr><td colspan="2">Maximum torque</td><td>191 Nm (19.5 kg*m; 141 ft*lb.) at 2,400 r.p.m</td></tr>
<tr><td colspan="2">Tire size</td><td>Front tires (195R15−6PRLT), Rear tires 195R15−8PRLT</td></tr>
<tr><td colspan="2">Minimum ground clearance</td><td>200mm</td></tr>
<tr><td colspan="2">Wheelbase</td><td>2570mm</td></tr>
<tr><td colspan="2">Front overhang</td><td>1050mm</td></tr>
<tr><td colspan="2">Rear overhang</td><td>1075mm</td></tr>
<tr><td colspan="2">Dimensions (width x length x height)</td><td>1690 x 4690 x 1980 mm</td></tr>
<tr><td colspan="2">Allowable maximum speed</td><td>100Kmph</td></tr>
<tr><td colspan="2">Maximum payload</td><td>1250 kg</td></tr>
<tr><td colspan="2">GVW</td><td>2800kg</td></tr>
<tr><td colspan="2">Electricals battery</td><td>12 volts, 150Ah</td></tr>
<tr><td rowspan="3">Brake Pedal</td><td>Free play</td><td>1-6mm</td></tr>
<tr><td>Height</td><td>162mm (average measured value)</td></tr>
<tr><td>Minimum pedal reserve distance with the pressure of 294N</td><td>115mm (average measured value)</td></tr>
<tr><td colspan="2">Driver seat</td><td>Adjustable driver seat</td></tr>
<tr><td colspan="2">Brakes</td><td>Both rear and front brakes are hydraulic brake</td></tr>
</table>

Source:https://www.beforward.jp/toyota/hiace-van/bf63992/id/57830/, https://www.engine-specs.net/toyota/5l.html, https://toyota.dreamhosters.com/pages/hiace-tmc/spec_van_standard.php.

Aoki measured the braking force of 60 men, 54 high school students (16 years old), and 37 disabled people of both sexes in a vehicle model. The author concluded that the resistance of the brake pedal should be less than 294 N and the optimal 196 N. If the pedal is pressed by the ankle joint, the resistance should be less than 196 N. According to Musta, the resistance of the accelerator pedal must be in the range of 36-53 N and the resistance of the brake pedal should be less than 267 N. The author briefly described the experiments that led to the recommendations. Nineteen participants were instructed to reproduce different force levels using multiple foot controls. The force participants thought they would exert on the pedals (intended force) was compared to the actual forces they exerted. The results showed that when the target force is less than 29 N, the accurate perception of the force level is lost, and when the target force is greater than 89 N, the level of leg fatigue increases. In addition, according to the author, a force of 36 N was calculated as the force level at which the foot rests on the gas pedal. (Xi et al., 2018). Researchers have concluded that the maximum active pedal force varies from 136.3 N to 387 N (Macuzic & Lukić, 2019). From the research of the above researchers, the maximum pedal force applied to this combined pedal is as follows.

- ✓ Suppose the maximum force required to step on the brake pedal is 294N.
- ✓ The maximum force required to apply the accelerator pedal is 89N.

A. Design of electric linear actuator

Therefore, the total force required by the linear electric actuator is 294N to depress the brake pedal. The components should be designed based on this force.

Electric linear actuators have various components as shown in Fig. 3.29. The inner tube is known as the extension tube or the motor tube. This tube is attached to the threaded drive nut and expands and retracts as the nut moves along the axis of rotation. The lead screw/rotary screw/lifting screw of the linear actuator rotates to extend or retracts the inner tube nut/tube, creating a linear motion. The drive nut can be tapered or spherical and connected to the inner tube and moving along the main shaft or rotary screw. A nut is a component that allows the inner tube to extend or retract. Using a gear, it is possible to decrease or increase the speed between the drive of the drive mechanism and the speed of the inner tube of the driven parts. The motor is where all the power is generated for the electric linear actuator (Team, 2018).

The motor housing contains all the internal parts of the gear motor without leaving anything exposed to external damage.

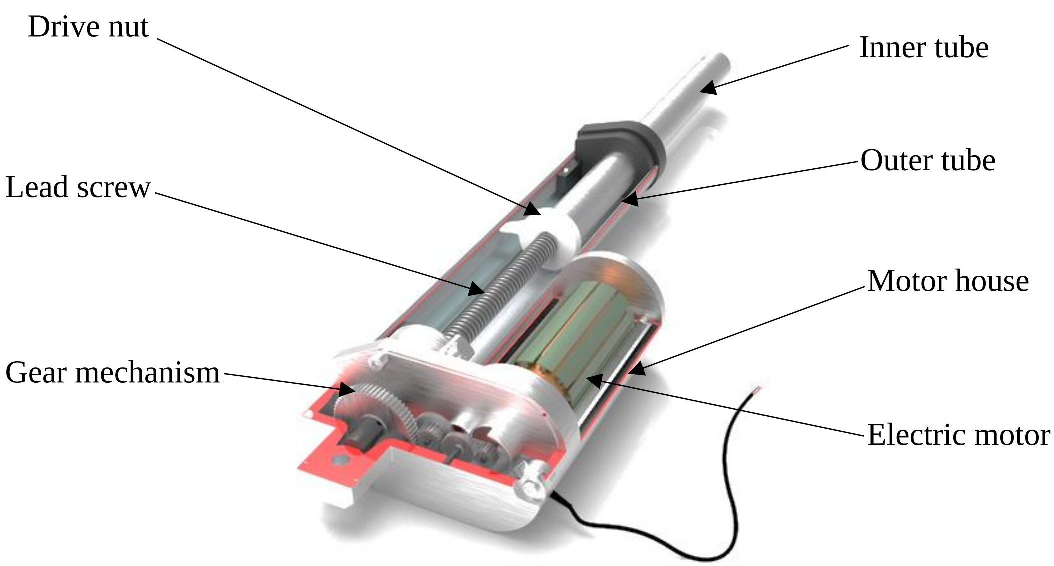

Figure 3.29: Linear actuator exploded view (Team, 2018)

i. Design of brake pedal actuator power screw

A screw is used as a coupling in a machine to convert rotational motion into linear motion. Threads are formed by cutting continuous spiral grooves on a cylindrical surface. The power screw is composed of two main parts: a screw and a nut, which can be operated when the Screw rotates in bearings and the nut moves axially, the screw rotates also moves axially while the nut is kept fixed and nut rotates and the screw moves in axial direction Power screws have the following advantages: (Khurmi, R.s.,&Gupta, 2005).

- ✓ The power screw has a large carrying capacity.
- ✓ The power screw is small in size and compact in structure.
- ✓ The design of the power screw is simple.

The screws are usually made from C30 or C40 steel. See the property of carbon steel in Table 3.11. Since the failure of the power propellers can lead to a serious accident, a higher safety factor is required. Nuts are made of a softer material than screws, so if they fail at all, the nut will fail, not the screw, which is more expensive and also difficult to replace. For the manufacture of nuts, plastic, bronze, or copper alloys are used. For steel screw and bronze nut. The values of the safety factor for the ultimate strength of soft materials and alloys are about six.

Table 3.11: Mechanical properties of carbon steel of the SAE1030 (Khurmi, R.s.,&Gupta, 2005)

Properties	Tensile strength	Yield Strength	Bulk modulus	Shear modulus	Elastic modulus	Poisson's ratio
Metric	525 MPa	440	140Mpa	80Gpa	200GPa	7872kg/m^3

The maximum force required to depress the brake pedal is 194N. Suppose the material, coefficient of sliding friction, safety factor, and bearing pressure for the brake pedal force screw are let:

- P = pitch
- d_o = Major diameter
- α = Helix angle
- φ = Friction angle
- w = load to be lifted
- μ = coefficient of friction
- h = Thread depth
- σ = Axial stress
- d_c = Minor diameter
- d = pitch diameter
- l = lead
- n = number of engaged Thread

The axial stress in the body of the power screw due to load W is

$$\sigma=\frac{W}{A}=\frac{4W}{\pi(d_c)2}\text{...} (3.1)$$

$$\sigma=\frac{\text{tensile stress}}{\text{FOS}}\text{ ....} (3.2)$$

$$d_c=\sqrt{\frac{4\text{W}}{\pi\sigma}}\text{..} (3.3)$$

Take the value of the minor diameter of the screw for the brake pedal power screw 4.001 mm. The brake pedal power screw minor diameter is approximately 4.02 mm from the basic standard of basic dimensions of ISO metric screw threads (Juvinall & Marshek, 2012) as shown in Table 3.12.

Table 3.12: Basic dimensions of ISO metric screw thread (Juvinall & Marshek, 2012)

Nominal or Major diameter (d_o) mm	3	3.5	4	5	6
Minor or core diameter (d_c) mm	2.39	2.76	3.14	4.02	4.77
Pitch (p) mm	0.5	0.6	0.7	0.8	1
Area of core (A_c) mm^2	5.03	6.78	8.78	14.2	20.1

For the minor diameter of 4.02 mm (see the above Table 3.12.) gas pedal Acme tread screw the nominal or major diameter meter do = 5 mm, Pitch (p) = 0.8mm, Thickness t = 0.37p = 0.296 mm and thread depth = h, for Acme screw h = 0.5p+0.25 = 0.65 mm and Pitch diameter = d= do – p/2 = 4.6 mm, Helix angle tan α =p π d = 0.8mmπ×4.6mm, α=3.17°.

Ham and Ryan showed that the coefficient of friction in screw threads is independent of axial load, practically independent of speed, decreases with heavier lubricants, changes little with material combinations, and is best suited for steel on bronze (Richard G. Budynas & J, 2011). Therefore, the nut material chosen for this system is bronze. The friction coefficient for dry steel screw and bronze nut is 0.14-0.21, see Table 3.13.

Table 3.13: Coefficients of sliding friction pair materials (Richard G. Budynas & J, 2011).

Screw material	Nut material			
	Steel	Bronze	Brass	Cast iron
Steel dry	0.15-0.25	0.15-0.21	0.15-0.19	0.15-0.25
Steel, machine oil	0.11-0.17	0.10-0.16	0.10-0.15	0.11-0.17
Bronze	0.08-0.12	0.04-0.06	-	0.06-0.09

From the friction coefficient, the friction angle φ can be found

$$tan\varphi=\mu,\ \varphi=tan-1(0.18)=10.20°$$

The torque required to rotate the screw is

$$T=W \times \tan(\alpha+\varphi)\ d/2 \ldots\ldots\ldots\ldots\ldots (3.4)$$

Shear stress in the screw due to torque

$$\tau = \frac{19T}{\pi(d_c)^3} \ldots\ldots\ldots\ldots\ldots (3.5)$$

Bearing pressure(P_b) Determination

To reduce the wear of the bolt and nut, the pressure of the bearing on the thread surfaces must be within the limits. In the design of power bolts, the bearing pressure depends on the materials of the bolt and nut, the relative speed between the nut and the bolt, and the nature of the lubrication (Tlomatic, 2021). See Table 3.14 for bearing pressure on different materials.

Table 3.14: Limiting values of bearing pressures (Khurmi, R.s.,&Gupta, 2005)

Application of screw	Material		Safe bearing pressure in N/mm^2	Rubbing speed at the thread pitch diameter
	Screw	Nut		
Hand press	Steel	Bronze	17.5 - 24.5	Low-speed, well lubricated
Lead screw	Steel	Bronze	1.05 – 4.25	High speed > 15m/min

This power screw is used for lead threads and the screw nut combinations are steel and bronze respectively, so the safe pressure is 1.05 to 4.25 N/mm^2. Suppose that the load is evenly distributed across the threads it is in contact with.

The number of meshes between threads and nuts is

$$n = \frac{W}{\frac{\pi}{4}((d_o)^2 - (d_c)^2)P_b} \qquad (3.6)$$

Bending (σ_b), Shear, compressive, and buckling stress

The maximum bending stresses

The maximum bending stress occurs at the root of the thread. It is calculated by assuming the thread is a simple cantilever beam built in at the root. The load is assumed to act at the mid-point of the thread (Gopinath, 2014).

$$\sigma_b = \frac{3Wh}{\pi d n t^2} \qquad (3.7)$$

The maximum Shear stresses

Both the nut and screw threads are subject to traverse shear stress resulting from the bending forces. For a rectangular section, the maximums shear stress occurs at the neutral axis and equals (Gopinath, 2014).

$$\tau = \frac{3W}{2\pi d_c n t} \qquad (3.8)$$

Tensile / compressive stresses

A loaded power screw is subject to a direct tensile or compressive load. The tensile stress area is generally provided in a screw using a stress area based on the root diameter may be used for conservative design studies (Gopinath, 2014).

$$\sigma_{t/c} = \frac{W}{A} \quad \text{...} \quad (3.9)$$

Where: $A = \frac{\pi d^2}{4}$

Combined stresses

According to the maximum shear stress theory and maximum normal stress theory, the maximum shear stress, the maximum normal stress is:

$$\tau_{max} = \frac{1}{2}\sqrt{(\sigma)^2 + 4\tau^2} \quad \text{and} \quad \sigma_{max} = \frac{1}{2}\sigma_b \frac{1}{2}\sqrt{(\sigma)^2 + 4\tau^2}$$

ii. Design of Brake pedal drive nut

Bronze is the ideal material selected for nut because of its excellent corrosion resistance, Higher tensile strength and excellent machinability, comfortability, and lower coefficient of friction. The elastic limit of bronze may be taken as shown in Table.3.15.

Table 3.15: Elastic limit of bronze

Conditions	The elastic limit of bronze
In tension	100MPa
In compression	90MPa
In shear	80MPa

Let:

- D_1 = Inner diameter of the nut
- D_2 = Outer diameter of nut collar
- N = Number of threads engaged
- σ_t = Tearing strength
- w = load to be lifted
- σ_c = Compression strength
- h = Axial length of nut ($h = n * p$)
- t_1= Thickness of nut col

Inner and Outer diameter of the nut

Inner diameter (D_1) is found by considering the tearing strength (σ_t) of the nut and the outer diameter (D_2) is found by considering the crushing strength as

$$D_1 = \sqrt{\frac{4W}{\pi\sigma_t} + d^2} \quad \dots (3.10)$$

Where: $W = \frac{\pi}{4}((D_1)^2 - (d)^2)\sigma_t$

$$D_2 = \sqrt{\frac{4W}{\pi\sigma_c} + {D_1}^2} \quad \dots (3.11)$$

Where $W = \frac{\pi}{4}((D_2)^2 - (D_1)^2)\sigma_c$

The thickness of the nut collar

By considering the shearing of the collar of the nut

$$W = \pi d t_1 \quad \dots (3.12)$$

$$t_1 = \frac{W}{\pi d \tau} \quad \dots (3.14)$$

The shear stress at the root of the threads in the nut and screw is given by

$$\tau = \frac{3W}{2\pi d n t} \quad \dots (3.15)$$

iii. Design of coupling between the lead screw shaft and stepper motor shaft

A good coupling should be easy to connect and disconnect, should transmit full power, should hold the shaft in perfect alignment also should reduce transmission of shock loads from one shaft to another shaft (Khurmi, R.s.,&Gupta, 2005).

Design of sleeve

Torque (T) transmitted by a hallow section is given by

$$T = \frac{\pi}{16} * \tau_c \left(\frac{D^4 - d^4}{D}\right) \quad \dots (3.16)$$

Where: T = Torque transmitted by the shaft

- F = Tangential force
- d = Diameter of shaft
- l = Length of key
- w = width of the key
- σ_c and τ = crushing and shear stresses
- τ_c = Permissible shear stress
- t = Thickness of key

Proportions of a cast iron sleeve coupling are

Outer diameter of sleeve, D = 2d +13mm, D = 2*5mm + 13mm = 23mm

Length of the sleeve, L = 3.5d, L = 3.5*5mm = 17.5mm

The safe value of shear stress for cast iron may be taken as 14 MPa (Khurmi, R.s.,&Gupta, 2005). The induced shear stress in the sleeve is less than the shear stress value of cast iron. Therefore, the design is safe.

Design of key

The length of the coupling key is at least the same as the length of the sleeve (that is, 3.5d). Table 3.16 shows standard parallel, taper, and Gib head key ratios by IS: 2292 and 2293-1974 (Khurmi, R.s.,&Gupta, 2005).

Table 3.16: Proportions of standard parallel, tapered keys (Khurmi, R.s.,&Gupta, 2005).

Shaft diameter (mm) up to and including	Key cross-section	
	Thickness	Width
6	2	2
8	3	3
10	4	4
12	5	5
17	6	6

The diameter of the shaft is 5 mm, the length of key L=17.5 mm, the Width of key w=2 mm, Thickness of key t=2 mm. The induced shear and crushing stresses are key.

Shearing of the key Considering shear stress (τ) and crushing stress (σ_c)

$$\tau = \frac{2T}{Lwd} \text{ and } \sigma_c = \frac{4T}{Ltd} \quad \text{(3.17}$$

The permissible crushing stress for the usual key material is at least twice the permissible shearing stress. Therefore, we have w = t. In other words, a square key is equally strong in shearing and crushing. Since the induced shear and crushing stresses are less than the permissible stresses (14 MPa), therefore the design of the key is safe.

iv. Determination of motor power required to control brake pedal

The maximum power required by a stepper motor to depress the automobile pedals can be determined by

$$p = T\omega_n \quad (3.18)$$

The distance that the drive nut travel to depress the pedals is equal to the maximum travel distance of the pedal. It is equal to the maximum pedal travel of the brake pedal (43mm).

v. Determination of speed of brake pedal motor

The driver's reaction time includes recognizing a change in the light signal, the decision to continue driving or to brake, and when stopping - applying the brake (remove the foot from the accelerator and apply the brake). In general, the normal reaction time of the driver is 0.5-3 seconds.

The standard driving regulations act requires 0.7 seconds for perfect reaction time (Yared, 2019). This includes 0.5 seconds for perception and 0.2 seconds for foot movement, which is the time it takes to move your foot from the gas pedal to the brake pedal.

A controlled study showed that total brake reaction time (defined as the period between the point at which the driver began to release the accelerator pedal to the maximum brake application point) was 2.2 seconds for the IDS and 2.3 seconds on the test track. Time to throttle release was also compared between the two studies (Mcgehee et al., 2000). This implies that the time required for foot movement is 0.2 and the time required to depress the brake pedal is (2.3sec – 0.2sec) equal to 2.1 seconds. In this case, since there is no need of moving your foot from the gas pedal to the brake pedal. Thus, 2.1sec can be taken as brake pedal application time excluding foot movement.

$$V = \frac{s}{t} = \frac{0.04m}{2.1sec} = 0.019m/s$$

Where: s is braking pedal travel which is 40mm (average pedal height (164mm) minus average reserve distance (124mm)) average value measured for three 5L Engine type minibus taxis.

Lead is the linear travel of the nut. The lead for a single start power screw is equal to the pitch of the screw and approximately equal to one revolution of the screw expressed as:

Lead (l) = pitch (p) ≈ 1 revolution

$$n = \frac{V}{l} = \frac{0.019m/s}{0.0008m} = 23.75rev/s = 1425rev/min$$

Angular velocity (ω)

$$\omega = 2\pi n = 149.15rad/s$$

The power required by motor (P)

$$P = 0.1308Nm * 149.15rad/s$$

$$P = 19.54watt$$

vi. Selecting the appropriate stepper motor

The type (see section 3.1.1) and Specification of the stepper motor should be within the following specifications see Table 3.17.

Table 3.17: Required specifications and type of stepper motor

Criteria's	Brake pedal motor
Maximum power	19.54watt
Maximum torque	0.1308Nm
Maximum rpm	1425rpm
Type of stepper motor	
Based on the arrangement of stator windings	Bipolar
Based on construction	Hybrid
Input voltage	12V

For the required data specification NEMA 17 bipolar stepper motor 12VDC which has a 5mm diameter shaft that fits screw diameter can meet the requirements (See Fig.3.30 for speed torque curve of bipolar drive).

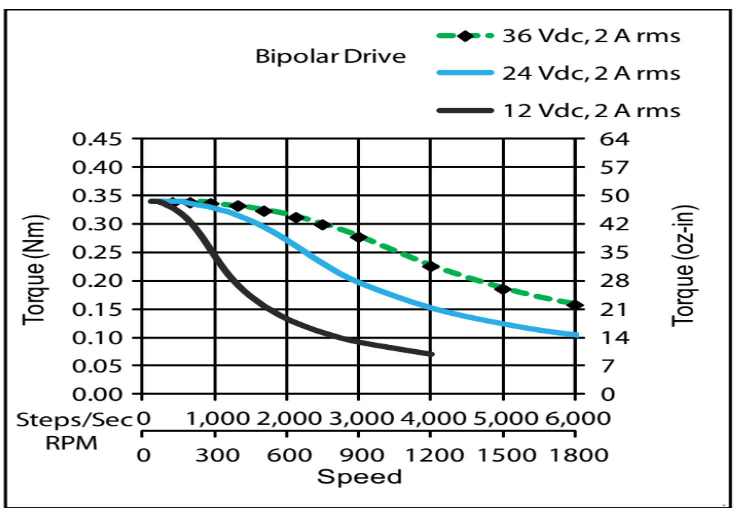

Figure 3.30: Stepper motor torque vs speed

vii. Design of brake pedal actuating inner tube

Inner tubes are also known as extension tubes, drive tubes, translating tubes, or pistons. This tube is usually made of aluminum or steel. While retracted, the inner tube is where the spindle is located. This tube is attached to a threaded drive nut that expands and contracts as the nut moves along the rotating spindle. For this task, the material chosen for the inner tube to reduce weight is aluminum (Elsherif et al., 2019). For material properties of aluminum alloy see Table 3.18.

Table 3.18: Material properties of aluminum alloy (Elsherif et al., 2019).

Properties	Ultimate tensile strength	Tensile Yield Strength	Compressive strength	Shear strength	Shear modulus	Elastic modulus	Young's modulus
Metric	310MPa	276MPa	280Mpa	207MPa	26Gpa	200GPa	68.9GPa

The inner tube is the hollow circular part of the linear electric actuator and is also considered a vertical rod subject to buckling and compressive stress, one end of which is free and the other end is fixed. The force on the inner tube, which is equal to the load required to operate the brake pedal, is 300 N with a rod length of about 31 mm. The minimum inner diameter must be greater than the outer diameter of the screw shaft and there must be sufficient clearance between the screw shaft and the inner tube. Suppose the gap between the screw and the inner tube is 1mm.

Determination of crippling stress for inner tube

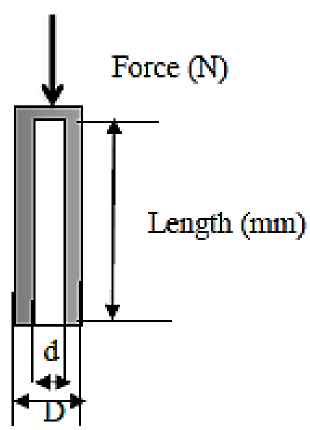

Figure 3.31: Inner tube

According to Euler's theory, the crippling or buckling load (W_{cr}) under various end conditions is represented by a general equation.

$$W_{cr} = C\pi^2 E \frac{I}{L^2} \quad \text{.................................} \quad (3.19)$$

$$I = AK^2 \ldots\ldots\ldots\ldots\ldots\ldots\ldots\ldots\ldots\ldots\ldots\ldots \text{ (3.20)}$$

Where: E= elasticity modules

- C = end fixing coefficient (c = 0.25 for one ended fixed)
- L= length
- A = area
- W_{cr} = Crippling load
- K= radius of gyration

By substituting Eq in Eq the buckling load become

$$W_{cr} = C\pi^2 E \frac{A}{(\frac{L}{K})^2} \ldots\ldots\ldots\ldots\ldots\ldots\ldots\ldots \text{ (3.21)}$$

Buckling stress σ_{cr} is also given by

$$\sigma_{cr} = \frac{W_{cr}}{A} = \frac{C\pi^2 E}{(\frac{L}{K})^2} \ldots\ldots\ldots\ldots\ldots\ldots\ldots\ldots \text{ (3.22)}$$

Where: $\frac{L}{K}$ = slenderness ratio (if $\frac{L}{K} < 80$ the bar is short bar otherwise long bar).

By equating the buckling stress equation with the buckling load equation $\frac{L}{K}\, is < 80$. Therefore, Euler's formula is not valid, thus Professor Johnson's formula for the short bar was used for the determination of the diameter of the inner tube.

$$D = \sqrt{\frac{4W_{cr}}{\pi[\sigma_y - \frac{2\sigma_y}{3\pi}(\frac{1}{k})\sqrt{\frac{\sigma_y}{3CE}}} + d^2} \ldots\ldots\ldots\ldots\ldots \text{ (3.23)}$$

viii. Design motor mounting bar

The distance between the mounting tape point and the load applied by the motor is approximately 150 mm (valley measurement). The maximum force applied to the rod is 294 N. The material used for the engine mounting rod can be aluminum or steel metal. Steel which has an ultimate tensile strength of 650Mpa is more suitable for rail installation because it has a higher resistance to bending, pressure, shear, and tensile strength than aluminum. The specified cross-section is a circular steel bar due to its higher resistance to bending than the sacred cross-section.

Maximum bending moment (σ_{bmax})

$$\sigma_{bmax} = \sigma_b \frac{\pi}{32}(D^3) \ldots\ldots\ldots\ldots\ldots\ldots\ldots\ldots\ldots\ldots\ldots \text{(3.24)}$$

Where: σ_b= allowable bending stress is given by:

$$\sigma_b = \frac{\sigma_{ultimate}}{\text{FOS}} = \frac{650\text{MPa}}{2} = 325\text{Mpa}$$

Determination of Maximum bending moment from free body diagram

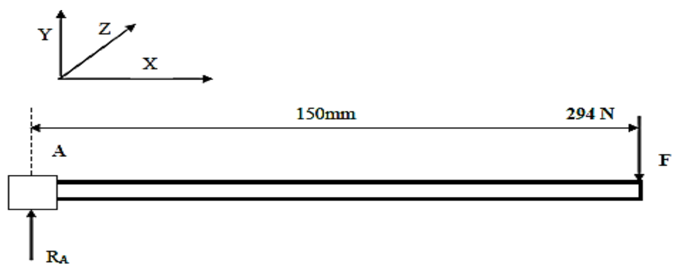

Free body diagram

Figure 3.32: Free body diagram

Maximum reaction force at the fixed end can be expressed as

$$R_A = F = 294N$$

The bending moment at A

$$\sum M_A = 0, 294N * 150mm = 44.1Nm$$

Shear force diagram

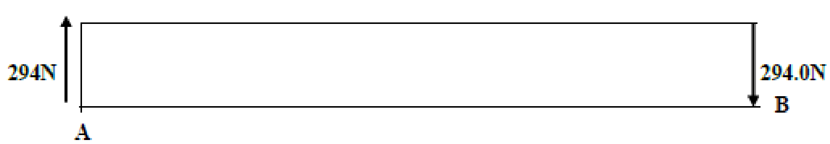

Figure 3.33: Shear force diagram

Shear force at A, $F_A = R_A = +294N$

The shear force between A and B is constant and equal to +294N.

Shear force at B, $F_B = -294N$.

Bending moment diagram

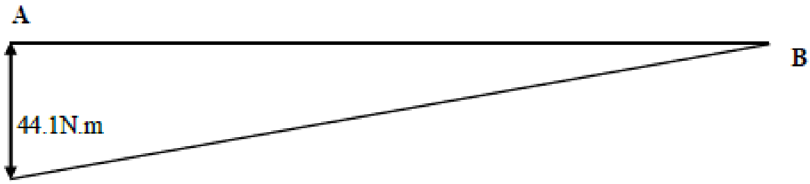

Figure 3.34: Bending moment diagram

The bending moment at A, $M_A = 44.1Nm$

The bending moment at A, $M_B = 0$

Therefore, the maximum bending moment at B is equal to 44.1Nm. thus, the diameter of the bar for the maximum bending moment is calculated as:

$$D = \sqrt[3]{\frac{32M}{\sigma_b \pi}} \quad \text{...} \quad (3.25)$$

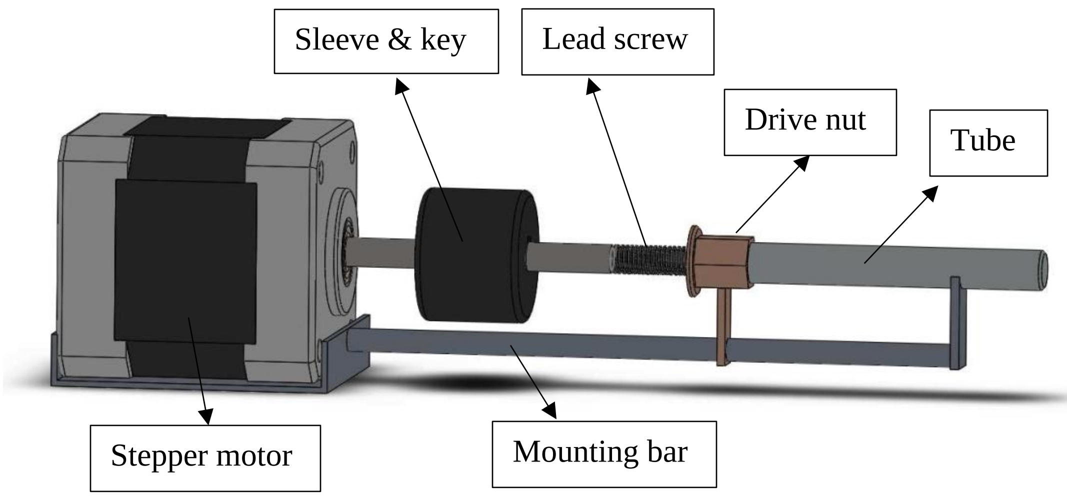

Figure 3.35: Actuation mechanism SOLIDWORKS model

The kinetic energy of the vehicle

Arduino Uno program relates the position sensor (potentiometric sensor) and actuator travel distance to activate the brake pedal.

Using the specification, the maximum speed of the TOYOTA 5L minibus taxi from the above data collection is 100kmph (27.78 meter per second).

The braking force required to stop 5L minibus can be found after the calculation of the kinetic energy of the vehicle using Eq.3.26.

For the body in motion, the kinetic energy is given by:

$$KE = \frac{1}{2} m_v V_v{}^2 \ldots\ldots\ldots\ldots\ldots\ldots\ldots\ldots\ldots\ldots\ldots\ldots\ldots (3.26)$$

Where: m_v= mass vehicle (kg)

V_v = vehicle speed (m/s)

KE = kinetic energy (kJ)

$$KE = \frac{1}{2} m_v V_v{}^2$$

The net weight of the demonstrate vehicle is 2800 kg and encompasses a greatest admissible speed of 27.78 meter per second.

$$KE = \frac{1}{2} 2800kg * (27.78\, m/s)^2$$

$$KE = 1{,}080.419KJ$$

Work done (W) is defined as

$$W = KE = F*Sd \ldots\ldots\ldots\ldots\ldots\ldots\ldots\ldots\ldots\ldots\ldots\ldots\ldots (3.27)$$

Where: Sd = stopping distance (m)

W = work done (kJ)

F = brake force (N)

Therefore, W = KE= $1{,}080.419KJ$

The vehicle stopping distance

One of the particular targets of this proposition is to diminish the ceasing separation of minibus taxis by progressing the execution of brakes utilizing the combined pedal. Hence, the ceasing remove of this minibus is decreased by minimizing the response time to apply the brake.

Braking distance (D_b)

When the minibus taxi is equipped with a combined pedal and travels at a maximum allowable speed of 27.78m/s. The braking distance is calculated as follows using equation 3.28.

$$D_b = \frac{V^2}{(2*\mu*g)} \quad \text{……………………………………………} (3.28)$$

(https://www.101computing.net/stopping-distance-calculator/)

Where: V = velocity before applying brake (m/s)

D_b= brake distance (m)

g = acceleration due to gravity (m/s2)

μ = coefficient of friction asphalt road 0.8

$$D_b = \frac{V^2}{(2*\mu*g)}$$

$$D_b = \frac{(27.78\, m/s)^2}{(2*0.8*9.81\, m/s^2)} = 49.167m$$

Reaction Distance (d_r)

Reaction distance is the distance the vehicle travels before the driver notices the danger and starts braking. The full response time takes 0.75 seconds from the standard driving regulation act. Of this, 0.5 second is for perception and at least 0.25 second is for foot movement or the average reaction time required to release the accelerator and to depress the brake pedal is ¾ of a second. Using equation 3.29.

$$d_r = {}^{(V*t_r)}/_{3.6} \quad \text{……………………………………...…… } (3.29)$$

Where: V = Vehicle speed (km/hr.)

t_r = reaction time (sec)

d_r = reaction distance (m)

$$d_r = \frac{(100\, km/h * 0.75)}{3.6} = 20.83m$$

Reaction distance resulting from delay in driver reaction time is reduced (It decreases misjudgment of operating the wrong pedal.) since there is no foot movement which requires at least 0.2 seconds. because the system will automatically apply the brake pedal by sensing the pedal position.

The new reaction distance becomes:

$$d_{nr} = \frac{(100\,km/h * 0.5)}{3.6} = 13.88m$$

Stopping distance (S_d)

The vehicle will not come to a stop immediately after the application of the brake. It takes some movement to come to a stop this distance is stopping distance. It depends on the speed of the vehicle, coefficient of friction (between the tire and the road), and brake system efficiency. Thus, it is calculated using Eq. 3.30.

$$\mathrm{S_d} = \text{Reaction distance} + \text{Braking distance} \ldots\ldots\ldots\ldots\ldots\ldots\ldots\ldots\ldots\ldots \text{(3.30)}$$

$$\mathrm{S_d} = \text{Reaction distance } (\mathrm{d_r}) + \text{Braking distance } (\mathrm{D_b})$$

$$S_d = 20.83m + 49.167m = 70m$$

When the vehicle is equipped with a combined pedal the new stopping distance (S_{nd}) is reduced to:

$$\mathrm{S_{nd}} = \text{Reaction distance } (\mathrm{d_{nr}}) + \text{Braking distance } (\mathrm{D_b})$$

$$S_{nd} = 13.88m + 49.167m = 63m$$

Therefore, for the vehicle equipped with a combined accelerator and brake pedal the stopping distance (S_d) of the vehicle is 63m at the maximum allowable speed.

According to the world speed limit used in Ethiopia in town is 60km/h and out of town 100km/h, 70km/h, and 60km/h depending on road conditions 1st, 2nd, and 3rd road levels respectively; for vehicles weighing up to 3500kg (Scale et al., 2022).

Table 3.19: The vehicle stopping distance.

		Vehicle speed, expressed in km/h				
		30	40	60	70	100
Distance in (m)	D_b	4.42	7.86	17.7	24.1	49.15
	d_r	6.25	8.33	12.5	14.58	20.83
	d_{nr}	4.16	5.55	8.33	9.72	13.88
	S_d	10.25	15.64	30.2	37.71	70
	S_{nd}	8.58	13.41	26.03	33.82	63.03

This show that the vehicle speed and vehicle stopping distance are directly proportional to each other.

Brake force (F)

From the general formula of work done equation 3.27 would get brake force.

$$\text{w} = F * S_d$$

From the above work done is $1{,}080.419KJ$

$$1{,}080.419kJ = F * S_d$$

$$1{,}080.419kJ = F * 70m$$

$$F = \frac{1{,}080.419kJ}{70m} = 15.43KN$$

For a vehicle equipped with a combined pedal, the stopping distance at maximum speed is 63m. Thus, the braking force is increased to 17.15 kN.

Braking time:

Covers the time from the fully developed brake achieved to the time vehicle stops its movement.

$$a = \frac{dv}{dt} \ldots\ldots\ldots\ldots\ldots\ldots\ldots\ldots\ldots\ldots\ldots\ldots\ldots\ldots (3.31)$$

The longest braking time happens by driving the loaded vehicle at a maximum speed.

$$\int dt = \int \frac{dv}{a} \quad \text{……………………………………………} (3.32)$$

$$a = \frac{F_b}{m_v}$$

$$t_b = \frac{v_v}{a}$$

The ratio of the product of vehicle mass and vehicle velocity to forces that contribute to overall braking effort equals braking force. (See Eq.3.33).

$$t_b = \frac{m_v v}{F} \quad \text{……..……………………..…………………….} (3.33)$$

Where: t_b = time to brake (s) (i.e., braking time)

m_v = mass of the vehicle (kg)

v = vehicle speed (m/s)

F = brake force (N)

$$S = ut - {}^{1}/_{2}\,(at^2) \quad \text{…….………………………………} (3.34)$$

s = the distance at which the vehicle stops (m)

u = speed of the vehicle (m/s)

t = time (s)

a = acceleration (m/s2)

Notice that, $t = t_b$ and $a = \frac{F}{m_v}$ so,

$$s = ut - {}^{1}/_{2}\,(\frac{F}{m_v}t^2) \quad \text{………………………………..…} (3.35)$$

The maximum engine rpm determines the maximum speed. This is achieved at the gear ratio: 1:1 (the minimum gear ratio).

Thus, the propeller shaft maximum rpm $= \frac{\text{The max.Engine speed}}{\text{The min.gear ratio}}$…………… (3.36)

Therefore, braking time at the maximum allowable speed of 27.78m/s is calculated from equation 3.33.

$$t_b = \frac{m_v v}{F}$$

$$t_b = \frac{2800kg * 27.78\, m/s}{15.43KN}$$

$$t_b = 5.04\, sec$$

Using the above equation for calculating stopping distance (Eq. 3.34).

$$S = ut - \frac{1}{2}\,(at^2)$$

$$S_d = 27.78\, m/s * 5.04sec - \frac{1}{2}\,(\frac{15.43KN}{2800Kg}\,(5.04\, sec)^2)$$

$$S_d = 70m$$

Table 3.20: Vehicle stopping distance and braking time (at selected speeds)

	Speed of the vehicle (in km/h)				
	30	40	60	70	100
t_b(s)	1.51	2.01	3.02	3.53	5.04
$t_{nb}(s)$	1.36	1.81	2.72	3.17	4.53

B. Design of Combined brake and accelerator pedal

The brake pedal is part of the car that initiates the entire brake system in a vehicle. Organ type pedal enables muscles of both the calf and the shin to completely relax and also for better control. In automatic cars, it’s the pedal on the left side, and in manual cars, it’s the middle pedal. When you press down on it, all the components of your braking system swing into action. From reviews of the existing design guidelines and standards on automotive pedal design which is organized by different aspects of pedal design, such as pedal position and pedal size the data in Table 2.1 in section 2.6 was obtained. The material for each of the components is listed (see Appendix E) with their properties.

By using the conventional pedal design guidelines and standards listed in Table 2.1: (Summary of relevant design recommendations) the combined accelerator and brake pedal model was made as shown in Fig. 3.36.

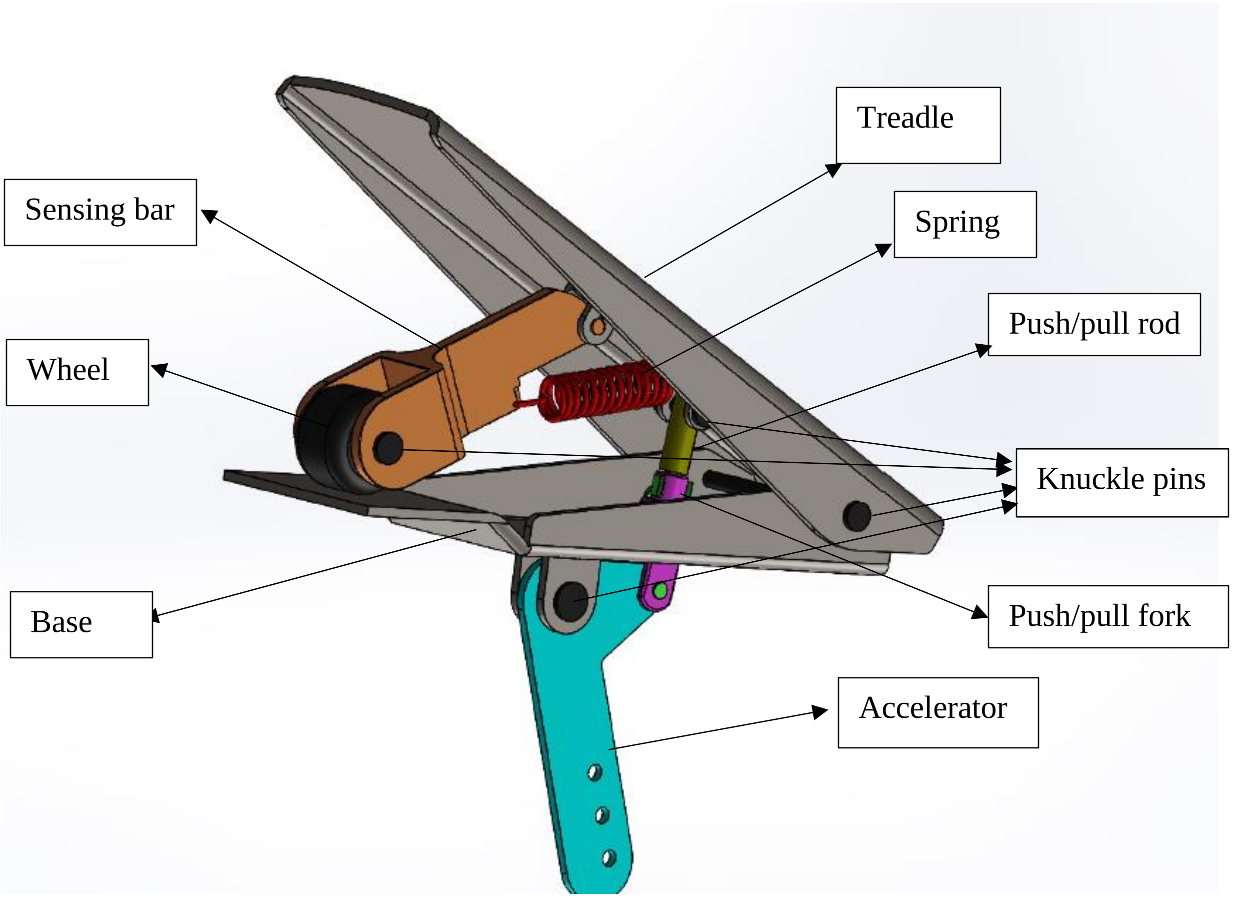

Figure 3.36: SOLIDWORKS model of combined brake and accelerator pedal

The analysis was carried out using the following consideration into account. High-quality mesh using high-quality elements.

- ✓ A tetrahedron ISH shape.
- ✓ Four curvy “Tri-angular ISH” sides.
- ✓ Six parabolic edges and
- ✓ Ten nodes result in more equations and more accurate results, as shown in Fig. 3.37.

Meshing: Representation of the model in tiny chunks that the computer can easily work with. Dicing model in tiny elements enables many simpler calculations. (Curvature-based mesh is used as shown in Fig. 3.37).

Quality: high quality (curved edges).

Level of detail: coarse.

A high aspect ratio is bad as it results in skinny elements. The aspect ratio should be <20.

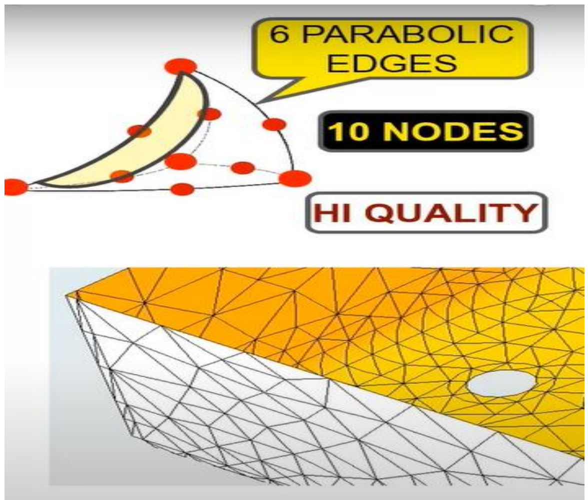

Figure 3.37: Combined pedal Mesh

The model is supported in such a way approximate reality. Some of the components are excluded from the analysis for the sake of reducing redundancy and their effect on analysis. Application of load that adequately and accurately validates the design.

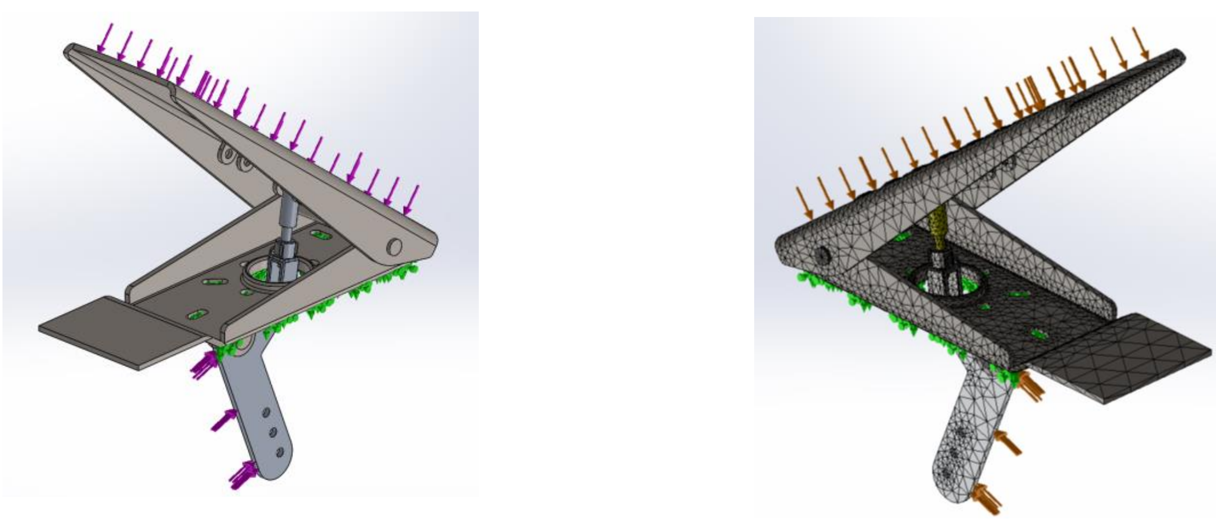

Figure 3.38: Combined pedal application of boundary conditions and mesh

Then finally SOLIDWORKS analysis is carried out to check the strength of the pedal in terms of:

- ✓ Stress (Von Mises)
- ✓ Strain and
- ✓ Displacement.

Major Conditions applied for simulation.

Table 3.21: Major conditions applied to the simulation

Study type	Static Study
Contact set	No penetration
External load	90N per item (see section 3.1.2)

Figure 3.41: SOLIDWORKS simulation for Displacement analysis

Finally, the motion analysis of the combined pedal was made after design in SOLIDWORKS.

Design of spring

Inadequate pedal design of spring often leads to fatigue and discomfort for drivers. The material used for spring is stated in Table 3.21 above with its properties. The model with SOLIDWORKS is shown in Fig. 3.39.

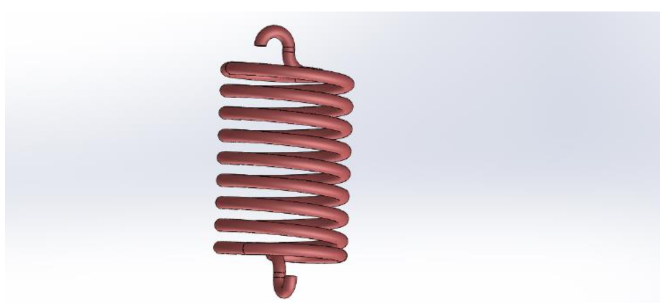

Figure 3.39: SOLIDWORKS Spring model

Spring design requirements (boundary conditions)

- ✓ Able to extend about 21.23mm during the pedal full depression at an average foot force of 58N (see section 3.1.2) for the accelerator pedal.

✓ The normal height should not exceed 48mm to satisfy the pedal design requirement (Xi et al., 2018). As shown in Fig. 3.40 and Fig. 3.41.

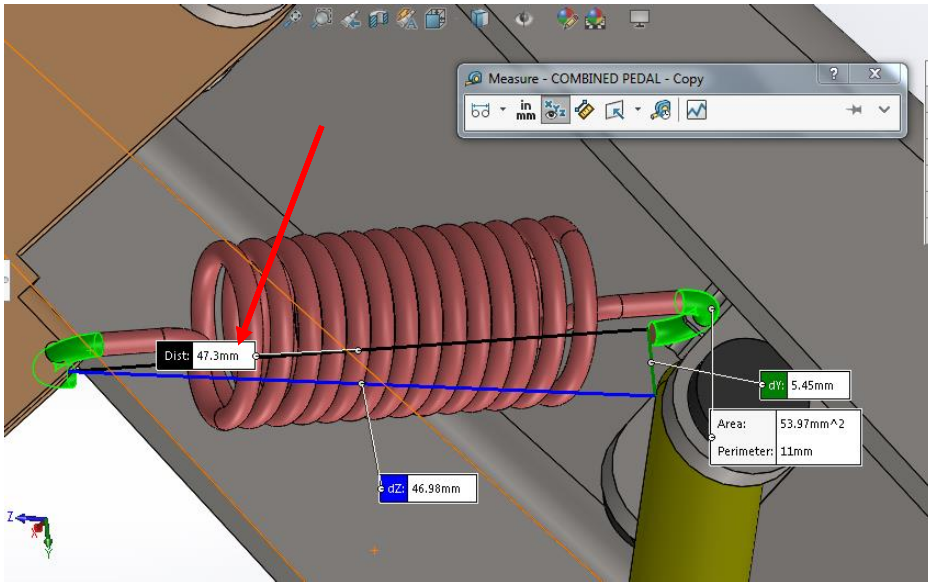

Figure 3.40: Undepressed pedal spring length

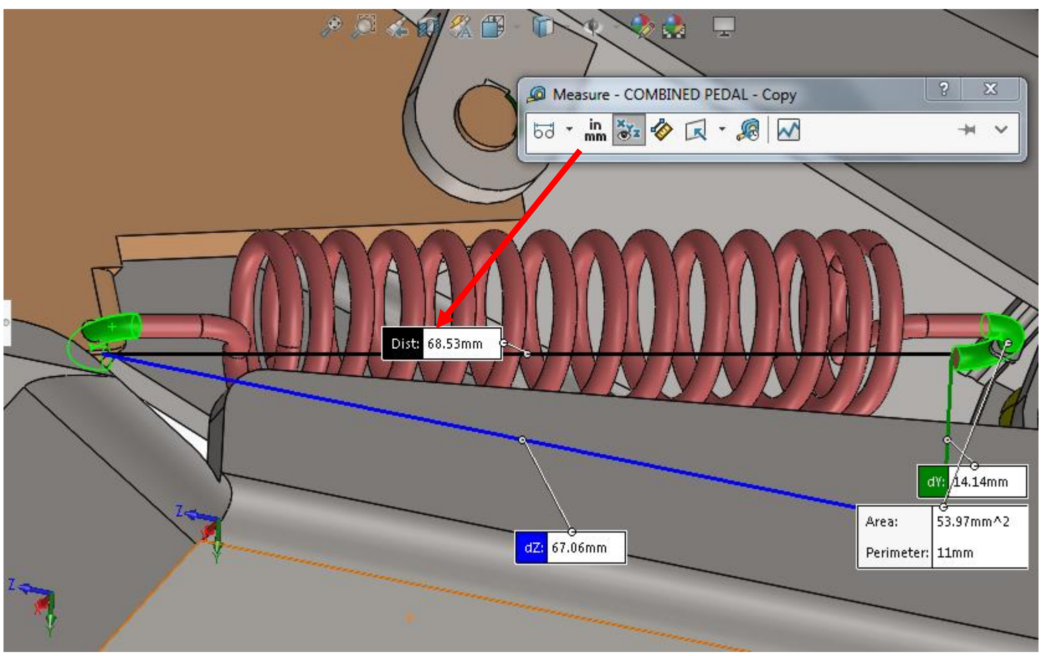

Figure 3.41: Fully depressed pedal spring length

Using spring design boundary conditions, the SOLIDWORKS simulation analysis for spring was carried out.

3.4.3 Motion Analysis

Finally, the motion analysis was made with the following boundary conditions in SOLIDWORKS software for both the combined pedal and actuation mechanism.

A. Combined Pedal Motion Analysis

The combined pedal motion analysis is carried out under the following conditions:

- ✓ The maximum force of 90N is applied on the pedal.
- ✓ The motion analysis is carried out for 5sec.
- ✓ Gravity (g = 9.81m/s^2) is applied to the system.
- ✓ The force is set to off condition at 4 sec.

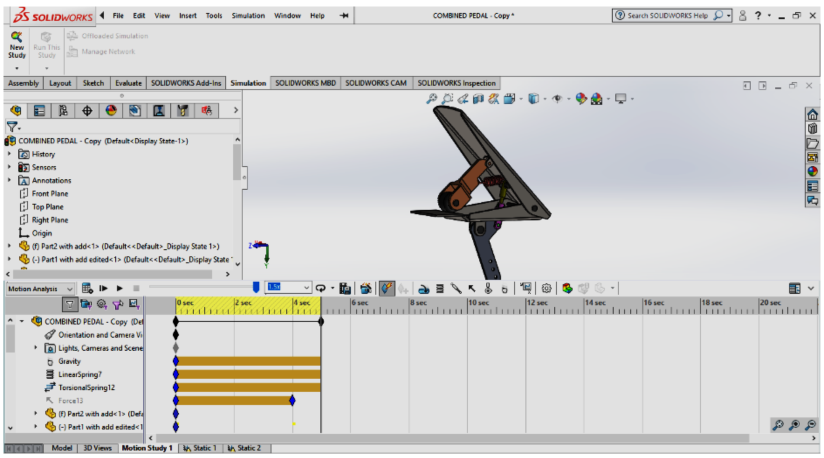

Figure 3.42: SOLIDWORKS combined pedal motion analysis setup

B. Actuation Mechanism Motion Analysis

The time (in seconds) needed to extend the brake actuation tube up to 40mm (brake pedal travel) under the following situations:

- ✓ Motor rpm: 1425 rpm (see section 3.1.2).

✓ The direction of rotation is clockwise.

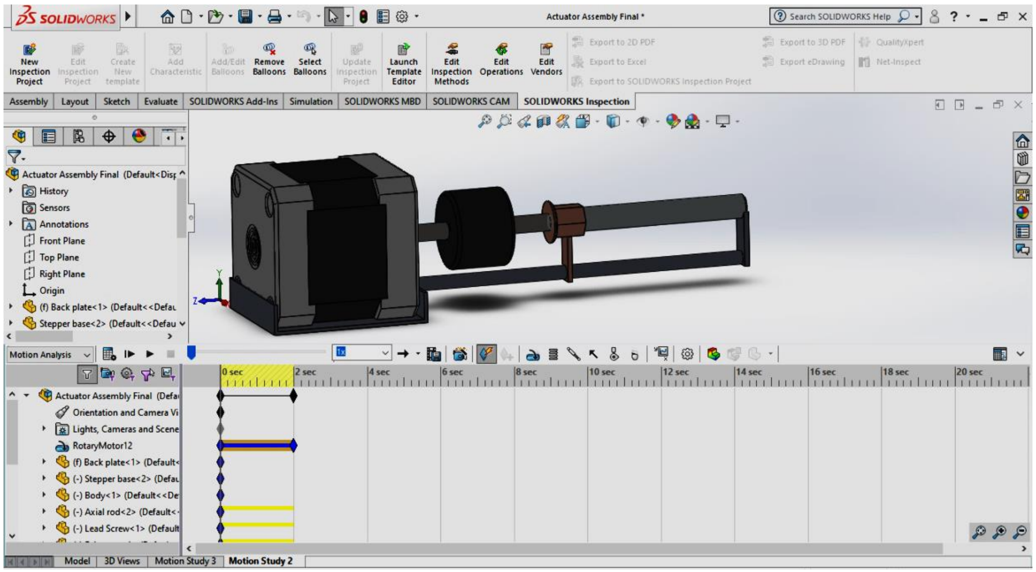

Figure 3.43: SOLIDWORKS Brake pedal actuator motion analysis setup

CHAPTER FOUR

RESULT AND DISCUSSION

4.1 Design results of combined pedal

Initially, in the design of the combined pedal, the model is made with SOLIDWORKS. The mesh detail result is shown in Table 4.1.

Table 4.1: Mesh detail

Study name	Static1 (default)
Mesh type	Solid mesh
Mesher used	Curvature based mesh
Jacobian points	4 points
Mesh control	Defined
Max element size	9.27581mm
Min element size	1.85516mm
Mesh quality	High
Total nodes	67130
Total elements	94933
Maximum aspect ratio	20.372
Percentage of elements with aspect ratio < 3	76
Percentage of elements with aspect ratio >10	0.746
% Of distorted elements (Jacobian)	0
Re-mesh elements failed parts with incompatible mesh	Off
Time to complete mesh (hh: mm: ss)	00:00:07
Computer name	DELLI5-PC

The result of the SOLIDWORKS simulation analysis was carried out to check the strength of the pedal in terms of Stress (Von Mises), Strain, and Displacement is shown in Fig 4.1, and 4.2 respectively.

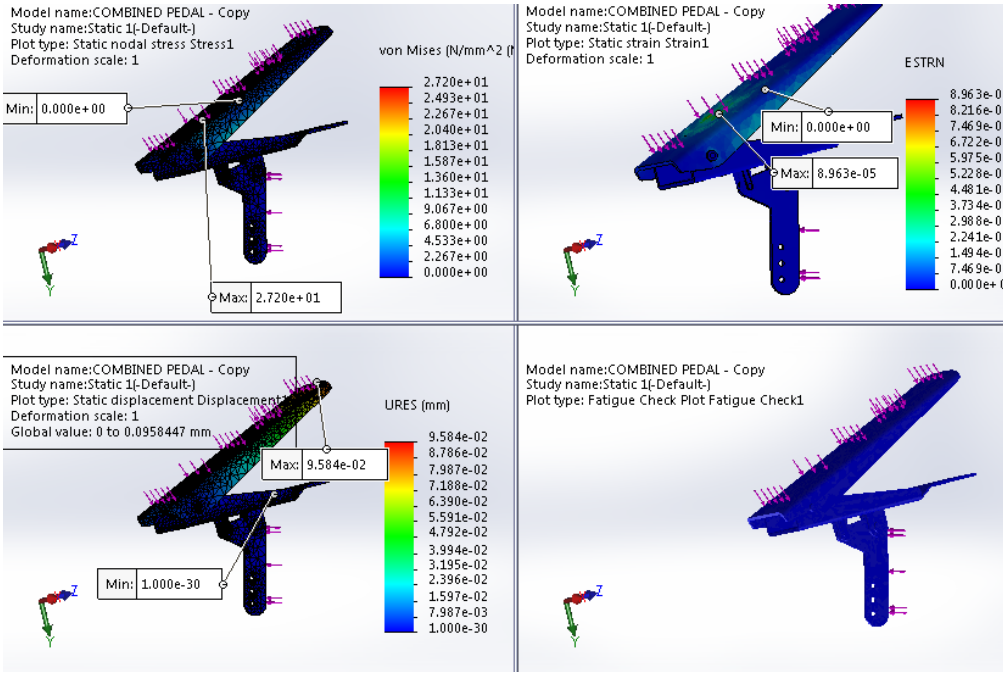

Figure 4.1: SOLIDWORKS Simulation of combined pedal results

Similarly, for return spring

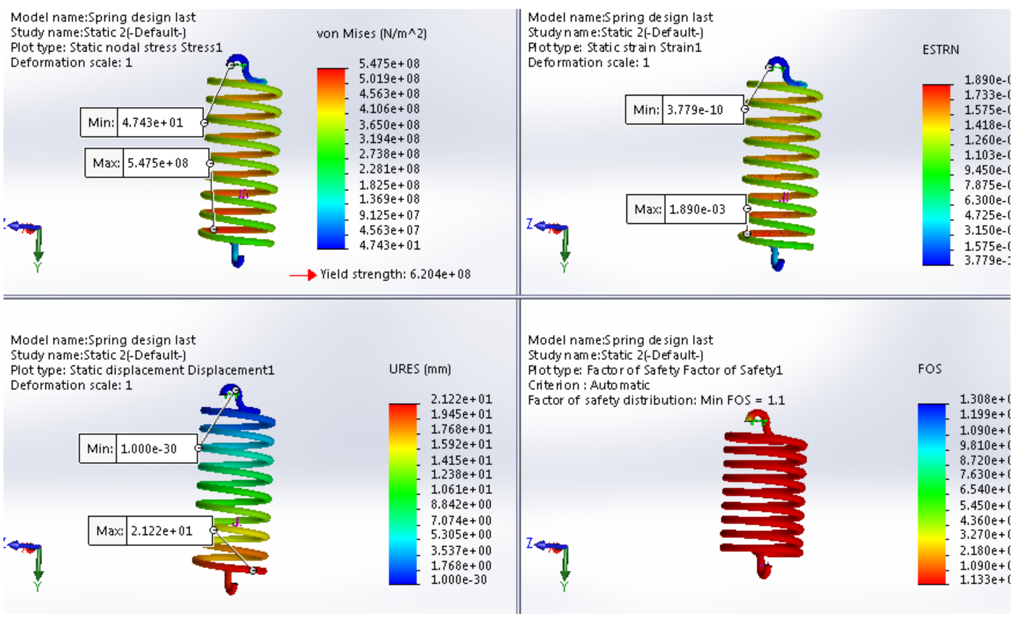

Figure 4.2: SOLIDWORKS simulation of spring results

Table 4.2: SOLIDWORKS simulation of combined pedal Result

Component	Stress (MPa)	Strain	Displacement (mm)	Remark
Pedal	27.20	8.963e -05	0.09584	Maximum stress and strain displacement are less than the ultimate yield strength of spring and pedal material alloy steel (620.4Mpa) and stainless-steel sheet metal (172.3Mpa) respectively.
Spring	547.5	1.890e-3	21.22	

The design and simulation of combined brake and accelerator pedal design analysis, SOLIDWORKS software (modeling, simulation, and motion analysis), and Arduino code and simulation in proteus were carried out with the assignment of various materials to each component, formulation of connections, fixtures, and constraints so that it resembles reality. The designed combined pedal components result shows that the maximum stress (27.2Mpa), strain ($8.963*10^{-5}$) displacement (0.09584) is less than the ultimate yield strength of combined pedal components materials alloy steel (620.4Mpa) and stainless-steel sheet metal (172.3Mpa) which implies safe design.

Combine pedal components were made based on the dimension of automotive pedal design guidelines as explained in Chapter 2. The Spring design geometric dimensions are shown in Table 4.3.

Table 4.3: SOLIDWORKS Simulation Spring design result

Component	Parameters	Symbols	Value (Unit)
Tension Spring	Height	H	37.3mm
	Revolutions	N	8.095
	Coil diameter	D_c	25 (mm)
	Spring constant	K	4 (N/mm)
	Number of coils	N	9
	Wire diameter	d_w	2.5 (mm)

The designed spring enables the driver to rest his/her foot freely (with pivoted toe) on the combined pedal without the risk of pressing the pedal (minimum force required 58N) and provides good sensitivity. In addition, in a manner that does not cause foot fatigue (maximum force needed 90N).

4.2 Motion analysis result of combined pedal

Motion analysis result for combined pedal treadle depressed for 4sec with the average accelerator pedal force of 58N is as shown in Fig.4.3.

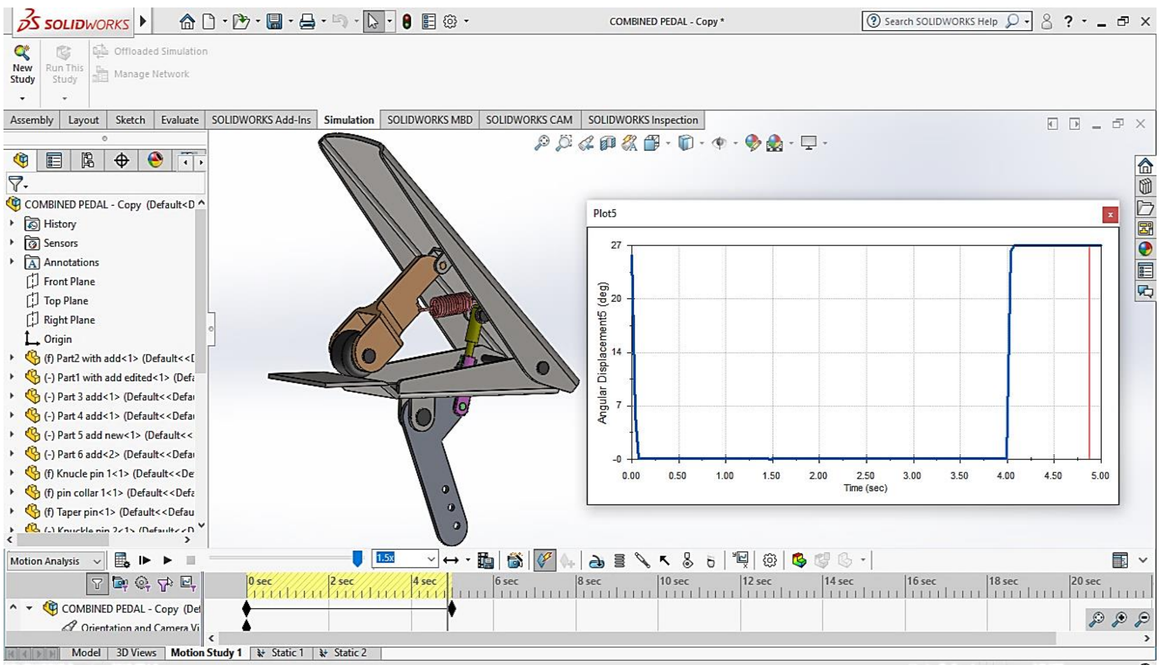

Figure 4.3: Motion analysis of Combined pedal results

From fig.4.3 motion analysis in SOLIDWORKS software (to know whether the combined pedal return to its initial position immediately after the applied force is removed.

Motion analysis result of combined pedal treadle depressed for 4sec with the average accelerator pedal force of 58N shows that the spring is strong enough to return the treadle to its original position without any delay (within less than 0.1sec). Also, the average force of 58N can depress the pedal fully which allows the application of the pedal effortless and good stability to control the gas.

4.3 Design results of brake pedal actuator components

The design geometric dimensions of brake pedal actuation system components are shown in Table 4.4. See Table 4.5 for maximum bending, shear, and bending stress.

Table 4.4: Brake pedal actuator dimensions.

Actuating system	Components	Parameters	Symbol	Values (Unit)
Brake pedal actuator	Lead screw	Minor diameter	d_c	4.02 (mm)
		Major diameter	d_o	5 (mm)
		Helix angle	A	3.07 (°)
		Friction angle	Φ	10.2 (°)
		Thread depth	H	0.65 (mm)
		Pitch	P	0.8 (mm)
		Thickness	T	0.296 (mm)
		Pitch diameter	D	4.6 (mm)
		Thread arrangement with nut	n	10
	Drive nut	Inner diameter	D_1	7 (mm)
		Outer diameter	D_2	8.5 (mm)
		Thickness	T	1.5 (mm)
		Axial length	L	10 (mm)
	Inner tube	Outer diameter	D	7 (mm)
		Inner diameter	D	6 (mm)
		Length	L	50 (mm)
Shaft coupling	Sleeve	Outer diameter	D_o	23 (mm)
		Inner diameter	D	5 (mm)
		Length	L	17.5 (mm)
	Key	Length	L	17.5 (mm)
		Width	W	2 (mm)
		Thickness	T	2 (mm)

Table 4.5: Maximum bending, shear, and bending stress for brake pedal actuators

Components	Parameter		Values (N/mm^2)	Remark
Brake pedal lead screw	Maximum bending stress		32.78	Maximum bending, shear, and combined stresses are less than the ultimate tensile stress of screw material ($150N/mm^2$)
	The maximum shear stress (for threads)		8.22	
	Tensile or compressive stress		28.11	
	Combined stress	Maximum shear stress theory	18.34	
		Maximum normal stress theory	36.67	

4.4 The motion analysis result of the brake pedal actuator

The motion analysis result of the brake pedal actuator shown in Fig. 4.4 indicates that the stepper motor with 1425 rpm actuates the brake pedal up to 44mm in 2sec. Motor actuation of brake pedal SOLIDWORKS motion analysis result. Motor actuation of brake pedal SOLIDWORKS motion analysis result

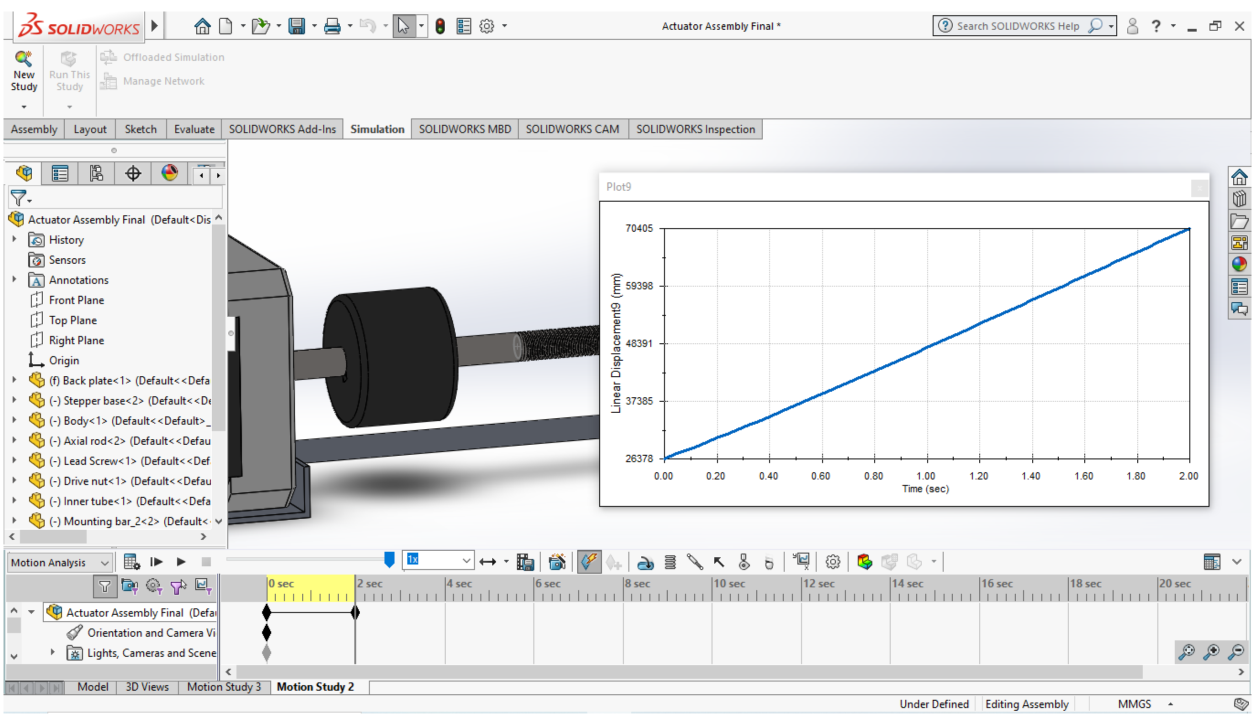

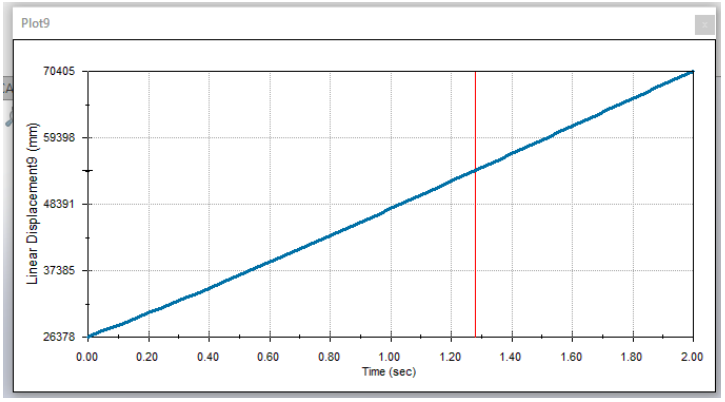

Figure 4.4: Motor actuation result

Actuation Mechanism Motion Analysis result shows that if the combined pedal is released suddenly the lead screw able to extend up to 44 mm within 2 seconds using a stepper motor with 1425rpm which is less costly and requires 12 DC which is already available on the vehicle to provide panic brake. Due to the use of this actuation mechanism instead of transferring the foot between the brake and the accelerator pedal is illuminated. As a result, the stopping distance was reduced to 63m from 70m (at maximum speed and load). Therefore, the combined pedal reduced the stopping distance by 7 (see Table 4.6).

4.5 Stopping distance comparison for existing pedal and combined pedal

When the braking system of the existing or conventional pedal type was compared to the combined pedal brake system the result in Table 4.6 was obtained.

Table 4.6: Combined pedal and conventional pedal comparison in terms of stopping distance.

Vehicle speed, expressed in km/h	Stop distance (m)	
	Conventional pedals	Combined pedal
30	10.25	8.58
40	15.64	13.41
60	30.2	26.03
70	37.71	33.82
100	70	63.03

As the speed of the vehicle increases the stopping distance also increases. They are directly proportional to each other (see Fig 4.5).

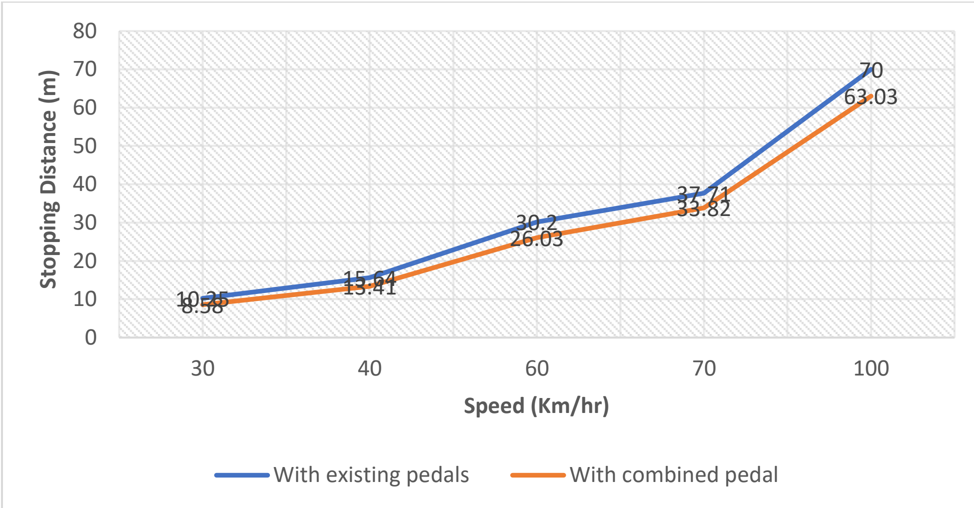

Figure 4.5: Combined pedal and existing pedal stopping distance comparison

4.6 Braking time and stopping distance combined pedal brake system

As the vehicle speed increases both braking and stopping distance increases (that means they are directly proportional to each other) (see Table 4.7).

Table 4.7: Optimized Combined pedal. Braking and stopping distance

Braking time (s)	Vehicle speed (m/s)	Stopping distance (m)
1.36	8.33	8.58
1.81	11.11	13.41
2.72	16.66	26.03
3.17	19.44	33.82
4.53	27.78	63.03

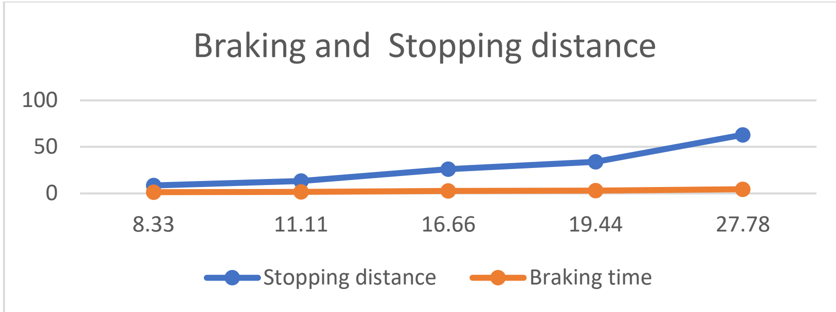

Figure 4.6: Combined pedal stopping and braking distance

4.7 Schematic circuit diagram of electronic system

The two working conditions simulated in the electronic system are normal and braking operating conditions (see Table 4.8).

Table 4.8: Normal operating conditions and braking conditions of a system

System components	Red LED	Green LED	Linear Actuator
Normal operating condition	Do not glow	Give light	Retracts
Braking condition	Give light	Do not glow	Extends

The proteus software was used for schematic circuit diagrams. As a result, the operation of individual components in the circuit was able to be observed.

All the system components were functioned as presented in Table 4.8, both during braking and normal operating conditions. The Arduino code is compiled as a HEX file and uploaded to Proteus. Proteus software is used to test the circuit to check whether the system is working properly. POT-HG in the Proteus library generates different input voltages for the microcontroller. POT-HG allows the resistance to be changed during the simulation run in Proteus. Based on the program developed by Arduino and burned on the microcontroller, the simulation model circuit shows the pedal status. Two conditions continuously measure the pedal position. The three combined pedal positions are shown in Fig. 4.7.

The first position is fully depressed position with pedal angle (measured from floor) 17^0. When it is released first it leaves acceleration region by combination of return spring of acceleration rod and sensing mechanism spring about 30^0 from floor. The further release of the pedal does not have any effect on throttling (stay at released position) as push rod has no any effect on accelerating fork.

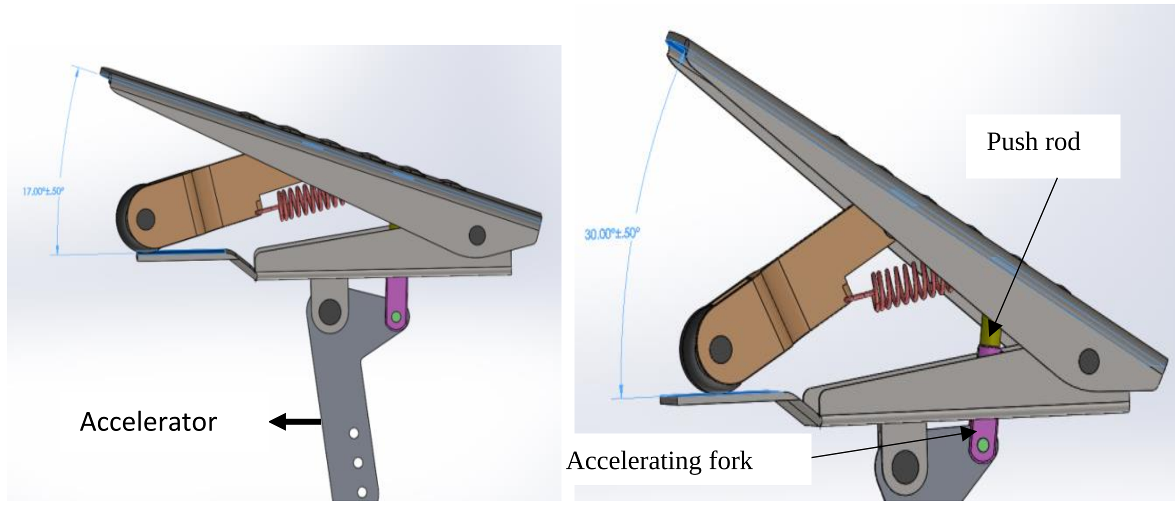

(a) Fully depressed position (b) Combined pedal released position

Figure 4.7: Combined pedal fully depressed position (a) and acceleration released position (b)

Finally, the combined pedal enters the braking region by further release of the pedal beyond 30^0 up to 44^0 measured from floor as shown in Fig. 4.8. During this time the sensor mounted under the pedal senses the movement of the pedal in this region as it released and apply the the brake-on-brake pedal accordingly through brake actuation mechanism (the amount of brake application is following the position of pedal release between 30^0 and 44^0). At 44^0 the brake is at fully applied position.

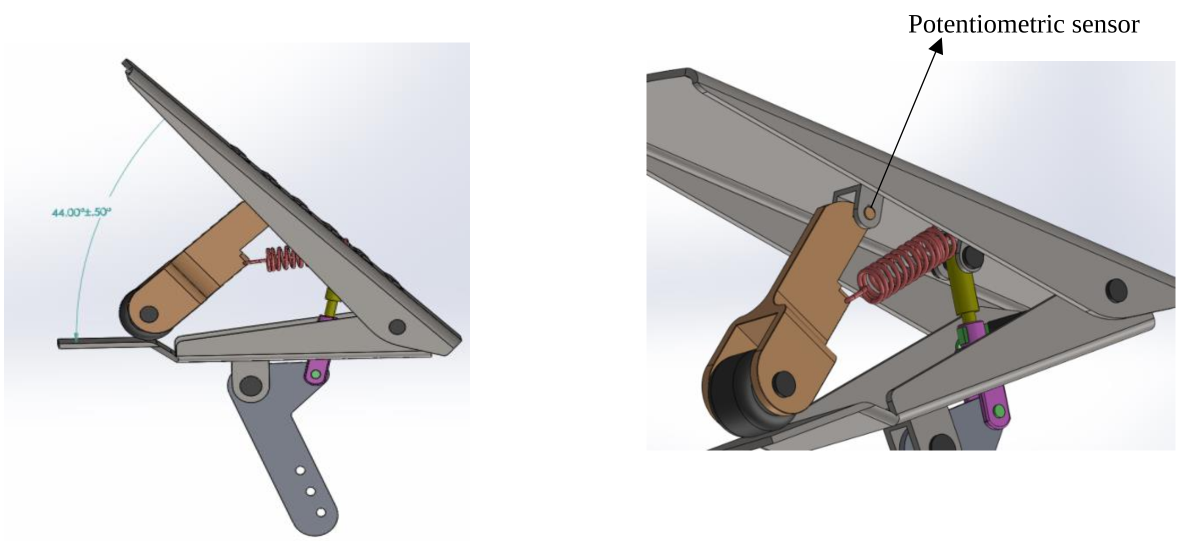

Figure 4.8: Combined pedal fully released position

Condition one: When the pedal is in the accelerating region the system shows the green LED glow-up. In addition, the combined pedal mechanism is designed in a manner that allows the driver to know the pedal position through foot feel as it touches the accelerating fork due to a change in pedal resistance. For the wiring and program simulation see Fig. 4.7. Also, for the imbedded program see Appendix F.

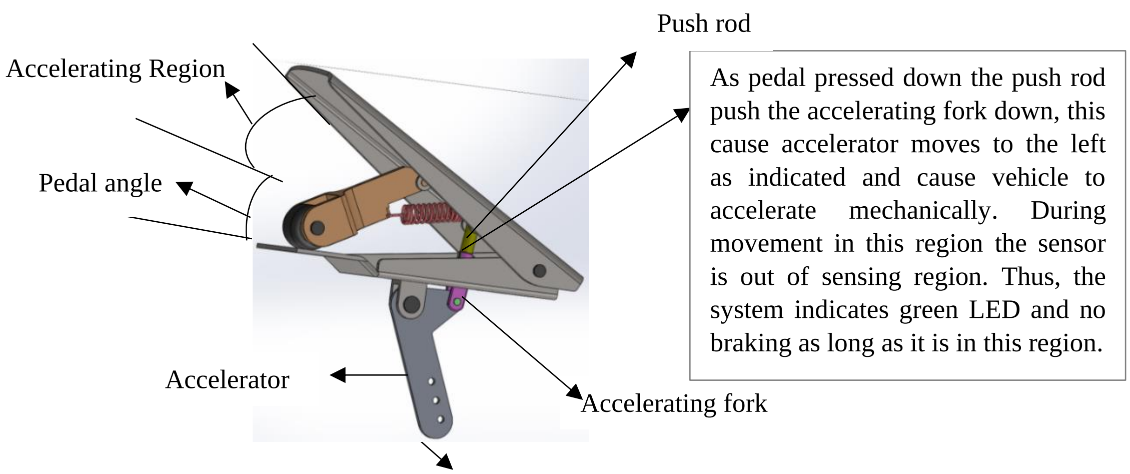

Figure 4.9: Mechanical condition of Combined pedal in accelerating region

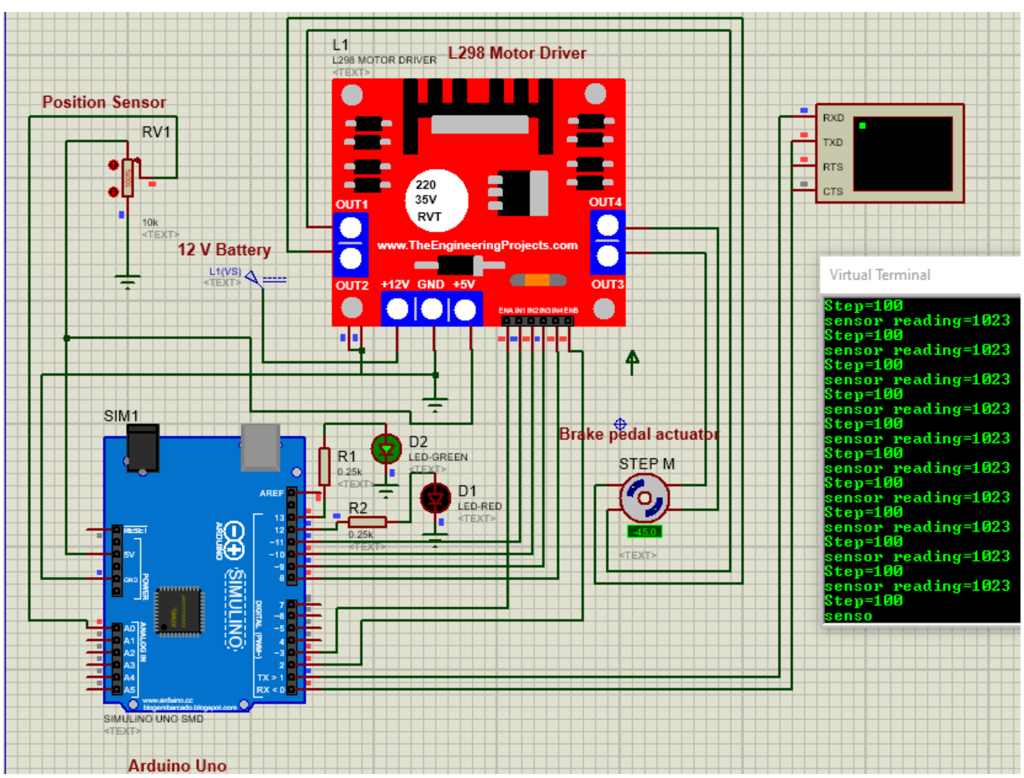

Figure 4.10: Electronic Circuit Diagram Simulation not braked condition

Condition two: When the pedal is in the braking region the system shows the red LED glow-up. In addition, the combined pedal mechanism is designed in a manner that allows the driver to know the pedal position through foot feel as it leaves the accelerating fork due to a change in pedal resistance. (see Fig.4.11.).

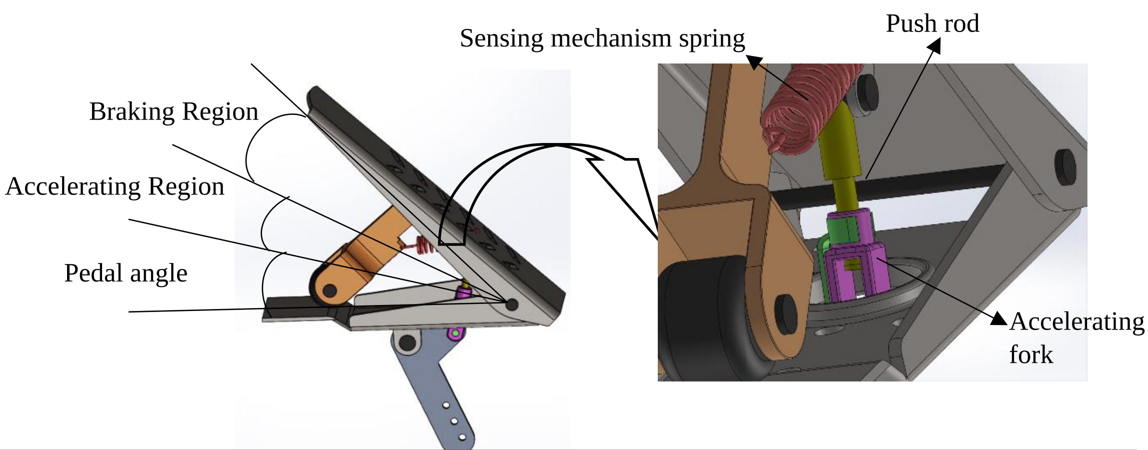

Up and down movement in braking region has no effect on acceleration because the push rod moves freely (due to change in diameter) in accelerating fork as long as the pedal is in Braking region. During movement in this region the foot feel is only by sensing mechanism spring and the sensor senses the position of pedal in this region and apply brake through actuation mechanism in accordance of amount of release. In this region the shows red LED as shown in Fig.4.12.

Figure 4.11 Mechanical condition of combined pedal in braking region

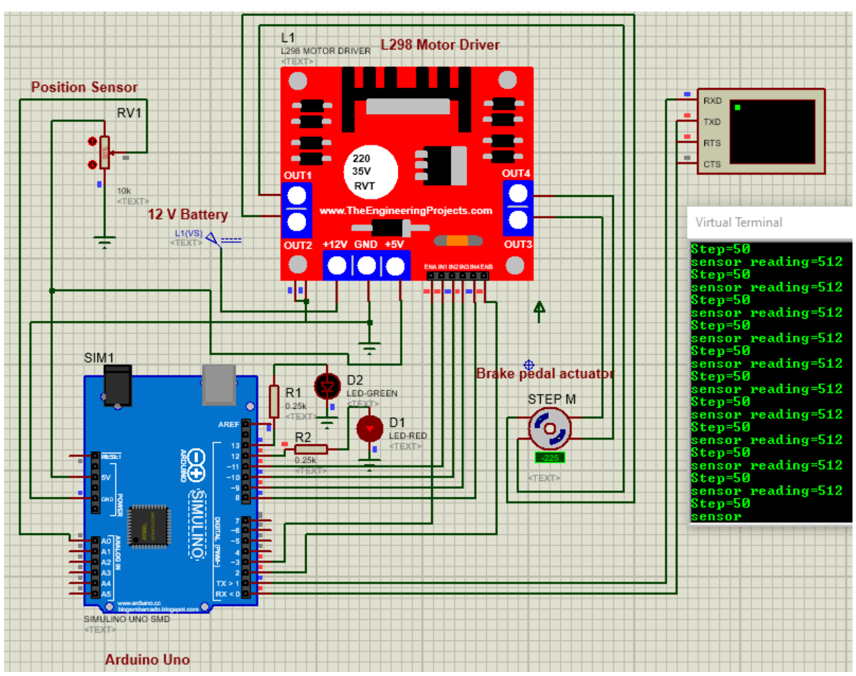

Figure 4.12: Electronic Circuit diagram simulation during Braking

The combined accelerator and brake pedal involves the indicators to inform the position or level of the pedal to the driver in addition to a design mechanism that involves a change in resistance as the driver enters or leaves the accelerating region. Finally, all of the electrical components of the combined accelerator and brake pedal such as; Arduino Uno, position sensor, led, etc. are less costly and can be easily replaced. It is designed in a manner that braking is carried out without the possibility of error, and without interfering with one function with the other.

CHAPTER FIVE

SUMMARY, CONCLUSIONS, AND RECOMMENDATIONS

5.1 Summary

For design of combined accelerator and brake pedal the required information or data are gathered from a reliable source. Then after organization, and analysis, modeling and simulation of the collected data was made using SLIDWORKS software. Finally, using proteus software the simulation of program written in Arduino software was made.

Combined pedal works using a different sensor and electrical component. The system is activated by starting the engine. As a pedal is in the region of the signal to the controller and controller controls brake through the stepper motor. If the pedal is out of range the microcontroller will not receive any signal and the brake will not be applied. The vehicle is in braking condition when the pedal is not pressed. It will first slowly disable braking. Half of the pedal play is given for braking in the combined pedal and with no acceleration at this stage. When the braking is completely disengaged, by further pressing the pedal it can throttle the vehicle. This can be achieved by setting the cable position to the point where the brake is completely released.

In general, Once the pedal is pressed the braking force is released, and when further pressed the car will accelerate. To apply the brake on the vehicle the operator has to slightly release the force off the brake pedal and an emergency situation he/ she has to take his/her foot off the pedal to apply sudden brake.

5.2 Conclusions

Based on result of the design analysis, motion analysis and simulation:

- ✓ The stopping distance at maximum speed and load is reduced to 63m from 70m. Therefore, the combined pedal is selected over the conventional one.
- ✓ As observed through analysis, combined pedal preferable over existing brake and accelerator pedals by reducing collision. so that using a combined one is better than the existing brake and accelerator pedals.

- ✓ All components of the combined accelerator and brake pedal like; potentiometric sensor Microcontroller, (Arduino), LED, and stepper motor are less expensive. And also, can be replaced easily.
- ✓ It designed in a manner that braking is carried out without the possibility of error, and without interfering one function with other.
- ✓ The combined pedal system is not costly for the implementation on any kind of vehicle simply by modifying the accelerator pedal components of the conventional accelerator pedal and motor size further, no need of additional skill of driving from driver.
- ✓ The combined is the best fit for automatic transmission vehicles, as a result, it reduces the foot pedal requirement to only one.
- ✓ In general, it covers both the past and future.

5.3 Recommendations

- ✓ During data collection through the visit of Federal Police Commission to collect the offices refused to provide data. Therefore, to fix the gap it is necessary to give at least one copy of the study.
- ✓ It is important if this combined pedal is used in vehicles such as buses, trucks, etc. (those involve frequent start and stop).
- ✓ The interested researcher can manufacture and assemble the design and interface the system to the minibus taxi vehicle.
- ✓ The other advantage of the combined pedal could be especially useful for elderly drivers.
- ✓ It is the best fit for even Automatic transmission vehicles.

5.4 Future work

Additional study of different scenarios related with a traffic accident is recommended related to a traffic accident. Therefore, it is better to add the following:

- ✓ To implement a combined pedal for the braking system, the design of the existing Engine Control Module is needed. So that it takes sensor information and implement it.
- ✓ Also, it needs further study so that the driver can select speed through his foot by involving a locking system to enable ease of foot control.

REFERENCES

Ahmed M.T.Ibraheem Al-Naib. (2019). *Stepper Motor Stepper Motor Stepper Motor*. *May*.

Bright, D., Daly, T., & Daly, T. (2011). *Identifying Solutions to Pedal Confusion in Buses*. *02*.

Chandra, R., & Kanuru, H. S. (2020). *Combined pedal for brake and accelerator*. *March*, 1–4.

Elsherif, D. M., Abd El-Wahab, A. A., Elgamsy, R. B. M., & Abdellatif, M. H. (2019). Material selection of wind turbine blade using finite element method. *International Journal of Scientific and Technology Research*, *8*(1), 22–32.

Fischer-Cripps, A. C. (2004). Materials data. *The Physics Companion*. https://doi.org/10.1887/0750309539/b1258b1

Gill, H. (2016). *Stepper Motor or Servo Motor : Which should it be ?* 1–8.

Girish, A. R., Safreed, M., Dcosta, A., Hashmi, A. M., & Arshak, M. M. (2021). *A COMBINED PEDAL FOR BRAKE AND*. *8*(8), 688–690.

Gopinath, R. (2014). Design of a power screw. *Middle - East Journal of Scientific Research*, *20*(5), 630–634. https://doi.org/10.5829/idosi.mejsr.2014.20.05.77

Gupta, M., & Bandyopadhyay, S. (2020). Regulatory and Road Engineering Interventions for Preventing Road Traffic Injuries and Fatalities Among Vulnerable Road Users in Low- and Middle-Income Countries: A Systematic Review. *Frontiers in Sustainable Cities*, *2*(May). https://doi.org/10.3389/frsc.2020.00010

Hs, D. O. T. (2015). *Driver Brake and Accelerator Controls and Pedal Misapplication Rates in North Carolina*. *May*.

av, H. K., Sale, O. G., Kumbhar, O. R., Shetti, S. B., Salokhe, S. S., & Sawant, V. V. (2019). Design of Combined Brake and Accelerator Pedal. *IRJET*, *06*(04 Apr), 1491–1493.

Juvinall, R. C., & Marshek, K. M. (2012). *Fundamentals of Machine Component and Design*.

Khakhar, A., Rao, K., Satam, S., & Bobere, F. (2018). *COMBINED PEDAL MECHANISM FOR BRAKING &*. *1*(6), 2320–2321.

Khurmi, R.s.,&Gupta, J. k. (2005). *Khurmi, R. et al.; Theory of Machines , 14th ed.; S. Chand & Co. Ltd., New Dehli 2005; ISBN 9788121925242*.

Macuzic, S., & Lukić, J. (2019). Application of digital human models in determination of the pedal force while driving. *IOP Conference Series: Materials Science and Engineering*, *659*(1), 0–6. https://doi.org/10.1088/1757-899X/659/1/012058

makerspaces. (2018). Arduino For Beginners. *Www.Arduino.Cc*, *4*(2), 457–463.

Matsunaga, K., Ph, D., Naruse, M., Muto, F., Kitamura, F., & Ph, D. (1996). *NEW BRAKE PEDAL AND ACCELERATOR BAR SYSTEM TO PREVENT THE MISTAKE OF PRESSING DOWN THE ACCELERATOR INSTEAD OF THE BRAKE IN EMERGENCY SITUATIONS*. *June*, 1–14.

Mcgehee, D. V, Mazzae, E. N., & Baldwin, G. H. S. (2000). *Iea2000_Abs51*.

Mehsen, J. T., Madhi, Z. S., & Madhi, I. S. (2020). *Spinal Stenosis : What Outcome Should be Expected ? Review the Latest Evidence Using the Assessment of Multiple Systematic Reviews Appraisal Tool (AMSTAR)*. 117–121. https://doi.org/10.4103/MJBL.MJBL

Mugundhan, K., Vishal, V. B., Prakash, B. A., & Raj, M. G. (2018). *COMBINED PEDAL FOR BRAKE AND*. *4*(8), 56–60.

Nilsson, R. (1989). *10 EVALUATION OF A COMBINED ACCELERATOR-BRAKE PEDAL*.

Nilsson, R. (2002). Evaluation of a combined brake-accelerator pedal. *Accident Analysis and Prevention*, *34*(2), 175–183. https://doi.org/10.1016/S0001-4575(01)00011-2

Prithiviraj, N., Balakrishnan, N., Nandhakumar, R., Mohankumar, S., Manikandan, R., Poovarasan, S., Scholar, U. G., Engg, M., & College, G. (2018). *DESIGN & FABRICATION OF COMBINED PEDAL FOR BRAKE & ACCELERATOR SYSTEM*. *1*(1), 6–9.

R. S. Khurmi. (2005). First Multicolour Edition Electrical. In *System: Vol. I* (Issue I).

Ramachandran, N., & Raghul, R. (2017). Design and Fabrication of Brake and Accelerator by using single pedal. *International Journal of Advance Research in Science and Engineering (IARSE)*, *No.6*(No.07), 276–283.

Rittenberry, R. (2005). Hands-on technology: L298N Dual H-Bridge Motor Driver. *Occup Health Saf*, *74*(2), 24.

Robbins, J. (2012). *THE BASICS of LEDs*. 1–72.

Runham, P., Stefanova, T., Skippon, S., Edwards, A., & Helman, S. (2018). *PPR984 The Transport for London Bus Safety Standard : Pedal Application Error Prevention & Recovery Evaluation of Safety Measure*.

Scale, T. H. E., The, O. F., & Safety, R. (2022). Sub-Saharan Africa. *GRSF*, *6/22/22*, 4–7.

Senthil Kumar, S., Palanivendhan, M., Kishore, L., Sameer, S., & Tej, M. (2020). Design and fabrication of combined Pedal for brake and accelerator. *IOP Conference Series: Materials Science and Engineering*, *993*(1). https://doi.org/10.1088/1757-899X/993/1/012148

Shanmugasundar, G., Krishna, A. J., Harish, M., Shankar, P. Y., & Muneeswaran, R. A. M. (2018). Design and Analysis of Automobile Pedal with Combined Brake and Accelerator. *IOSR Journal of Engineering (IOSRJEN)*, *08*(7), 36–40.

Tlomatic. (2021). *Selecting the Optimal Screw Technology*. 24.

Wevj-, P., Boekel, J. J. P. Van, Besselink, I. J. M., & Nijmeijer, H. (2015). *Design and realization of a One-Pedal-Driving algorithm for the TU / e Lupo EL*. *7*, 226–237.

Whitfield, D. (1967). A Review.of: "Man and Motor Cars: An Ergonomic Study." By S. Black. (Seeker and Warburg, 1966.) [Pp. 373.] 63s. *Ergonomics*, *10*(3), 363–364. https://doi.org/10.1080/00140136708930879

WHO. (2018). *GLOBAL STATUS REPORT ON ROAD SAFETY*.

Winner, H., Hakuli, S., Lotz, F., & Singer, C. (2017). Handbook of driver assistance systems:

Basic information, components and systems for active safety and comfort. *Handbook of Driver Assistance Systems: Basic Information, Components and Systems for Active Safety and Comfort*, 1–1602. https://doi.org/10.1007/978-3-319-12352-3

Xi, Y., Brooks, J., Venhovens, P., Rosopa, P., Desjardins, J., McConomy, S., Belle, L., Drouin, N., Hennessy, S., Kopera, K., McKee, J., Tanner, S., Truesdail, C., Lococo, K., & Staplin, L. (2018). Understanding the Automotive Pedal Usage and Foot Movement Characteristics of Older Drivers. *SAE Technical Papers*, *2018-April*. https://doi.org/10.4271/2018-01-0495

Yared, A. (2019). *Design and Development of Automated Pneumatic Braking Control System for Sinotruck.*

Yukon community and transportation services. (2019). *Air brake manual* (pp. 129–132).

.

B-E-N. (2022). *what is an Arduino*. (Sparkfun) Retrieved March 22, 2022, from https://learn.sparkfun.com/tutorials/what-is-an-arduino/all#:~:text=Arduino%20is%20an%20open%2Dsource%20platform%20used%20for%20building%20electronics%20projects.

Nilsson, R. (2018). Evaluation of a combined brake-accelerator pedal. *www.elsevier.com/locate/aap*, 175-183.

Richard G. Budynas & J, K. N. (2011). *Shigleys's Mechanical Engineering Design.* Kate Gleason College of Engineerig, Rochester Institute of Technology New York: Mc Graw Hill.

Team, F. A. (2018, August 01). *Firgelli Automations*. Retrieved from Inner working of a linear Actuators: https://www.firgelliauto.com/blogs/news/inside-a-linear-actuator-how-a-linear-actuator-works

APPENDICES

Appendix A: Traffic accident report by different vehicle types (Four year's)

የ ፌ ዴ ራ ል ፖ ሊ ስ ኮ ሚ ሽ ን

የ2009 አገር አቀፍ የትራፊክ አደጋ ስታትስቲክስ መንጠሪያ

የሚሸፍነው ጊዜ ከሐምሌ 1/2008 እስከ ሰኔ 30/2009 ዓ/ም

		አደጋ የፈፀሙ ተሽከርካሪዎች ዓይነት																			
		1	2	3	4	5	6	7	8	9	10	11	12	13	14	15	16	17	18	19	
ተራ ቁጥር	አደጋው ያስከተለው ጉዳት	ተራ ብስክሌት	ሞተር ብስክሌት	አውቶሞቢል	ስቴሽን ዋገን	ፒክአፕ እስከ 10 ኩንታል	የጭነት ከ11 - 40 ኩንታል	የጭነት ከ41 -100 ኩንታል	የጭነት ከተሳቢ	ቦቴ	ታክሲ	የሕዝብ እስከ 1200 መቀመጫ	የሕዝብ ከ13-45 መቀመጫ	የሕዝብ ከ46 በላይ	ልዩ ተንቀሳቃሽ መሳሪያ	ልዩ ተንቀሳቃሽ ከተሳቢ	ጋሪ	ባቡር	ሌላ	ያልታወቀ	ድምር
1	ሞት	34	156	214	131	195	397	486	213	125	462	410	415	110	22	21	36		54	94	3,575
2	ከባድ የአካል ጉዳት	19	291	301	274	554	324	297	103	24	859	636	274	118	20	15	18		79	145	4,351
3	ቀላል የአካል ጉዳት	17	193	184	91	260	194	184	69	41	540	410	109	169	24	22	24		99	59	2,.689
4	የንብረት ጉዳት	57	241	4,264	1,873	3,941	2,300	1,792	829	114	6,066	3,374	1434	651	58	34	97		474	236	27,835
ድ ም ር		127	881	4,963	2,369	4,950	3,215	2,759	1,214	304	7,927	4,830	2,232	1,048	124	92	175	0	706	534	38,450

የፌደራል ፖሊስ ኮሚሽን

የ2010 አገር አቀፍ የትራፊክ አደጋ ስታትስቲክስ ሠንጠረዥ

የሚሸፍነው ጊዜ ከሐምሌ 1/2009 እስከ ሰኔ 30/2010 ዓ/ም

		አደጋ የፈፀሙ ተሽከርካሪዎች ዓይነት																			
ተራ ቁጥር	አደጋው ያስከተለውጉዳት	1	2	3	4	5	6	7	8	9	10	11	12	13	14	15	16	17	18	19	ድምር
		ተራ ብስክሌት	ሞተር ብስክሌት	አውቶሞቢል	ስቴሽን ዋገን	ፒክአፕ እስከ 10 ኩንታል	የጭነት ከ11 - 40 ኩንታል	የጭነት ከ41 -100 ኩንታል	የጭነት ከነተሳቢ	ቦቴ	ታክሲ	የሕዝብ እስከ 12 መቀመጫ	የሕዝብ ከ13-45 መቀመጫ	የሕዝብ ከ46 በላይ	ልዩ ተንቀሳቃሽ መሳሪያ	ልዩ ተንቀሳቃሽ ከነተሳቢ	ጋሪ	ባቡር	ሌላ	ያልታወቀ	
1	ሞት	19	201	182	129	269	370	434	195	123	266	536	625	103	24	19	35	0	148	142	3,820
2	ከባድ የአካል ጉዳት	25	482	501	251	478	376	253	90	30	868	573	433	48	25	18	11	1	149	128	4,740
3	ቀላል የአካል ጉዳት	26	215	220	156	282	227	157	63	45	663	357	176	80	17	16	22	0	254	97	3,073
4	የንብረት ጉዳት	43	773	5798	1839	4756	2314	1646	825	54	4679	3236	2015	436	105	38	103	1	411	293	29,365
ድ ም ር		113	1,671	6,701	2,375	5,785	3,287	2,490	1,173	252	6,476	4,702	3,249	667	171	91	171	2	962	660	40,998

የፌዴራል ፖሊስ ኮሚሽን

የ2011አገር አቀፍ የትራፊክ አደጋ ስታትስቲክስ ሠንጠረዥ

የሚሸፍነው ጊዜ ከሐምሌ 1/2010 እስከ ሰኔ 30/2011ዓ/ም

ተራ ቁጥር	አደጋው ያስከተለው ጉዳት	አደጋ የፈፀሙ ተሽከርካሪዎች ዓይነት																				ድምር
		1	2	3	4	5	6	7	8	9	10	11	12	13	14	15	16	17	18	19	20	
		ተራ ብስክሌት	ሞተር ብስክሌት	አውቶሞቢል	ስቴሽን ዋገን	ፒክአፕ እስከ 10 ኩንታል	የጭነት ከ11 - 40 ኩንታል	የጭነት ከ41 -100 ኩንታል	የጭነት ከተሳቢ	ሎቤድ	ታንከር	የሕዝብ እስከ 1200 መቀመጫ	የሕዝብ ከ13-45 መቀመጫ	የሕዝብ ከ46መቀመጫ በላይ	ልዩ ተንቀሳቃሽ መሳሪያ	ልዩ ተንቀሳቃሽ ከተሳቢ	ጋሪ	[illegible]	ባጃጅ	ሌላ	ያልታወቀ	
1	ሞት	28	238	136	104	256	348	402	161	121	358	599	532	193	22	14	32	1	-	81	112	3,738
2	ከባድ የአካል ጉዳት	34	378	500	240	468	320	238	112	25	768	646	246	64	17	10	15	-	-	105	138	4,324
3	ቀላል የአካል ጉዳት	12	143	375	202	220	158	140	40	23	517	305	129	62	16	13	17	-	-	155	60	2,587
4	የንብረት ጉዳት	48	552	6,288	2,055	3,984	1,919	1,727	599	134	6,641	3,532	1,360	647	74	48	68	-	-	192	354	30,222
ድ ም ር		122	1,311	7,299	2,601	4,928	2,745	2,507	912	303	8,284	5,082	2,267	966	129	85	132	1	-	533	664	40,871

2012 ዓ/ም የተሽከርካሪው ዓይነት

ተራ ቁጥር	አደጋው ያስከተለው ጉዳት	1	2	3	4	5	6	7	8	9	10	11	12	13	14	15	16	17	18	19	20	ድምር
		[illegible]	[illegible]	[illegible]	[illegible]	[illegible]	[illegible]	[illegible]	[illegible]	[illegible]	[illegible]	[illegible]	[illegible]	[illegible]	[illegible]	[illegible]	[illegible]	[illegible]	ባጃጅ	ሌላ	[illegible]	
1	ሞት	63	265	126	123	177	227	397	146	143	438	542	289	158	54	46	81	3	49	84	166	3,577
2	ከባድ የአካል ጉዳት	33	398	553	238	301	376	285	82	23	588	739	165	76	28	20	20	-	54	111	196	4,286
3	ቀላል የአካል ጉዳት	22	180	339	123	161	131	75	38	16	379	273	157	70	23	23	17	-	42	130	48	2,247
4	የንብረት ጉዳት	76	303	7,934	2,065	3,160	1,981	1,456	403	198	5,267	3,895	1,134	1,041	106	73	62	-	45	166	342	29,707
ድምር		194	1,146	8,952	2,549	3,799	2,715	2,213	669	380	6,672	5,449	1,745	1,345	211	162	180	3	190	491	752	39,817

Appendix B: Accident reports of traffic (three year's)

<u>ከሐምሌ 1 ቀን 2008 እስከ ሰኔ 30 ቀን 2009 ዓ/ም ድረስ ባለው የአንድ ዓመት ጊዜ በአገር አቀፍ ደረጃ የደረሰ የትራፊክ አደጋና</u>

<u>በትራፊክ አደጋ ተጎጂ የሆኑ ሰዎች ብዛት በጉዳት ዓይነትና በጾታ</u>

ክልል መስተዳድር	የደረሰው የትራፊክ አደጋ ብዛት					በትራፊክ አደጋ ተጎጂ የሆኑ ግለሰቦች ብዛት								ጠቅላላ ድምር	በትራፊክ አደጋ በንብረት ላይ የደረሰ ጉዳት በገንዘብ ሲተመን	REGION
						ሞት		ከባድ የአካል ጉዳት		ቀላል የአካል ጉዳት		ድምር				
	ሞት	ከባድ የአካል ጉዳት	ቀላል የአካል ጉዳት	የንብረት ጉዳት	ድምር	ወንድ	ሴት	ወንድ	ሴት	ወንድ	ሴት	ወንድ	ሴት			
ትግራይ	303	339	55	489	1,186	254	117	471	193	254	102	979	412	1,391	59,191,154.70	Tigray
አፋር	90	50	14	201	355	112	19	124	40	58	21	294	80	374	80,558,700.00	Afar
አማራ	796	502	565	1,167	3,030	807	228	860	330	1,355	635	3,022	1,193	4,215	366,798,848.10	Amhara
ኦሮሚያ	1,188	568	518	1,626	3,900	1,157	384	1,068	391	1,056	429	3,281	1,204	4,485	153,004,478.00	Oromia
ሶማሌ	125	171	10	15	321	128	29	327	81	257	139	712	249	961	35,276,000.00	Somalia
ቤን/ጉሙዝ	31	98	114	44	287	26	7	180	44	254	141	460	192	652	9,711,900.00	Ben.Gumuz
ደቡብ	523	553	210	181	1,467	486	148	734	256	688	249	1908	653	2561	28,744,008.00	S N N P
ጋምቤላ	13	23	49	68	153	12	4	30	8	56	45	98	57	155	6,983,860.00	Gambella
ሐረሪ	42	55	206	248	551	43	10	82	41	165	119	290	170	460	23,047,644.08	Harari
አ/አበባ	466	1,996	973	23,510	26,945	367	110	1,619	466	885	347	2,871	923	3,794	417,922,804.00	A/ Ababa
ድሬዳዋ	29	94	89	330	542	26	5	98	43	112	68	236	116	352	6,247,405.00	Dire Dawa
ድምር	3,606	4,449	2,803	27,879	38,737	3,41	1,061	5,593	1,893	5,140	2,295	14,151	5,249	19,400	1,187,486,802.88	Total
						4,479		7,486		7,435		19,400				
	Death	Serious Injury	Slight Injury	Property Damage	General Total	Male	Female	Male	Female	Male	Female	Total Male	Total Female	General Total	Total Property Damage Estimate In Birr	
						Death		Serious Injury		Slight Injury						
	NUMBER OF TRAFFIC ACCIDENTS					VICTMS OF MOTOR VEHICLE TRAFFIC ACCIDENTS						ALL CASES				

ከሐምሌ 1 ቀን 2009 እስከ ሰኔ 30 ቀን 2010 ዓ/ም ድረስ ባለው የአንድ ዓመት ጊዜ በአገር አቀፍ ደረጃ የደረሰ የትራፊክ አደጋና

በትራፊክ አደጋ ተጎጂ የሆኑ ሰዎች ብዛት በጉዳት ዓይነትና በጾታ

ክልል መስተዳድር	የደረሰው የትራፊክ አደጋ ብዛት					በትራፊክ አደጋ ተጎጂ የሆኑ ግለሰቦች ብዛት: ሞት		ከባድ የአካል ጉዳት		ቀላል የአካል ጉዳት		ድምር		ጠቅላላ ድምር	በትራፊክ አደጋ በንብረት ላይ የደረሰ ጉዳት በገንዘብ ሲተመን	REGION
	ሞት	ከባድ የአካል ጉዳት	ቀላል የአካል ጉዳት	የንብረት ጉዳት	ድምር	ወንድ	ሴት	ወንድ	ሴ ት	ወንድ	ሴት	ወንድ	ሴት			
ትግራይ	301	459	97	550	1,407	268	106	632	226	447	137	1,347	469	1,816	47,397,561.18	Tigray
አፋር	53	24	6	71	154	66	6	40	9	26	5	132	20	152	89,781,800.00	Afar
አማራ	857	502	575	1098	3,032	882	270	848	333	1349	575	3,079	1,178	4,257	326,101,815.1	Amhara
ኦሮሚያ	1319	729	532	1806	4,386	1475	407	1286	424	1072	514	3,833	1,345	5,178	236,362,117.	Oromia
ሶማሌ	142	219	33	16	410	164	40	391	142	369	78	924	260	1,184	35,850,000.00	Somalia
ቤን/ጉሙዝ	24	78	122	42	266	32	4	97	29	157	58	286	91	377	4,970,550.00	Ben.Gumuz
ደቡብ	582	608	199	154	1,543	557	163	829	292	648	274	2,034	729	2,763	29,557,590.00	S N N P
ጋምቤላ	15	15	21	38	89	13	5	13	7	30	18	56	30	86	3,894,677.50	Gambella
ሐረሪ	31	102	286	346	765	25	9	146	78	277	230	448	317	765	22,972,900.00	Harari
አ/አበባ	456	1903	1074	24928	28,361	392	193	1481	323	819	413	2,692	929	3,621	109,882,371	A/ Ababa
ድሬዳዋ	40	101	128	316	585	31	10	97	31	169	110	297	151	448	13,999,933.00	Dire Dawa
ድምር	3,820	4,740	3,073	29,365	40,998	3,905	1,213	5,860	1,894	5,363	2,412	15,128	5,519	20,647	920,771,314.78	Total
						5,118		7,754		7,775		20,647				
	Death	Serious Injury	Slight Injury	Property Damage	General Total	Male	Female	Male	Female	Male	Female	Total Male	Total Female	General Total	Total Property Damage Estimate In Birr	
						Death		Serious Injury		Slight Injury						
	NUMBER OF TRAFFIC ACCIDENTS					VICTMS OF MOTOR VEHICLE TRAFFIC ACCIDENTS						ALL CASES				

ከሐምሌ 1 ቀን 2010 እስከ ሰኔ 30 ቀን 2011 ዓ/ም ድረስ ባለው የአንድ ዓመት ጊዜ በአገር አቀፍ ደረጃ የደረሰ የትራፊክ አደጋና

በትራፊክ አደጋ ተጎጂ የሆኑ ሰዎች ብዛት በጉዳት ዓይነትና በጾታ

ክልል መስተዳድር	የደረሰው የትራፊክ አደጋ ብዛት					በትራፊክ አደጋ ተጎጂ የሆኑ ግለሰቦች ብዛት								ጠቅላላ ድምር	በትራፊክ አደጋ በንብረት ላይ የደረሰ ጉዳት በገንዘብ ሲተመን	REGION
						ሞት		ከባድ የአካል ጉዳት		ቀላል የአካል ጉዳት		ድምር				
	ሞት	ከባድ የአካል ጉዳት	ቀላል የአካል ጉዳት	የንብረት ጉዳት	ድምር	ወንድ	ሴት	ወንድ	ሴት	ወንድ	ሴት	ወንድ	ሴት			
ትግራይ	329	483	60	640	1,512	290	96	618	236	257	124	1,165	456	1,621	96,524,434.82	Tigray
አፋር	36	33	11	114	194	52	4	66	7	13	7	131	18	149	35,480,300	Afar
አማራ	881	441	376	893	2,591	833	271	765	267	897	355	2,495	893	3,388	305,167,314	Amhara
ኦሮሚያ	1,209	535	480	1,738	3,962	1,096	382	1,057	391	1,046	340	3,199	1,113	4,312	189,972,568	Oromia
ሶማሊ	93	73	20	15	201	109	23	94	33	80	54	283	110	393	24,400,000	Somalia
ቤን/ጉሙዝ	43	89	114	45	291	88	3	95	41	172	94	355	138	493	3,808,500	Ben.Gumuz
ደቡብ	594	536	105	85	1,320	584	128	865	287	511	214	1,960	629	2,589	30,600,469	S N N P
ጋምቤላ	14	23	22	46	105	12	7	28	15	46	35	86	57	143	7,501,198.17	Gambella
ሐረሪ	48	87	119	152	406	38	17	133	70	113	75	284	162	446	23,891,986	Harari
አ/አበባ	460	1,926	1,143	26,019	29,548	406	122	1,745	465	1,006	268	3,157	855	4,012	141,822,992	A/ Ababa
ድሬዳዋ	31	98	137	475	741	24	12	101	28	178	64	303	104	407	13,715,119	Dire Dawa
ድምር	3,738	4,324	2,587	30,222	40,871	3,532	1,065	5,567	1,840	4,319	1,630	13,418	4,535	17,953	872,884,881	Total
						4,597		7,407		5,949		17,953				
	Death	Serious Injury	Slight Injury	Property Damage	General Total	Male	Female	Male	Female	Male	Female	Total Male	Total Female	General Total	Total Property Damage Estimate In Birr	
						Death		Serious Injury		Slight Injury						
	NUMBER OF TRAFFIC ACCIDENTS					VICTMS OF MOTOR VEHICLE TRAFFIC ACCIDENTS						ALL CASES				

Appendix C: Accident causes by vehicles their output

2011ዓ/ም አሽከርካሪውን ለአደጋ ያበቁ ምክንያቶች

ተራ ቁጥር	ምክንያቶች	አደጋው ያስከተለው ጉዳት				ድምር
		ሞት	ከባድ የአካል ጉዳት	ቀላል የአካል ጉዳት	የንብረት ጉዳት	
1	ሰክሮ መንዳት	3	1	-	90	94
2	በእጽ ደንዝዞ መንዳት	-	-	1	46	47
3	ቀኝን ለቆ መንዳት	138	166	74	1,380	1,808
4	ለተሽከርካሪ ቅድሚያ ባለመስጠት	100	239	154	7,259	7,752
5	ለእግረ ቅድሚያ ባለመስጠት	1,112	1,970	1,086	574	4,742
6	ርቀት ጠብቆ አለመከተል	362	171	183	8,074	8,790
7	ኮረብታ ሜዳ ላይ በመቅደም	17	15	2	22	56
8	ጠምዛዛ (ኩርባ) መንገድ ላይ በመቅደም	3	4	3	43	53
9	ከቀደመ በኋላ ድንገት ታጥፎ በመግባት	9	25	9	1,091	1,134
10	ከተ ሰን ፍጥነት በላይ በመንዳት	702	671	344	2,974	4,691
11	አላግባብ በመቅደም	150	158	25	2,350	2,683
12	አላግባብ በመታጠፍ	35	30	20	2,229	2,314
13	የትራፊክ ፖሊስ ትዕዛዝ በመጣስ	1	-	-	74	75
14	የትራፊክ መብራት በመጣስ	-	1	-	206	207
15	የትራፊክ መብራት በመጣስ	1	1	-	78	80
15	የቁም ምልክት በመጣስ					
16	ቅድሚያ ስጥ የሚል ምልክት በመጣስ	1	42	3	840	886
17	ከቆመበት አላግባብ በመነሳት	13	13	6	342	374
18	አላግባብ በማቆም	8	3	4	281	296
19	በድካም ወይም በመተኛት	3	3	3	17	26
20	በሌሳብ በመዋዋ	1	10	7	1	19
21	አላግባብ በማብራት	2	2	2	1	7
22	አላግባብ በመጫን	44	113	114	259	530
23	የፍሬን ጉድለት	194	85	90	219	588
24	የጎማ መ ለቅ	172	86	76	304	638
25	የጎማ መፈንዳት	8	15	10	9	42
26	የመሪ ጉድለት	173	99	95	300	667
27	የመንገድ ጉድለት	13	7	8	15	43
28	የእግረኛ ጉድለት	53	24	40	32	149
29	ሌላ	148	218	160	722	1,248
30	ያልታወቀ	222	152	68	390	832
	ድ ም ር	3,738	4,324	2,587	30,222	40,871

2012 ዓ/ምዓ/ም አሽከርካሪውን ለአደጋ ያበቁ ምክንያቶች

ተራ ቁጥር	ምክንያቶች	አደጋው ያስከተለው ጉዳት				ድምር
		ሞት	ከባድ የአካል ጉዳት	ቀላል የአካል ጉዳት	የንብረት ጉዳት	
1	ሰክሮ መንዳት	24	11	11	46	92
2	በእጽ ደንዝዞ መንዳት	5	8	1	9	23
3	ቀኝን ለቆ መንዳት	140	239	100	1,299	1,778
4	ለተሽከርካሪ ቅድሚያ ባለመስጠት	101	210	112	8,212	8,635
5	ለእግረኛ ቅድሚያ ባለመስጠት	958	1,847	1,015	1,097	4,917
6	ርቀት ጠብቆ አለመከተል	248	209	186	7,912	8,555
7	ከረብታ ጫፍ ላይ በመቅደም	3	11	3	692	709
8	ጠምዛዛ (ከርቭ) መንገድ ላይ በመቅደም	17	15	4	261	297
9	ከተፈቀደ በላይ ደንነት ታቀዶ በመግባት	13	13	5	792	823
10	ከተወሰነ ፍጥነት በላይ በመንዳት	854	807	338	1,517	3,516
11	አላግባብ በመቅደም	57	93	34	1,635	1,819
12	አላግባብ በመታጠፍ	37	31	13	2,254	2,335
13	የትራፊክ ፖሊስ ትዕዛዝ በመጣስ	8	2	3	500	513
14	የትራፊክ መብራት በመጣስ	2	2	-	362	366
15	የትራፊክ መብራት በመጣስ	1	9	10	123	143
15	የቁም ምልክት በመጣስ					
16	ቅድሚያ ስጥ የሚል ምልክት በመጣስ	2	3	-	407	412
17	ከቆመበት አላግባብ በመነሳት	13	16	13	358	400
18	አላግባብ በማቆም	12	7	2	246	267
19	በድካም ወይም በመተኛት	10	5	1	31	47
20	በአሳብ በመዋጥ	8	3	3	28	42
21	አላግባብ በማሳለፍ	3	20	-	1	24
22	አላግባብ በመጫን	53	90	8	100	251
23	የፍሬን ጉድለት	182	128	58	345	713
24	የጎማ መላቅ	125	8	60	188	381
25	የጎማ መፈንዳት	9	76	7	3	95
26	የመሪ ጉድለት	222	6	50	160	438
27	የመንገድ ጉድለት	14	7	3	13	37
28	የእግረኛ ጉድለት	30	29	12	-	71
29	ሌላ	163	182	122	753	1,220
30	ያልታወቀ	262	199	73	363	897
	ድ ም ር	3,576	4,286	2,247	29,707	39,816

Appendix D: Up to 2012 Vehicle statics in Ethiopia.

From Information Communication Technology Directorate

Type of Vehicles and Number in the Regions (up to sene 30.2013) Registration												
Descriptio	AA	AM	AF	BN	DD	SO	TG	GM	HA	SN	OR	Total
Ambulance	322	0	90	56	6	45	187	0	4	65	590	1365
Automobil	255793	1834	86	56	2413	648	1994	0	1303	104	5758	269989
Bajaj	0	11381	4608	0	3302	0	0	1439	4909	12901	65218	103758
Tri Cyle	0	0	0	0	0	0	0	0	0	0	0	0
Bus(< 12 Se	31330	9787	494	393	1666	979	5656	2125	80	13874	29068	95452
Bus(> 11 S	19206	14802	713	526	860	871	4473	859	3000	12579	39631	97520
Combiner	106	61	0	0	2	1	5	0	0	0	78	253
Dozer	16	1	3	3	0	1	4	0	0	0	0	28
Dry Cargo(	52338	3825	351	109	1083	1104	1298	0	0	176	2187	62471
Dry Cargo(	139376	3767	267	117	4670	2604	5148	0	0	233	8201	164383
Dual Purpo	56063	4258	486	343	1704	989	2266	0	56	1712	3028	70905
Field Vehic	53233	2066	389	164	524	1148	1282	0	300	206	3266	62578
Grader	6	2	0	0	2	1	4	0	0	0	2	17
Forklift	351	0	4	1	10	1	18	0	0	0	2	387
Not Specifi	21185	1621	72	57	327	511	397	0	0	2540	2293	29003
Gotach	7235	0	0	0	67	5	624	0	0	0	0	7931
Liquid Carg	8307	331	39	2	244	186	658	0	0	67	184	10018
Liquid Trail	0	14	0	0	0	0	0	0	0	0	0	14
Motor Bicy	28235	48997	1454	7385	8111	1651	14405	2643	1076	80466	63359	257782
Other	12526	778	35	39	137	33	485	0	0	44	4304	18381
Three whe	17	281	0	56	10	250	1874	0	0	0	9	2497
Three whe	350	13807	0	3111	0	8523	16647	0	0	0	0	42438
Tractor	1505	415	54	146	21	0	317	0	0	33	1015	3506
Trailer	32676	381	8	1	450	1	2913	0	0	1	408	36839
Vehicle wit	1004	158	21	1	134	27	145	0	0	0	0	1490
Total	**721180**	**118567**	**9174**	**12566**	**25743**	**19579**	**60800**	**7066**	**10728**	**125001**	**228601**	**1339005**

ማሳሰቢያ፡- የአዲስ አበባ ተሽከርካሪ ከሁሉም ክፍለከተሞች የተሰበሰበው መረጃ መርጅ በሚደረግበት ጊዜ ካለፈው ቁጥር ጋር ሲነፃፀር ዝቅ በማለቱ ከ6ወር በፊት በተሰጠው መረጃ መሰረት እንዲሆን እንገልፃለን፡፡

Appendix E: Parts and assembly drawings for combined pedal and its actuation system

Table: Properties of components materials for combined pedal (Fischer-Cripps, 2004).

Components	Materials	Tensile strength	Yield Strength	Shear modulus	Elastic modulus	Poisson's ratio
Treadle and Base	Stainless steel sheet	580 Mpa	172.369 Mpa	-	1.99e+11 Mpa	0.27
Push rod	Stainless Steel	685 Mpa	292 Mpa	-	2.07e+11 Pa	0.27
Spring and Mounting bracket	Alloy steel	723.8256 Mpa	620.422 Mpa	7.9e+10 Pa	2.1e+11 Pa	0.32
Collars /washers	Carbon steel	482.549 Mpa	248.168 Mpa	7.6000 Mpa	2e+11 Pa	0.32
Knuckle pins	Alloy Steel	723.8256 Mpa	620.422 Mpa	7.9e+10 Pa	2.1e+11 Pa	0.28
Sensing bar	Aluminum	689.356 Mpa	275.742 Mpa	2.7e+10 Pa	6.9e+10 Pa	0.33
Wheel	Rubber	20 Mpa	-	-	10 Kpa	0.45
Accelerator lever and Fork	Aluminum (6061) alloy	124.084 Mpa	551.485 Mpa	2.6e+10 Pa	6.9e+10 Pa	0.33

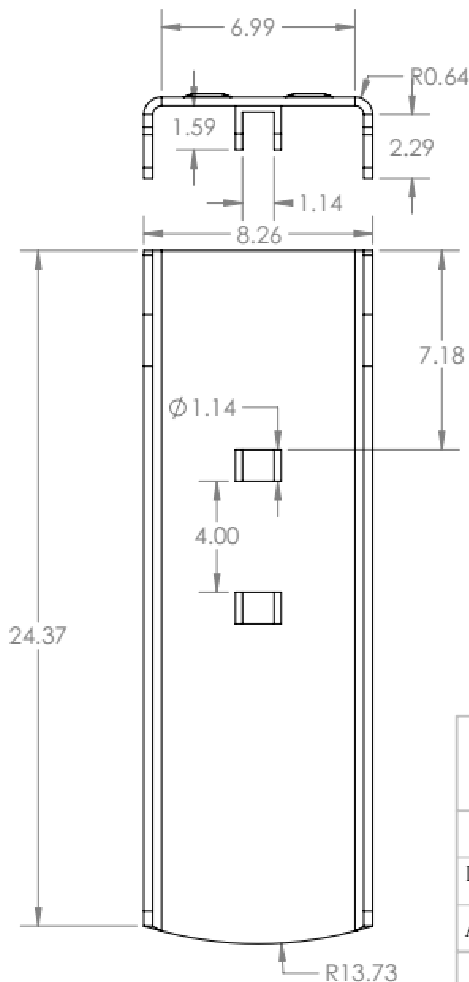

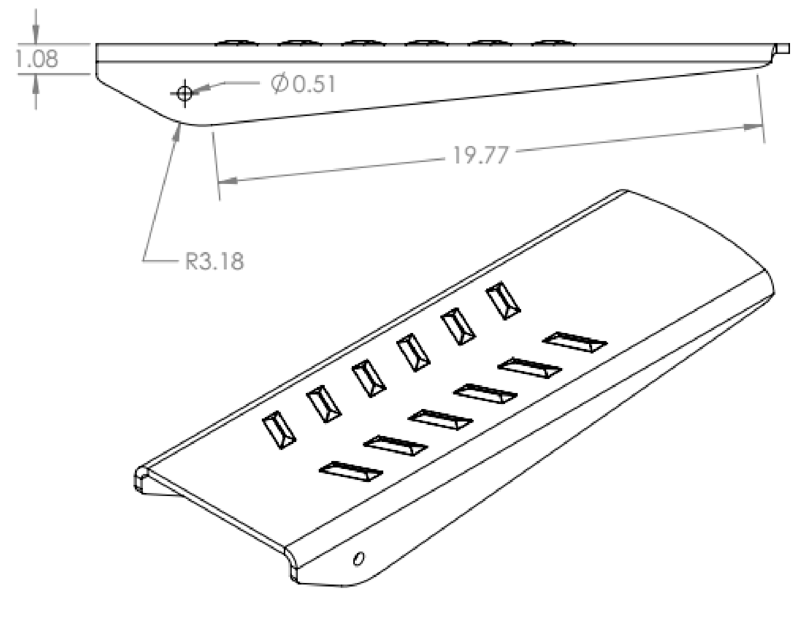

ASTU

	NAME	DATE
DRAWN BY	Udesa G.	
APPV'D		xxx

All dimensions are in cm

DRAWING TITLE

Treadle

MATERIAL
Stainless steel sheet

DRAWING NO XXX

A4

WEIGHT XXX

SCALE:1:5

SHEET 1 OF 1

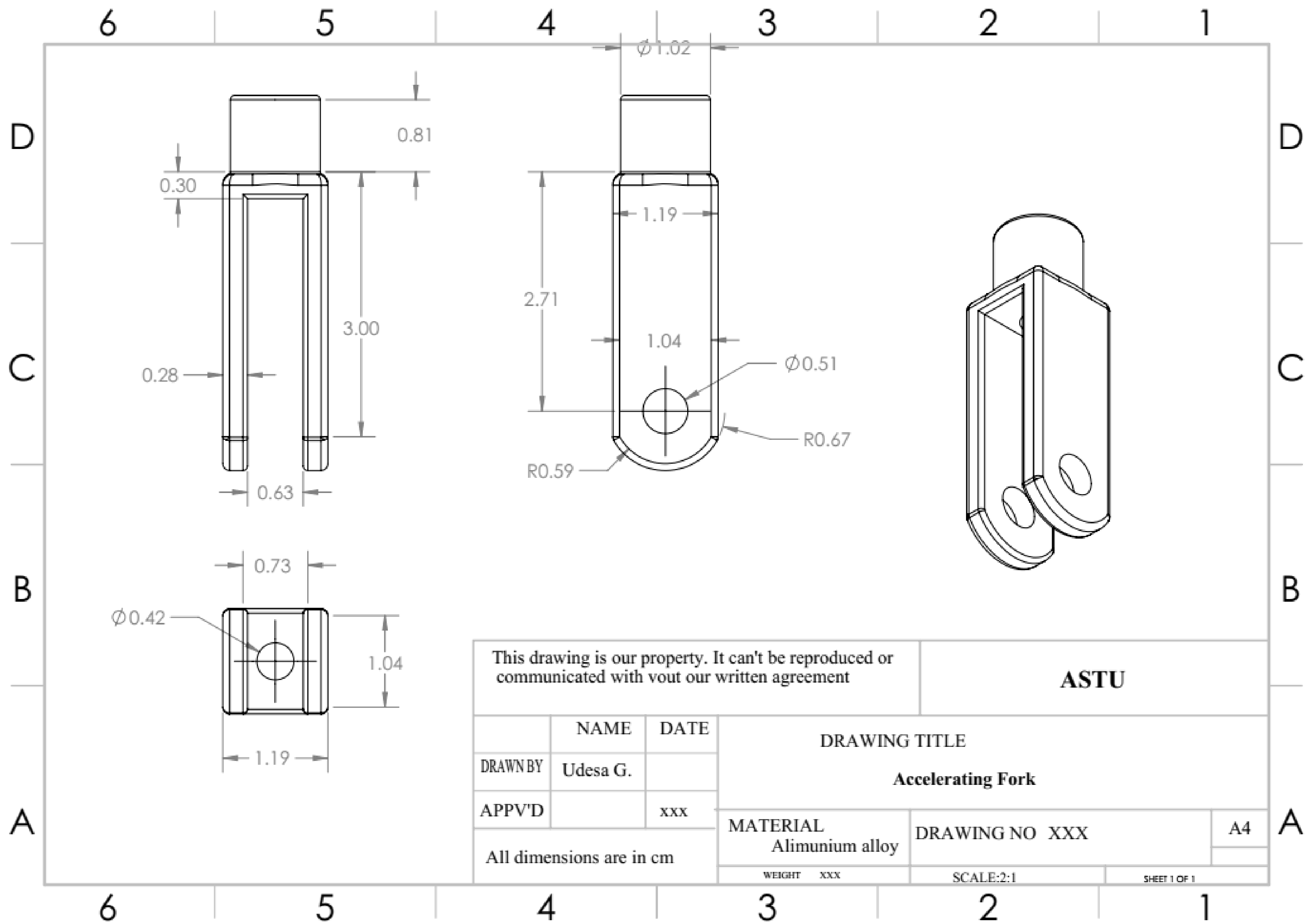

Ø1.02
0.81
0.30
3.00
2.71
1.19
1.04
Ø0.51
R0.67
R0.59
0.28
0.63
0.73
Ø0.42
1.04
1.19
This drawing is our property. It can't be reproduced or communicated with vout our written agreement
ASTU
NAME
DATE
DRAWN BY
Udesa G.
APPV'D
xxx
All dimensions are in cm
DRAWING TITLE
Accelerating Fork
MATERIAL
Alimunium alloy
DRAWING NO XXX
A4
WEIGHT XXX
SCALE:2:1
SHEET 1 OF 1

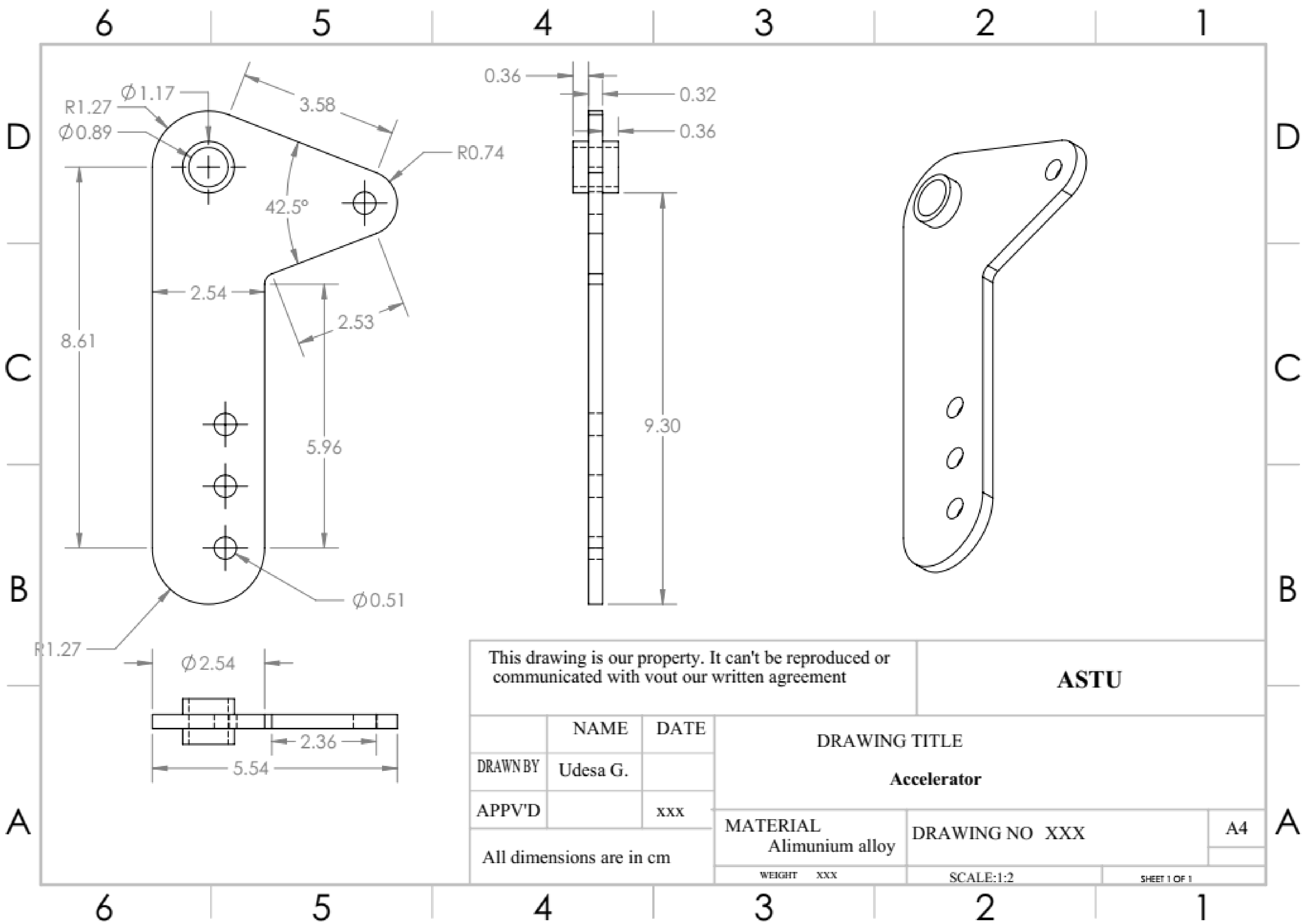
6
5
4
3
2
1
D
C
B
A
R1.27
Ø1.17
Ø0.89
3.58
R0.74
42.5°
8.61
2.54
2.53
5.96
Ø0.51
R1.27
0.36
0.32
0.36
9.30
Ø2.54
2.36
5.54
This drawing is our property. It can't be reproduced or communicated with vout our written agreement
ASTU
NAME
DATE
DRAWN BY
Udesa G.
APPV'D
xxx
All dimensions are in cm
DRAWING TITLE
Accelerator
MATERIAL
Alimunium alloy
DRAWING NO XXX
A4
WEIGHT XXX
SCALE:1:2
SHEET 1 OF 1

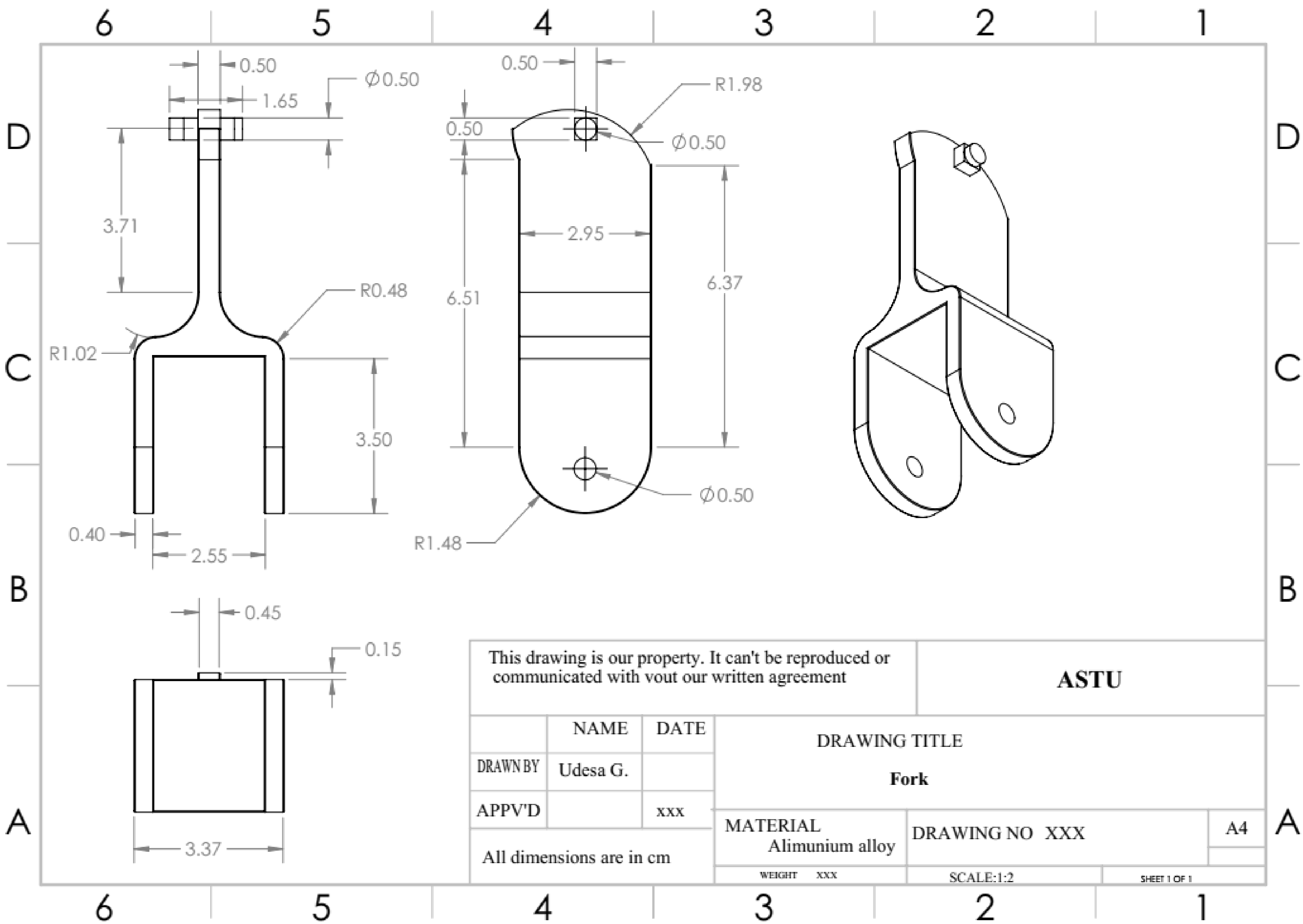

0.50
1.65
Ø0.50
3.71
R0.48
R1.02
3.50
0.40
2.55
0.50
R1.98
0.50
Ø0.50
2.95
6.51
6.37
Ø0.50
R1.48
0.45
0.15
3.37
This drawing is our property. It can't be reproduced or communicated with vout our written agreement
ASTU
NAME
DATE
DRAWN BY
Udesa G.
APPV'D
xxx
All dimensions are in cm
DRAWING TITLE
Fork
MATERIAL
Alimunium alloy
DRAWING NO XXX
A4
WEIGHT XXX
SCALE:1:2
SHEET 1 OF 1

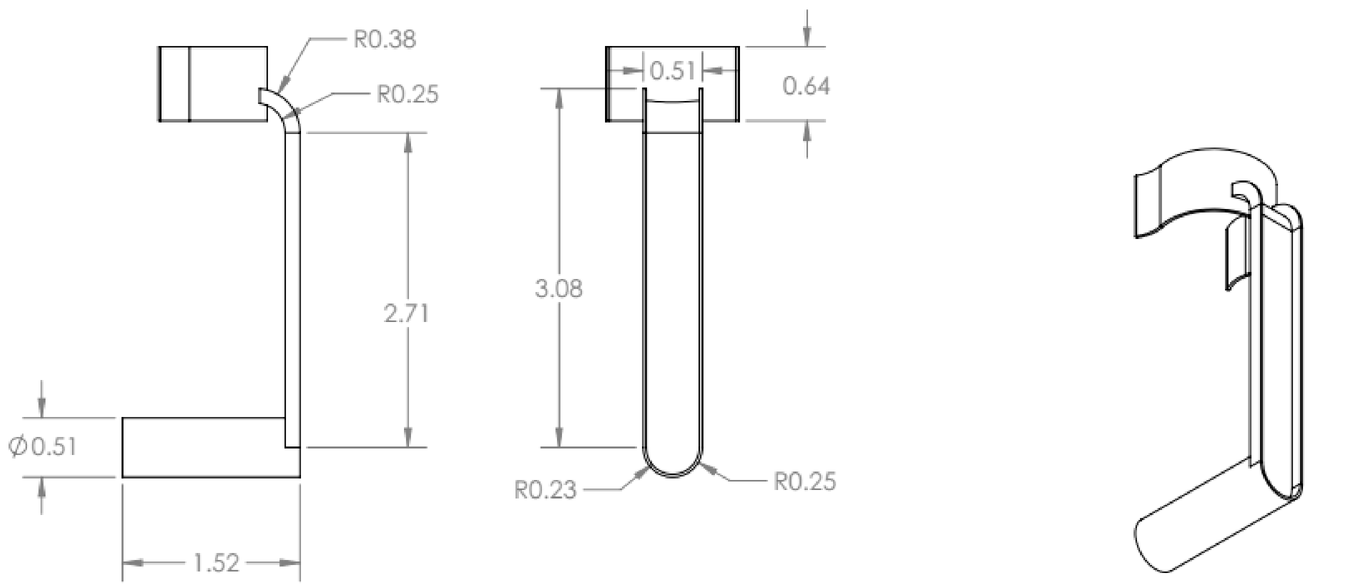

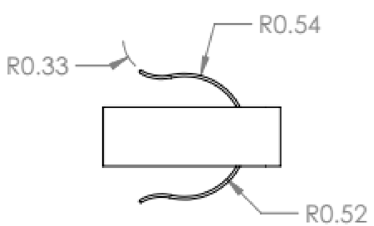

This drawing is our property. It can't be reproduced or communicated with vout our written agreement			**ASTU**	
	NAME	DATE	DRAWING TITLE **Mounting Braket**	
DRAWN BY	Udesa G.			
APPV'D		xxx	MATERIAL Carbon Steel	DRAWING NO XXX	A4
All dimensions are in cm			WEIGHT XXX	SCALE:2:1	SHEET 1 OF 1

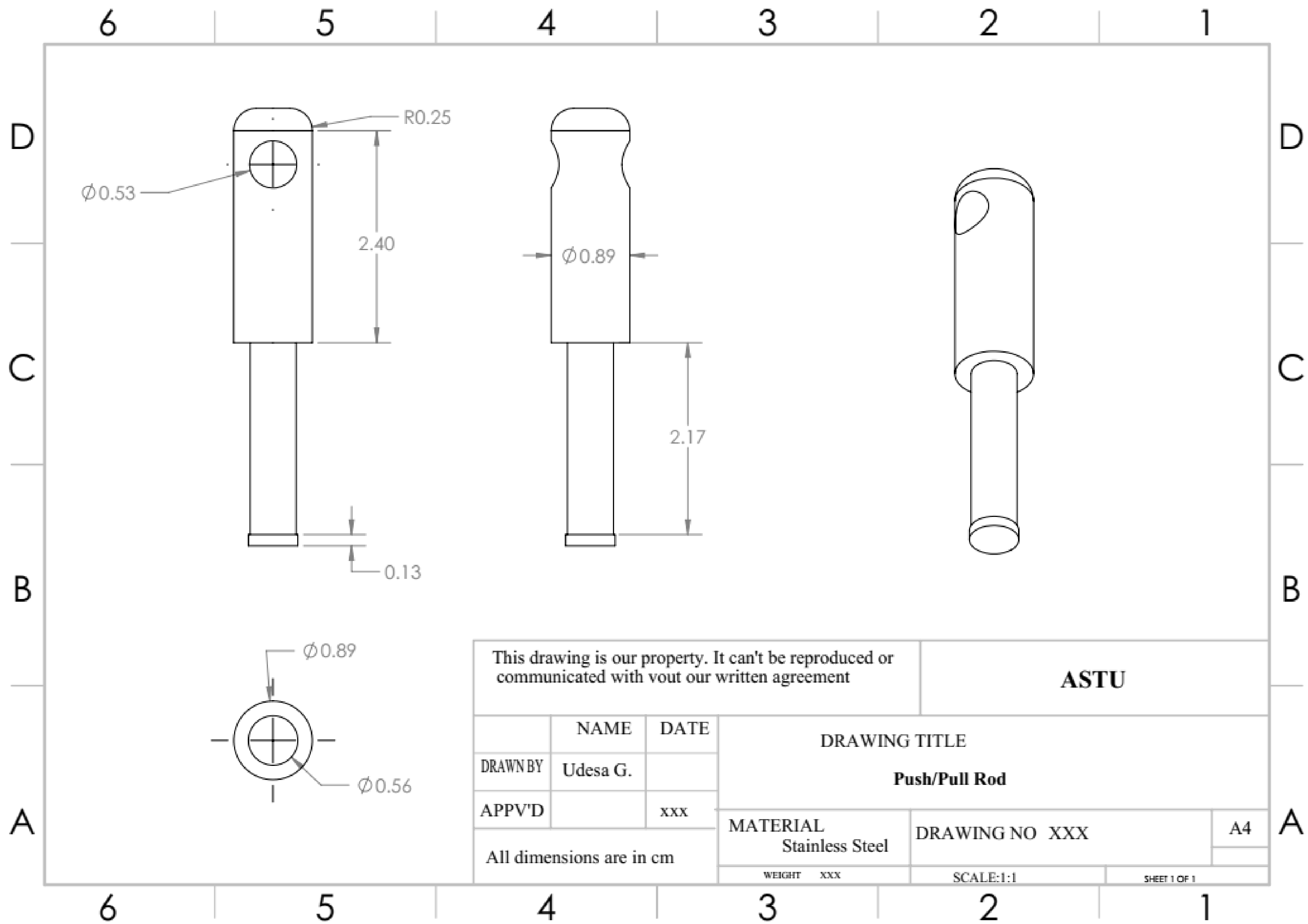
R0.25
∅0.53
2.40
∅0.89
2.17
0.13
∅0.89
∅0.56
This drawing is our property. It can't be reproduced or communicated with vout our written agreement
ASTU
NAME
DATE
DRAWN BY
Udesa G.
APPV'D
xxx
All dimensions are in cm
DRAWING TITLE
Push/Pull Rod
MATERIAL
Stainless Steel
DRAWING NO XXX
A4
WEIGHT XXX
SCALE:1:1
SHEET 1 OF 1

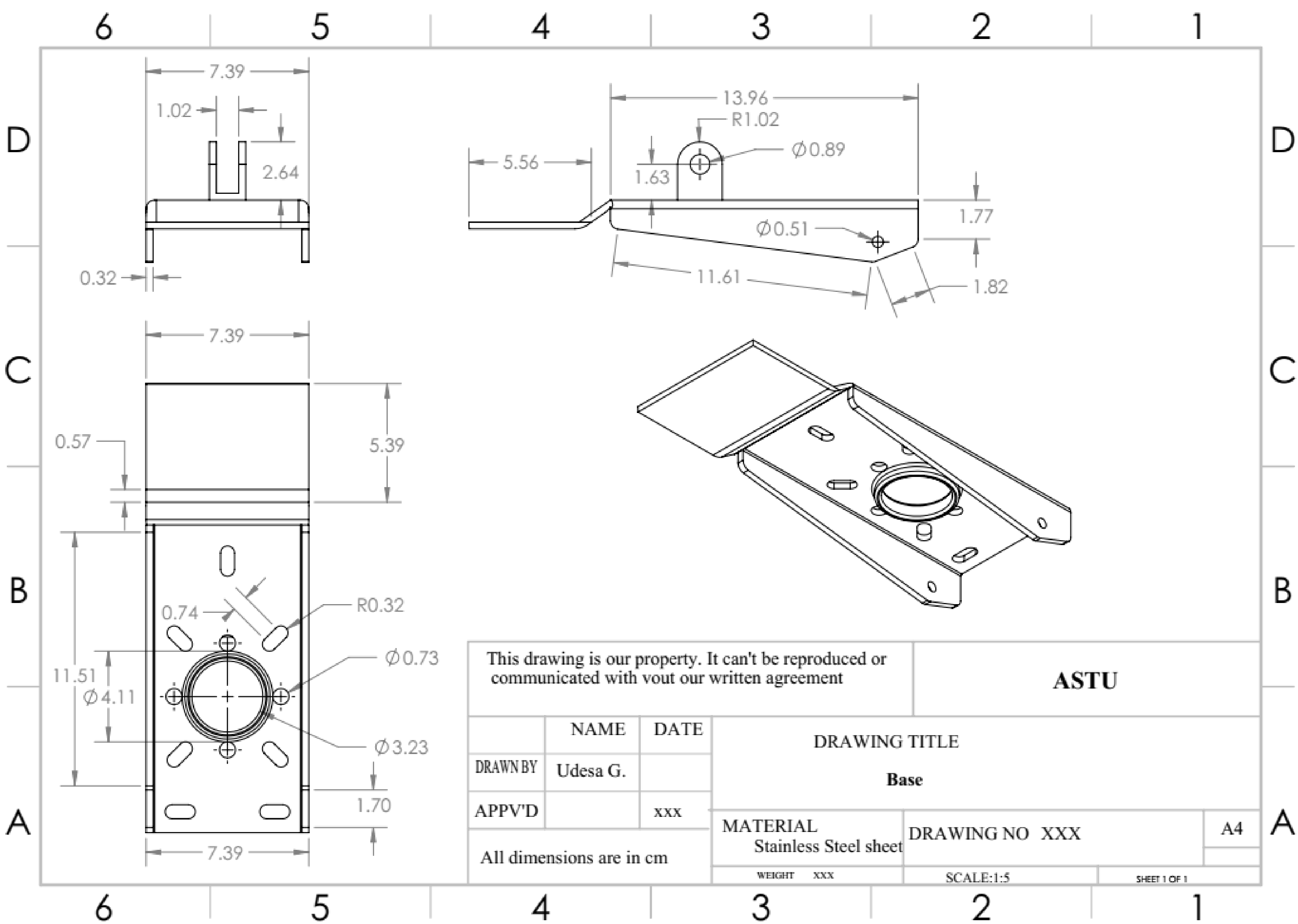
7.39
1.02
2.64
0.32
13.96
R1.02
∅0.89
5.56
1.63
1.77
∅0.51
11.61
1.82
7.39
0.57
5.39
0.74
R0.32
11.51
∅0.73
∅4.11
∅3.23
1.70
7.39
This drawing is our property. It can't be reproduced or communicated with vout our written agreement
ASTU
NAME
DATE
DRAWN BY
Udesa G.
APPV'D
xxx
All dimensions are in cm
DRAWING TITLE
Base
MATERIAL
Stainless Steel sheet
DRAWING NO XXX
A4
WEIGHT XXX
SCALE:1:5
SHEET 1 OF 1

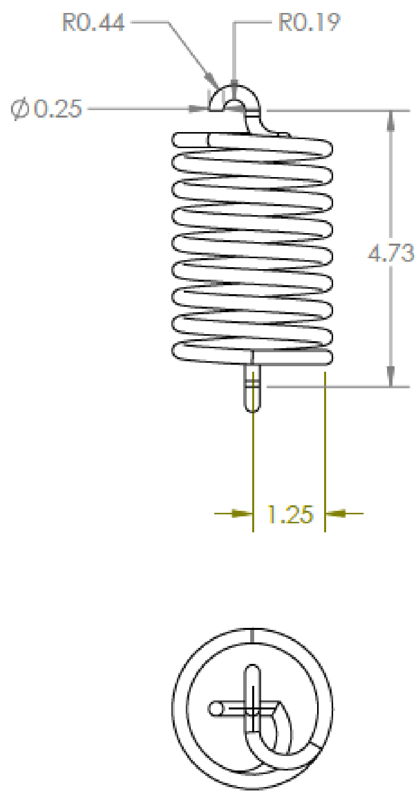

This drawing is our property. It can't be reproduced or communicated with vout our written agreement		ASTU

	NAME	DATE	DRAWING TITLE
DRAWN BY	Udesa G.	07/2022	Return spring
APPV'D		xxx	

All dimensions are in cm	MATERIAL Alloy steel	DRAWING NO XXX	A4
	WEIGHT XXX	SCALE:1:2	SHEET 1 OF 1

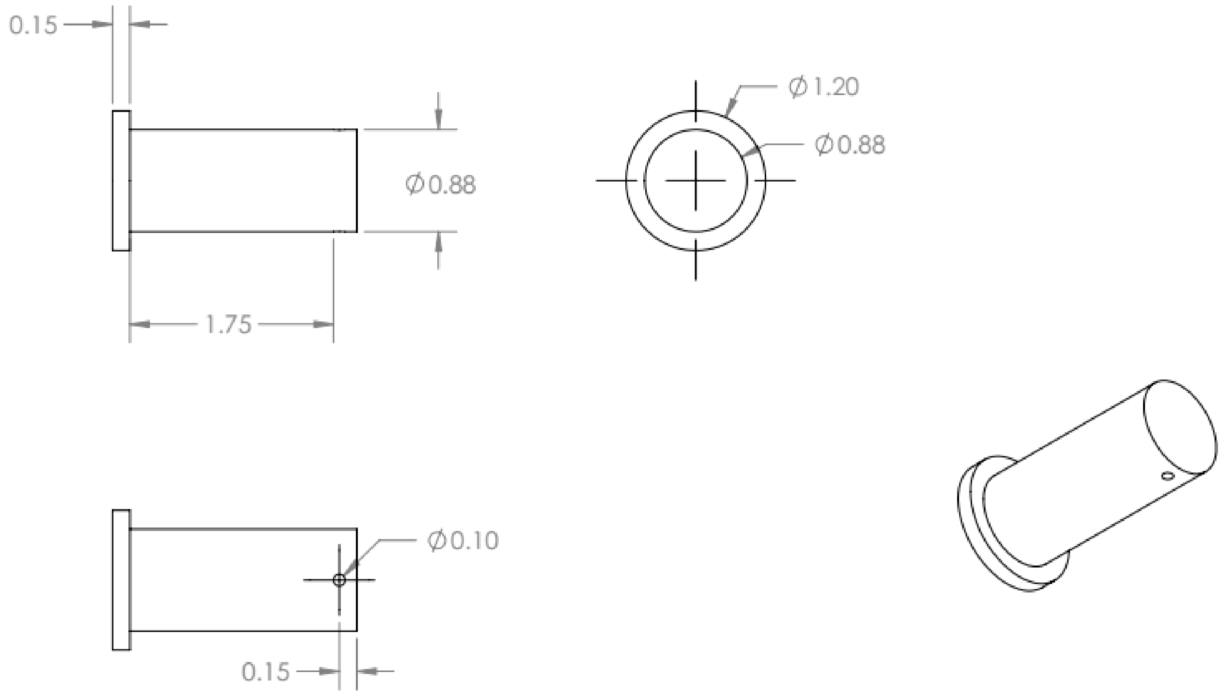

This drawing is our property. It can't be reproduced or communicated with vout our written agreement

ASTU

	NAME	DATE
DRAWN BY	Udesa G.	
APPV'D		xxx

All dimensions are in cm

DRAWING TITLE

Knucle pin

MATERIAL Alloy Steel	DRAWING NO XXX	A4
WEIGHT XXX	SCALE:2:1	SHEET 1 OF 1

xx

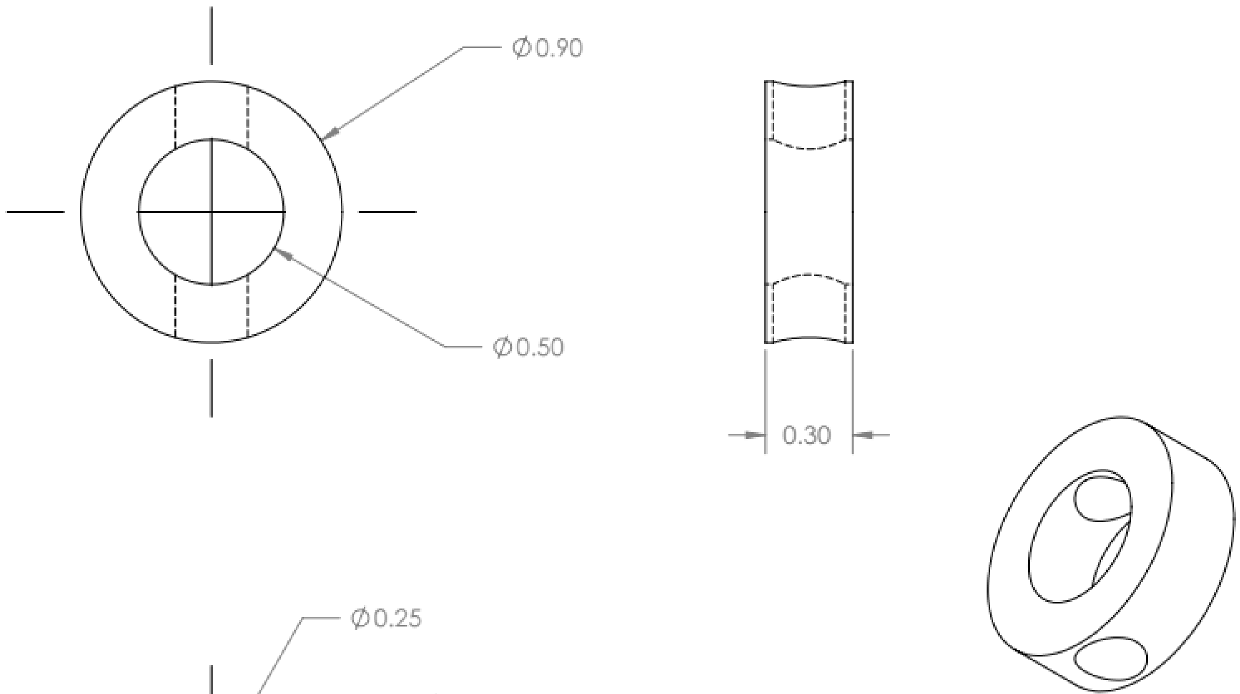

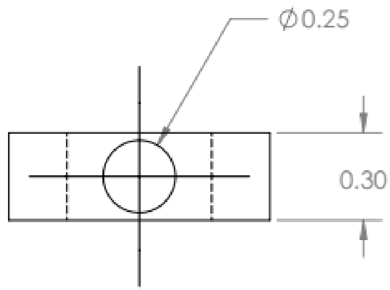

This drawing is our property. It can't be reproduced or communicated with vout our written agreement			**ASTU**		
	NAME	DATE	DRAWING TITLE **Collar**		
DRAWN BY	Udesa G.				
APPV'D		xxx	MATERIAL Alloy Steel	DRAWING NO XXX	A4
All dimensions are in cm			WEIGHT XXX	SCALE:5:1	SHEET 1 OF 1

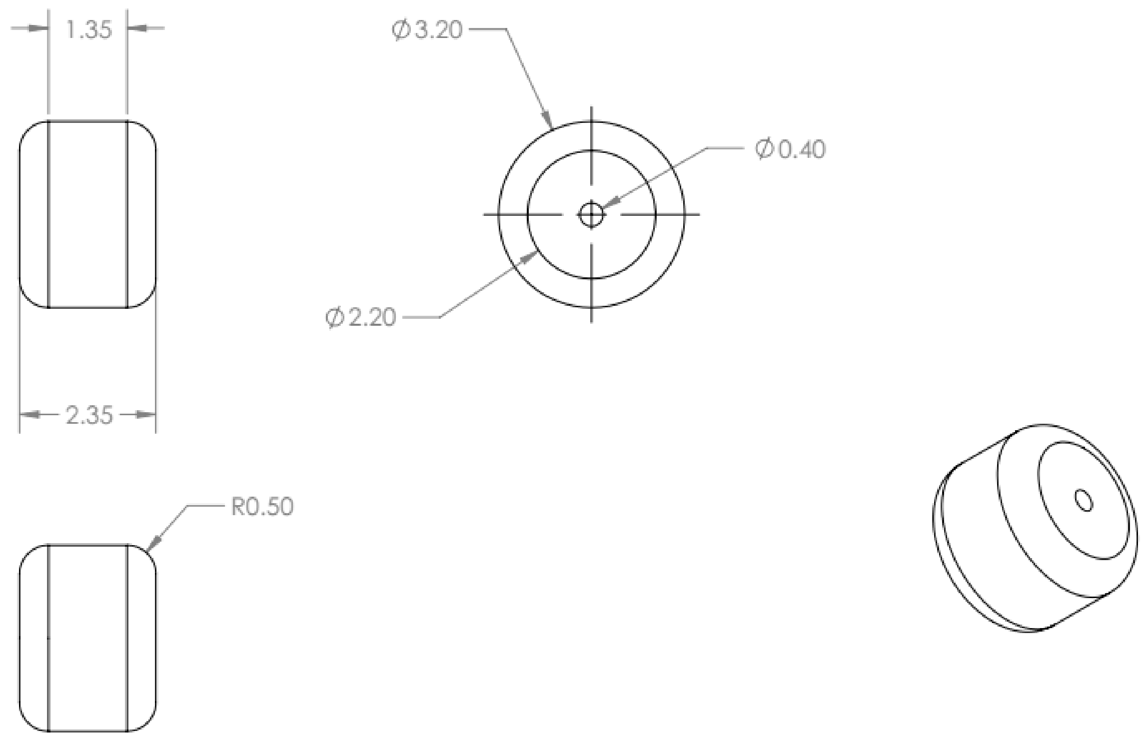

This drawing is our property. It can't be reproduced or communicated with vout our written agreement			ASTU		
	NAME	DATE	DRAWING TITLE **Wheel**		
DRAWN BY	Udesa G.				
APPV'D		xxx	MATERIAL Rubber	DRAWING NO XXX	A4
All dimensions are in cm			WEIGHT XXX	SCALE:1:1	SHEET 1 OF 1

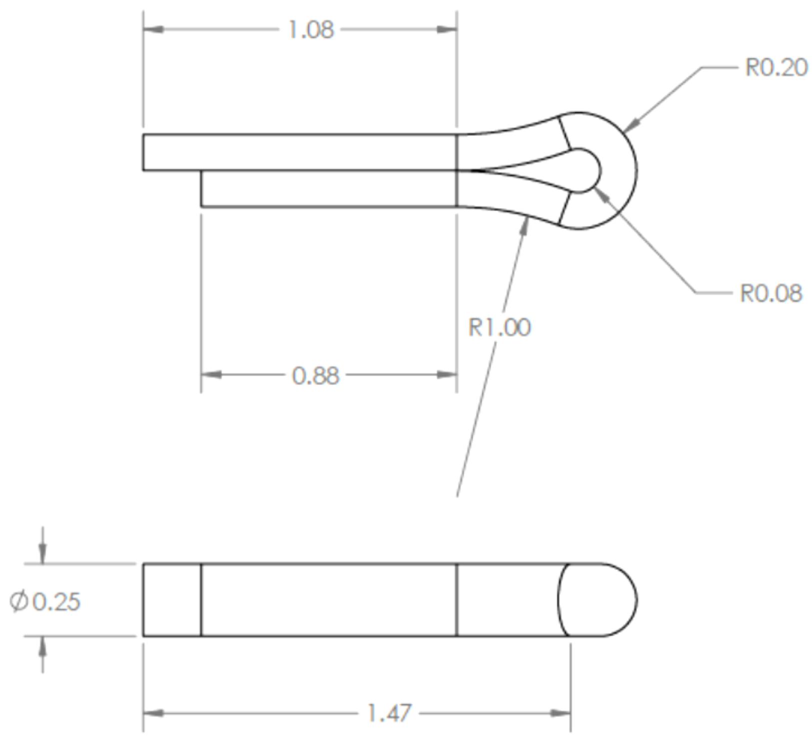

This drawing is our property. It can't be reproduced or communicated with vout our written agreement

ASTU

	NAME	DATE
DRAWN BY	Udesa G.	07/2022
APPV'D		xxx

All dimensions are in cm

DRAWING TITLE

Pin

MATERIAL

Carbon steel

WEIGHT XXX

DRAWING NO XXX

A4

SCALE:1:2

SHEET 1 OF 1

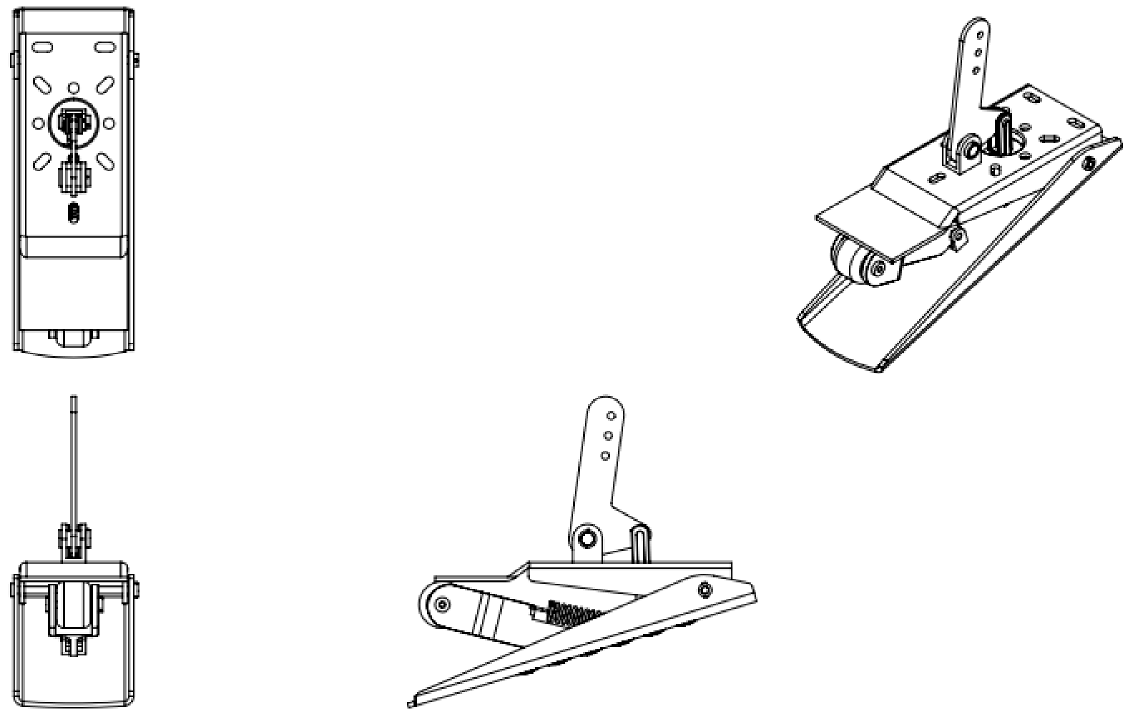

This drawing is our property. It can't be reproduced or communicated with vout our written agreement			**ASTU**		
	NAME	DATE	DRAWING TITLE Combined pedal		
DRAWN BY	Udesa G.				
APPV'D		xxx	MATERIAL	DRAWING NO XXX	A4
All dimensions are in cm			WEIGHT XXX	SCALE:1:5	SHEET 1 OF 1

Part and assembly drawing for actuation system

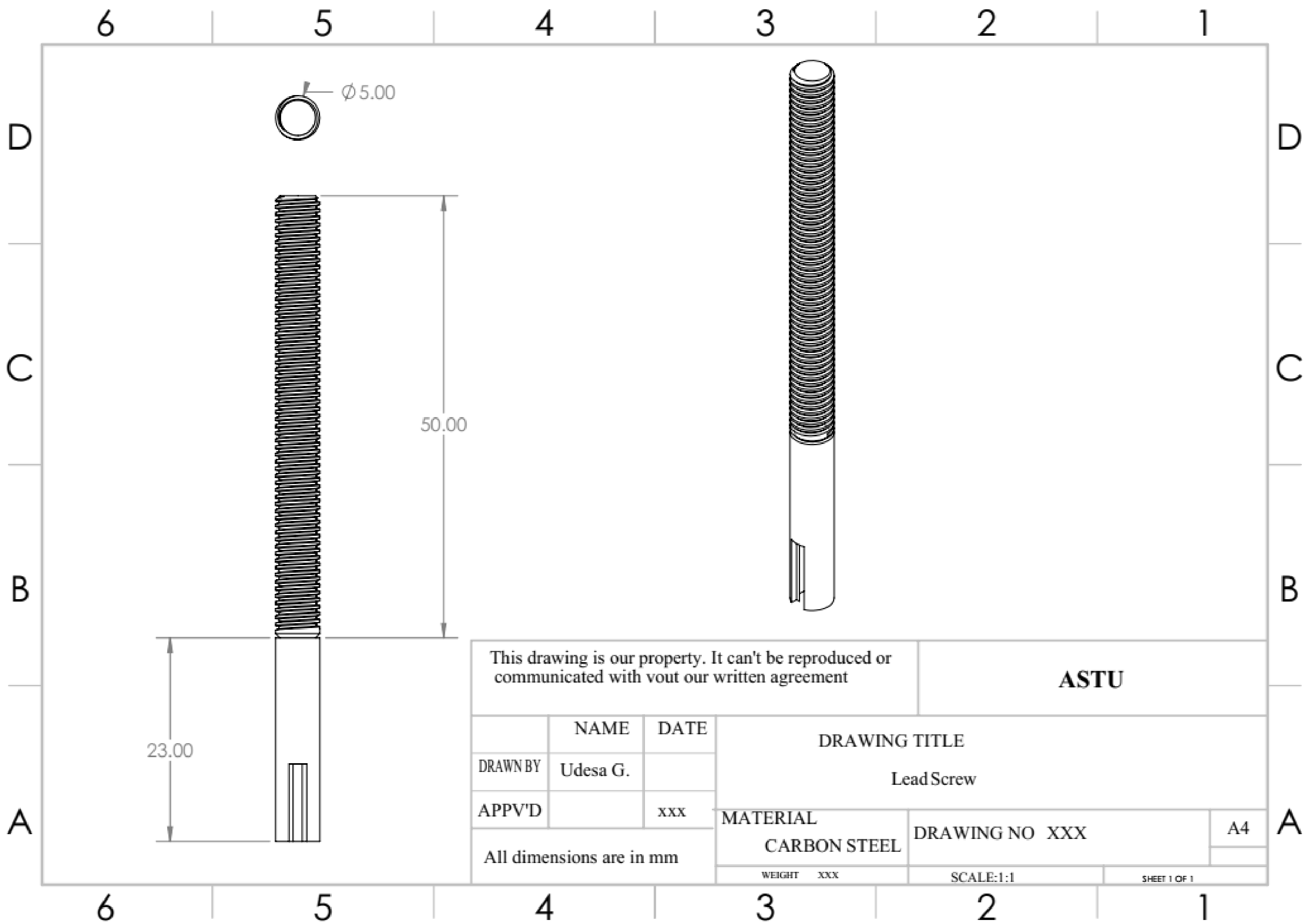

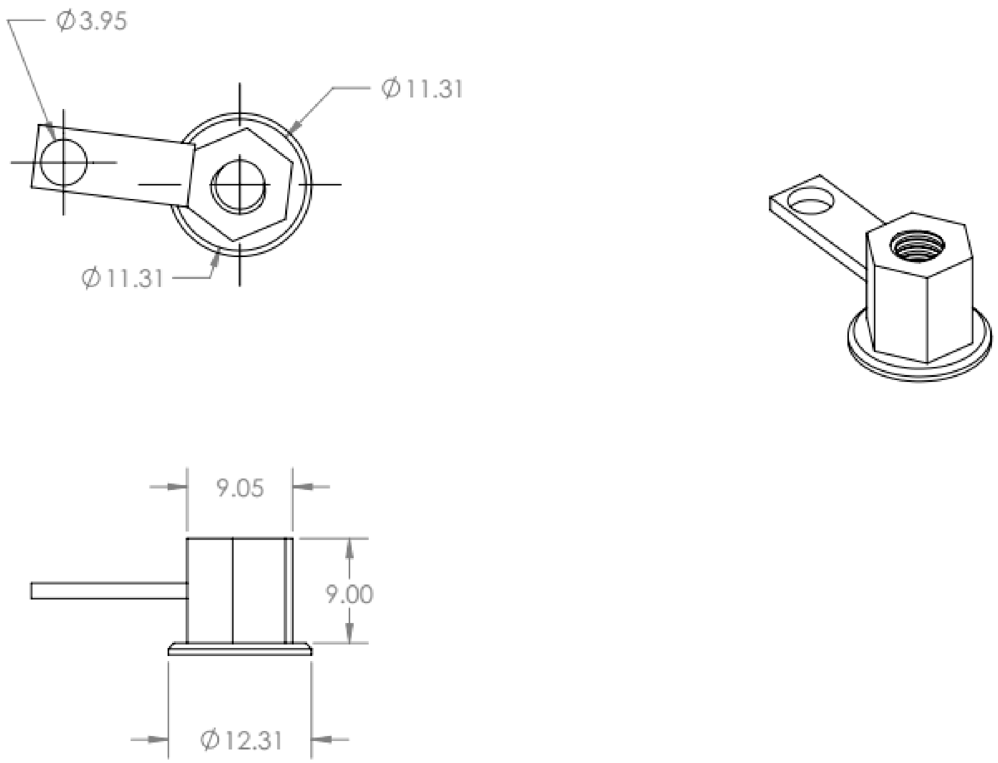

This drawing is our property. It can't be reproduced or communicated with vout our written agreement			ASTU		
	NAME	DATE	DRAWING TITLE		
DRAWN BY	Udesa G.		Drive nut		
APPV'D		xxx	MATERIAL Bronze	DRAWING NO XXX	A4
All dimensions are in mm			WEIGHT XXX	SCALE:2:1	SHEET 1 OF 1

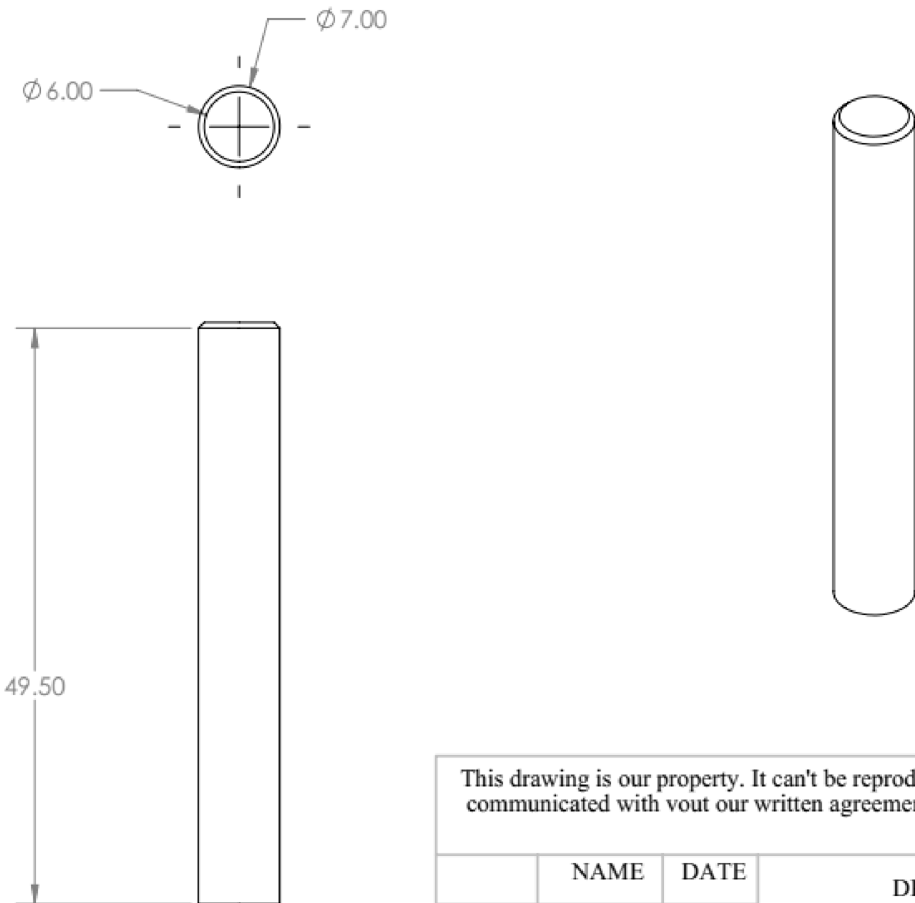

This drawing is our property. It can't be reproduced or communicated with vout our written agreement		**ASTU**

	NAME	DATE	DRAWING TITLE		
DRAWN BY	Udesa G.		Inner Tube		
APPV'D		xxx	MATERIAL Aluminum	DRAWING NO XXX	A4
All dimensions are in mm			WEIGHT XXX	SCALE:2:1	SHEET 1 OF 1

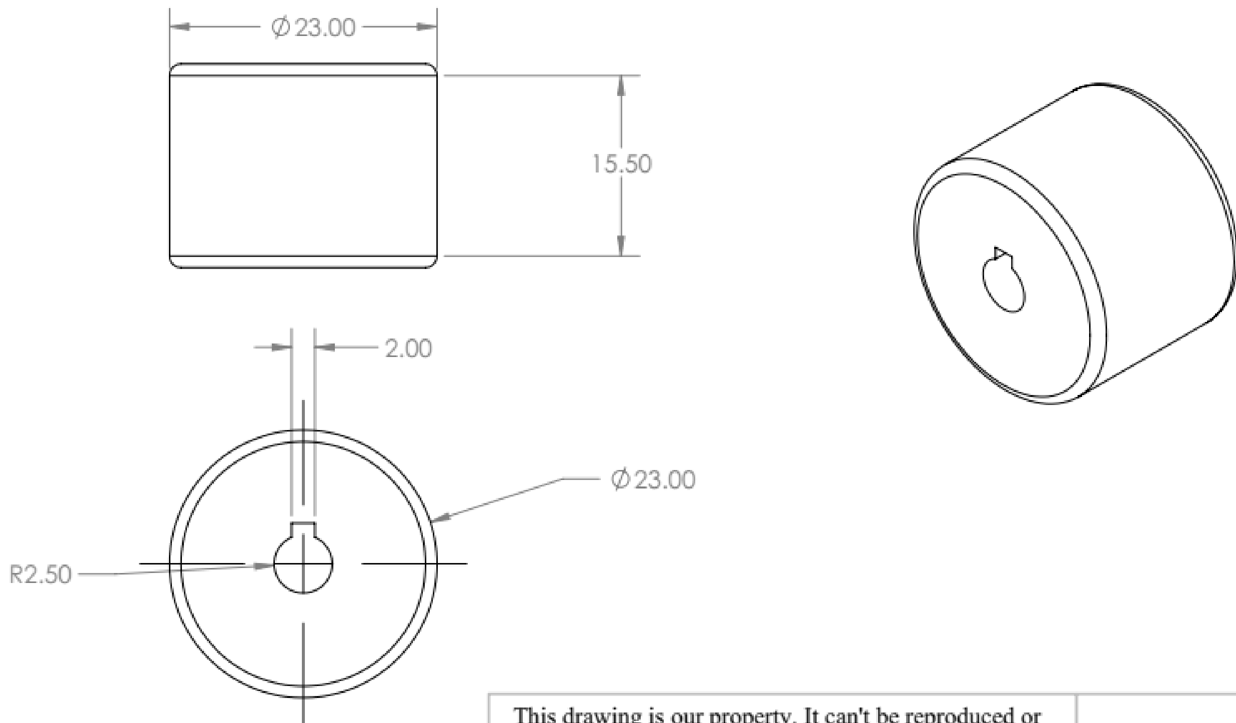

This drawing is our property. It can't be reproduced or communicated with vout our written agreement			**ASTU**
	NAME	DATE	DRAWING TITLE
DRAWN BY	Udesa G.		Sleeve
APPV'D		xxx	MATERIAL Cast iron
All dimensions are in mm			DRAWING NO XXX
			A4
WEIGHT XXX	SCALE:2:1	SHEET 1 OF 1	

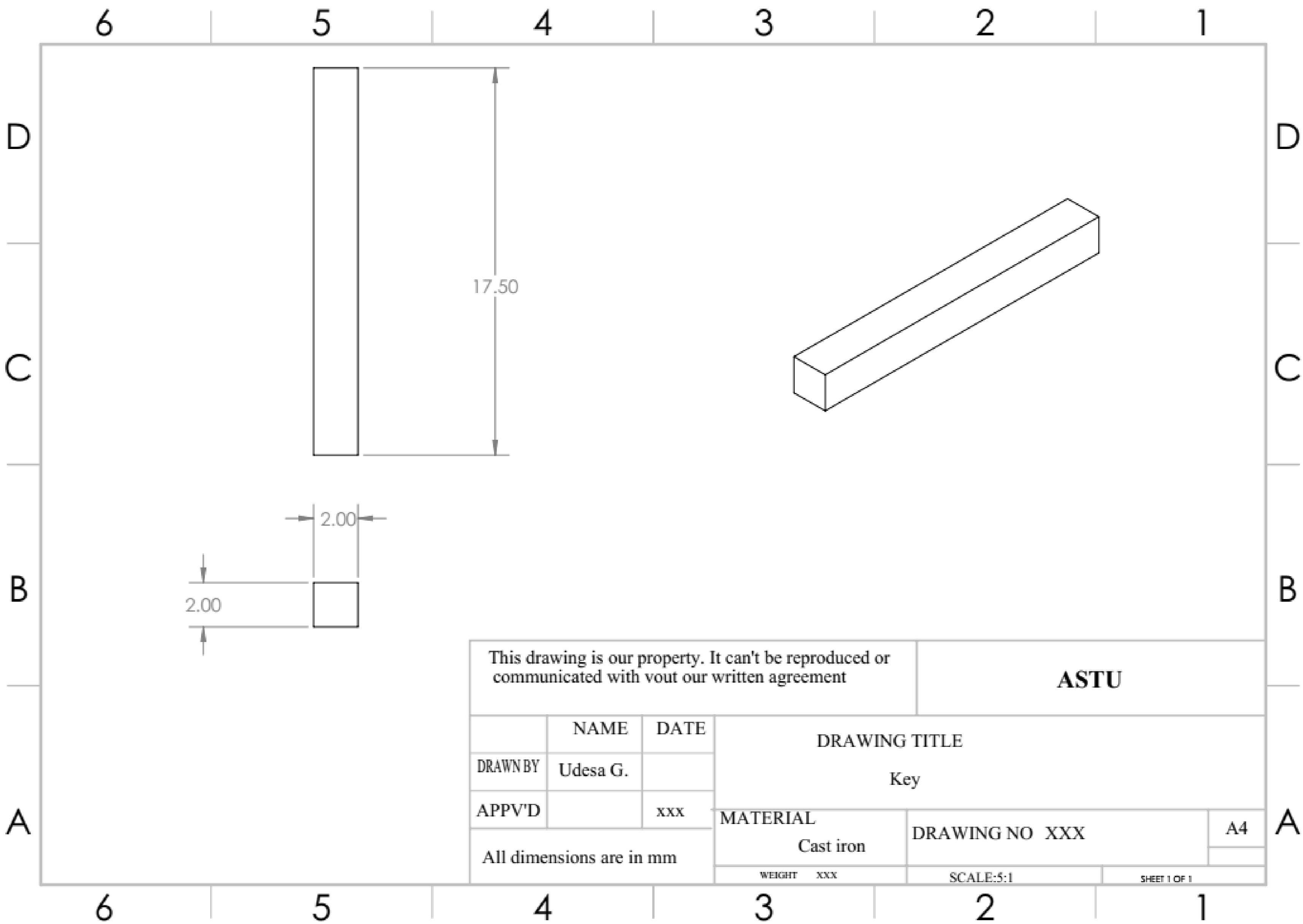
6
5
4
3
2
1
D
C
B
A
17.50
2.00
2.00
This drawing is our property. It can't be reproduced or communicated with vout our written agreement
ASTU
NAME
DATE
DRAWN BY
Udesa G.
APPV'D
xxx
All dimensions are in mm
DRAWING TITLE
Key
MATERIAL
Cast iron
DRAWING NO XXX
A4
WEIGHT XXX
SCALE:5:1
SHEET 1 OF 1

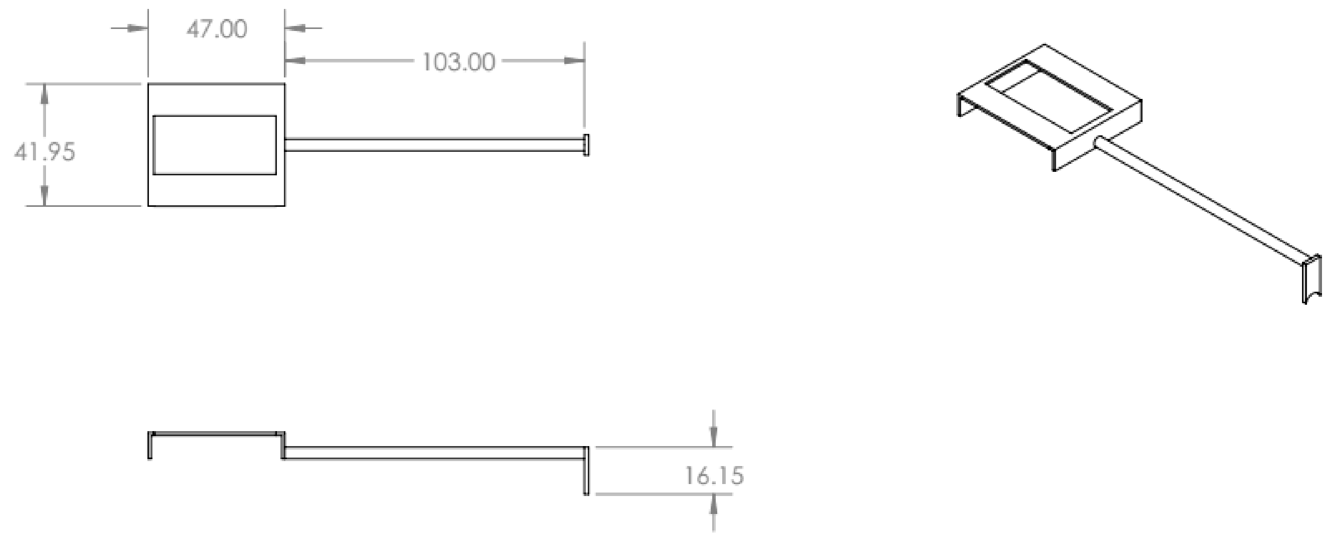

This drawing is our property. It can't be reproduced or communicated with vout our written agreement

ASTU

	NAME	DATE	DRAWING TITLE
DRAWN BY	Udesa G.		Mounting Bar
APPV'D		xxx	MATERIAL Aluminum

All dimensions are in mm

DRAWING NO XXX

A4

WEIGHT XXX

SCALE:1:2

SHEET 1 OF 1

xxx

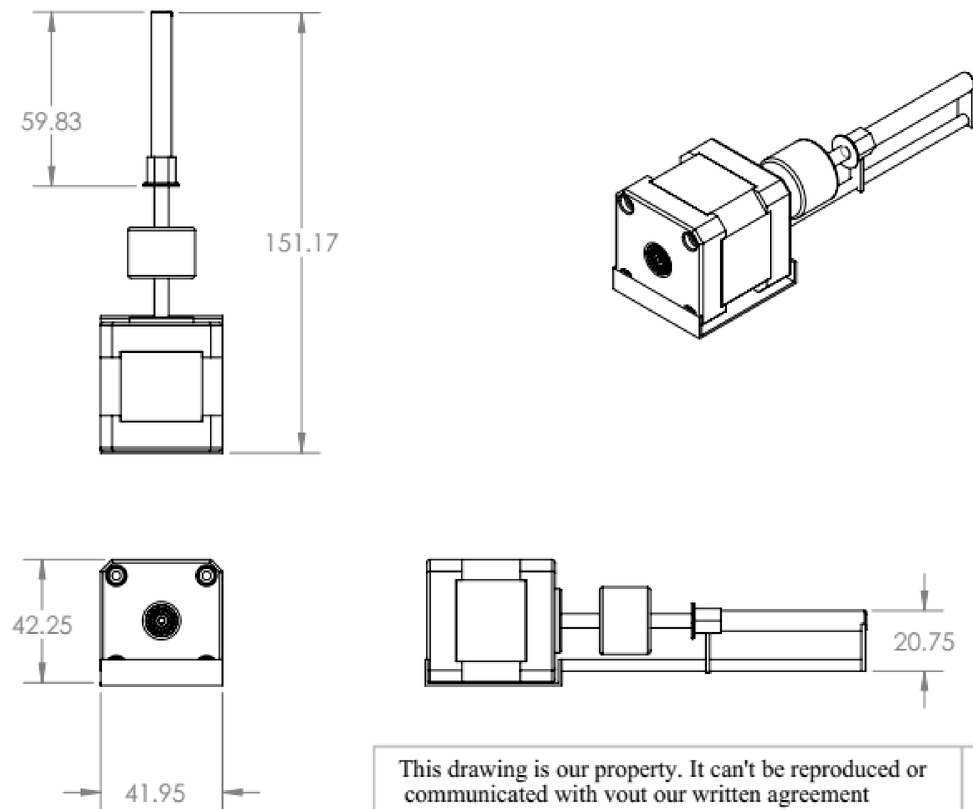

This drawing is our property. It can't be reproduced or communicated with vout our written agreement			ASTU		
	NAME	DATE	DRAWING TITLE Assembly of actuator		
DRAWN BY	Udesa G.				
APPV'D		xxx	MATERIAL	DRAWING NO XXX	A4
All dimensions are in mm			WEIGHT XXX	SCALE:1:2	SHEET 1 OF 1

Appendix F: Electronic Circuit and Arduino Code for Proteus simulation

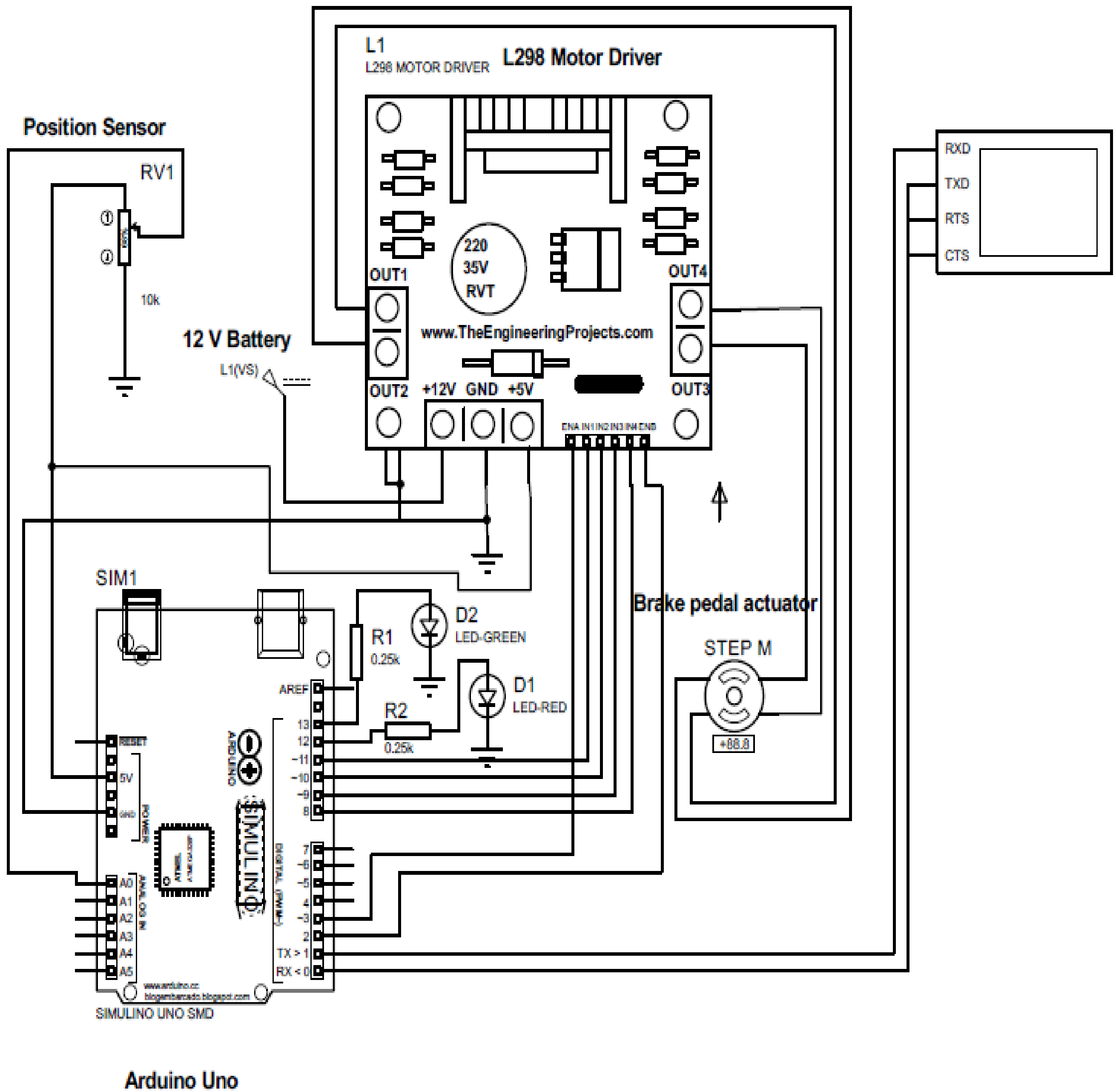

Arduino Code for Proteus simulation

```
///Udesa Getachew Shunu////

#include <Stepper.h>

// Change this to the number of steps on your motor

#define STEPS 100

// Create an instance of the stepper class, specifying

// the number of steps of the motor and the pins it’s

// attached to

Stepper stepper(STEPS, 8, 9, 10, 11);

// The previous reading from the analog input

int previous = 0;

int greenLed = 13;

int redLed = 12;

void setup() {

// set the speed of the stepper motor to 1425 RPMs


  Stepper setSpeed(1425);

  pinMode(greenLed,QUTPUT);

  // The determination of output pins

 pinMode(redLed,OUTPUT);

  pinMod(3,OUTPUT);

  pinMode(2,OUTPUT);

  digitalWriter(3,HIGH);
```

```
 // Continuously working Arduino pins
  digitalWrite(2,HIGH);
  //To operate L298 motor driver
  Serial begin(9600);
}
void loop() {
  // Get the potentio sensor value
  int sensorReading = analogRead(A0);
  // Asigniin arduino pins for sensor reading
int step=map(sensorReading,0,1023,0,STEPS);
  // Mapping sensor total step to sensor readings
 // Move a number of steps equal to the change in
  // sensor reading
 stepper.step(step - previous);
  // Remember the previous value of the sensor
  previous = step;
 if (sensorReading > 0 && sensorReading < 1023)
{
  digitalWrite(redLed, HIGH);
  digitalWrite(greenLed, LOW);
}
else {
  digitalWrite (greenLed, HIGH);
```

```
  digitalWrite (redLed, LOW);
}
// determination cases for LED operation
Serial.prinln("sensor reading=");
Serial.println(sensorReading);
Serial.print("Step=");
Seral.println(step);
}
```